M

NASA
Technical
Paper
2573

March 1986

Analysis of Jimsphere Pairs for Use in Assessing Space Vehicle Ascent Capability

Charles K. Hill

NASA

NASA Technical Paper 2573

1986

Analysis of Jimsphere Pairs for Use in Assessing Space Vehicle Ascent Capability

Charles K. Hill

George C. Marshall Space Flight Center
Marshall Space Flight Center, Alabama

National Aeronautics and Space Administration

Scientific and Technical Information Branch

TABLE OF CONTENTS

LIST OF ILLUSTRATIONS

LIST OF ILLUSTRATIONS (Continued)

LIST OF ILLUSTRATIONS (Continued)

LIST OF ILLUSTRATIONS (Continued)

LIST OF ILLUSTRATIONS (Continued)

LIST OF ILLUSTRATIONS (Concluded)

LIST OF SYMBOLS

Symbol	Definition
A	Azimuth
A_{EXT}	Azimuth extrapolation
A_{int}	Azimuth interpolation
cm	Centimeter
E	Elevation angle
E_{EXT}	Elevation extrapolation
E_{int}	Elevation interpolation
GMD	Ground Meteorological Direction Finder
GMT	Greenwich Mean Time
H	Rise rate velocity
H_k	One-tenth-second rise rate velocity
H_1	One-second rise rate velocity
hr	Hour
km	Kilometer
kips	Thousands of pounds
m	Meter
m/s	Meter per second
$msec^{-1}$	Meter per second
N	Number
NASA	National Aeronautics and Space Administration
NW	Number of points in the smoothed interval
R	Range
R_E	Earth radius, constant for a given location and dependent on station latitude
R_{EXT}	Range extrapolation

LIST OF SYMBOLS (Concluded)

Symbol	Definition
RMS	Root mean square
R_{int}	Range interpolation
STS	Space Transportation System
sec	Second
U	Wind component along the flight azimuth
V	Wind component perpendicular to flight azimuth
W_x	Zonal velocity
W_z	Meridional velocity
W_{x_k}	One-tenth-second zonal velocity
W_{z_k}	one-tenth-second meridional velocity
W_{x_1}	One-second zonal velocity
W_{z_1}	One-second meridional velocity
X_c	Zonal with respect to the Earth curvature
Y	Altitude
Y_c	Altitude with respect to the Earth curvature
Y_k	One-tenth second altitude
Y_1	One-second altitude
Z_c	Meridional with respect to the Earth curvature

Other Symbols

[ ]	Denotes intergral portion

TECHNICAL PAPER

ANALYSIS OF JIMSPHERE PAIRS FOR USE IN ASSESSING SPACE VEHICLE ASCENT CAPABILITY

I. INTRODUCTION

A. Introductory Remarks

The physical characteristics of the Earth are the result of the interaction between many processes. The transfer of the energy and momentum within the Earth atmosphere and oceans and the absorption of solar radiation produce the terrestrial climate in which we live. The terrestrial part of the aerospace environment has been defined as being from the surface of the Earth to about 90 km. In considering the design and operation of aerospace systems, one should remember that 99 percent of the Earth atmosphere is below 30 km and 50 percent is below approximately 7 km altitude. Therefore, the major structural and control system forcing functions, insofar as the environment is concerned, occur in the lower layers of the atmosphere.

With the advent of high flying rockets in World War II, the need to know more about the aerospace environment became a necessity as we moved toward the goal of progressive accumulation of knowledge concerning space and space travel. In striving for this goal, we have gone from the V-2s to the Space Shuttle, but by spanning this bridge, much has been learned about the composition and structure of the atmosphere and space. It is known that the atmosphere is structured with a troposphere, in which most weather occurs and within which the temperature generally decreases with altitude, extending from the surface to approximately 13 km and a stratosphere from approximately 13 km to approximately 48 km in which initially the temperature is essentially constant then increases. Above the troposphere and stratosphere, the mesosphere exists from approximately 48 km to approximately 80 km altitude in which the temperature increases. An electrically charged ionosphere extends from the upper part of the stratosphere to approximately 966 km.

B. Background Information

Atmospheric phenomena play a significant role in the design and flight of aerospace vehicles and in the integrity of the associated control systems and structures. Environmental design criteria are important inputs and major building blocks for any aerospace vehicle development. They are based on statistics and models of environmental phenomena relative to various aerospace industrial, test, and vehicle operational launch locations [1]. The design parameters are scaled to show the probability of reaching or exceeding certain limits determined by the mission requirements and desired operational lifetime for the aerospace system of concern.

Careful assessment of the natural environment operational requirements in the early stages of an aerospace vehicle development program will be advantageous in developing a vehicle with a minimum of mission constraints. For those areas of the environment that need to be monitored prior to and during tests and operations, this early planning will permit development of the required measuring and communication systems for accurate and timely decisions for deployment of the aerospace system.

For environmental (terrestrial or space) extremes, there is no known physical upper or lower bound except for certain conditions; for example, wind speed does have a strict physical lower bound of zero. Therefore, for any observed extreme environment condition, there is a finite probability of it being exceeded. Consequently, environmental extremes for design must be accepted with the knowledge that there is some risk of the values being exceeded. Also, the accuracy of measurement of many environmental parameters is not as precise as desired. In some areas, theoretical model estimates of extreme values are believed to be more representative than those indicated by empirical distributions from short periods of record. Therefore, values derived from detail modeling studies are given considerable weight in selecting design values for some parameters, i.e., the peak surface winds [2].

Aerospace vehicles are not normally designed for launch and flight in severe atmospheric conditions such as hurricanes, thunderstorms, and squalls. Atmospheric parameters associated with these conditions, which would be hazardous to aerospace vehicles if operated under these conditions, include ground and inflight winds, wind shears, turbulence, icing conditions, and electrical activity. Guidelines provide information relative to these severe environmental characteristics, which may be included in design studies if required, but most often would be considered, if safeguards to avoid encountering these conditions can be developed. For civilian missions, this is more practical than for military operations. A trade-off system, costs versus operational safety and flexibility, is often required.

The wind data to be presented in this document are focused on information below 20 km in the so-called terrestrial environment. Specific aerospace vehicle natural environment design criteria are not normally specified in the appropriate organizational space vehicle design ground rules and design criteria data documentation. References are given for the environmental design information referred to as terrestrial and the space planetary environments [3,4,5]. The data are based on conditions which actually occurred or are based on statistical or physical models for a longer reference period than the available data base.

A knowledge of the Earth atmospheric environmental parameters is necessary for the establishment of design requirements for aerospace vehicles and associated equipment. Such data are required to define the design condition for fabrication, storage, transportation, test, preflight, and inflight design conditions and should be considered for both the whole system and the components which make up the system [6].

Good engineering judgment must be exercised in the application of any environmental data to aerospace vehicle design analysis. Consideration must be given to the overall vehicle mission and performance requirements. Knowledge still is lacking on the relationship between some of the environmental variates which are required as inputs to the design of aerospace vehicles. Also, interrelationships between aerospace vehicle parameters and atmospheric variables cannot always be clearly defined. Therefore, a close working relationship and team philosophy should exist between the design/operational engineers and the aerospace meteorologists and space technologists of the respective organization. Although, ideally, an aerospace vehicle design should accommodate all expected operational environmental conditions, it is neither economically nor technically feasible to design space vehicles to withstand all environmental extremes. For this reason, consideration should be given to the protection of aerospace vehicles from some extremes by use of support equipment and by using specialized environment-monitoring personnel to advise on the expected occurrence of critical environmental conditions. The services of specialized monitoring personnel may be very economical in comparison with more expensive designing which would be necessary to cope with all environmental possibilities.

As a rule, environmental criteria guideline documents do not specify how the designer should use the data in regard to a specific aerospace vehicle design. Such specifications may be established only through collaborative analysis and study of a particular design problem.

The environment in which an aerospace system must operate consists of natural and induced forces. The induced environment is the environment which is a result of the system being present. The natural environment is the environment existing naturally and undisturbed in the presence of the system.

Induced environments (vehicle caused) may be more critical than natural environments for certain vehicle operational situations, and in some cases the combination of natural and induced environments will be more severe than either environment alone. Therefore, induced environments and natural environments must be considered in the final analysis.

Wind data given in this document were formulated based on discussions with engineers and experimenters involved in aerospace vehicle development and operations; therefore, they represent the response to actual engineering problems and are not just a general compilation of wind data.

Inflight winds constitute the major atmosphere forcing function in aerospace vehicle and missile design [7]. A frequency content of the wind profile near the beginning mode frequencies, wind shear with the characteristics of a step input, may exceed the vehicle structural capabilities (especially on forward stations for the small-scale variations of the wind profiles). Wind profiles with high wind speeds and shears exert high structural loads at all stations on a large space vehicle, and when the influences of bending dynamics are high, even a profile with low speeds and high shears can create large loads. Because of the possibility of launch into unknown winds, operational missile systems must accept some inflight loss risk in exchange for a rapid-launch capability [8]. But research and development aerospace vehicles, in particular, cost so much that the overall success of a flight often outweighs the consideration of launch delays caused by excessive inflight wind loads. If the exact wind profile detail structure could be known in advance, it would be a relatively simple task to decide upon the launch date and time. However, there is little hope of accurately predicting the detailed wind profile very much into the future. Over the years, these situations have increasingly put emphasis on prelaunch monitoring of inflight winds. Finally, prelaunch wind profiles determination techniques essentially preclude the risk of launching an aerospace vehicle or research and development missile into an inflight wind condition that would cause it to fail.

The development and operational deployment of the FPS-16 Radar/Jimsphere System (Fig. 1) significantly minimized vehicle failure risks when properly integrated into a flight simulation program. Figure 2 shows an example of the jimsphere profile data. The jimsphere sensor (Fig. 3), when tracked with the FPS-16 or other radar with equal tracking capability, provides a very accurate "all weather" detailed wind profile measurement. In general, the system provides a wind profile measurement from the surface to an altitude of 17 km in slightly less than 1 hr, a vertical spatial frequency resolution of 1 Hz per 100 m, and an RMS error of about 0.5 $msec^{-1}$ for wind velocities averaged over 50-m intervals. The resolution of these data permits calculating the structural loads associated with the first bending mode and generally the second mode of missiles and space vehicles during the critical high dynamic pressure phase of flight. This provides better than order-of-magnitude accuracy improvement over the conventional rawinsonde wind profile measuring system. However, the recently developed Meteorological Sounding System (Fig. 4) in use at some test ranges approach the wind profile resolution accuracy of the jimsphere system and may be adequate for many prelaunch monitoring requirements. By employing the appropriate data transmission resources, a detailed wind profile from the FPS-16 radar can be ready for input to the vehicle flight simulation program within a few minutes after tracking of the jimsphere. The flight simulation program provides flexibility relative to vehicle dynamics and other parameters in order to make maximum use of the detailed wind profiles [9].

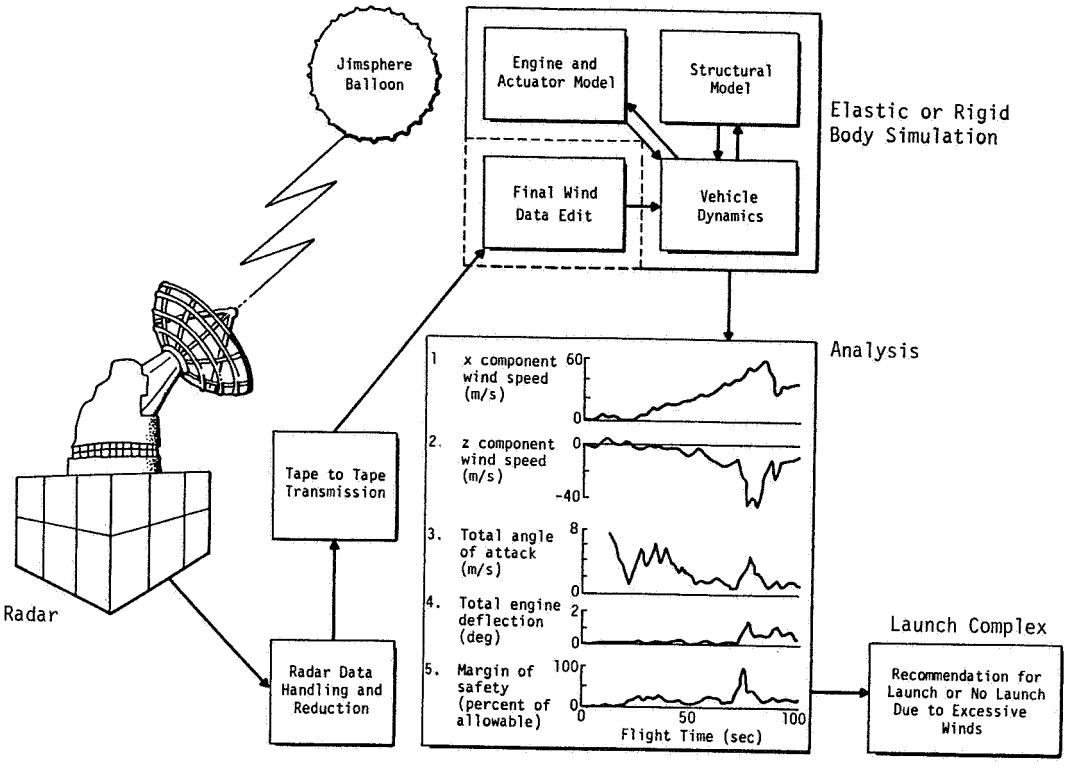

Figure 1. Operation of the FPS-16 Radar/Jimsphere System.

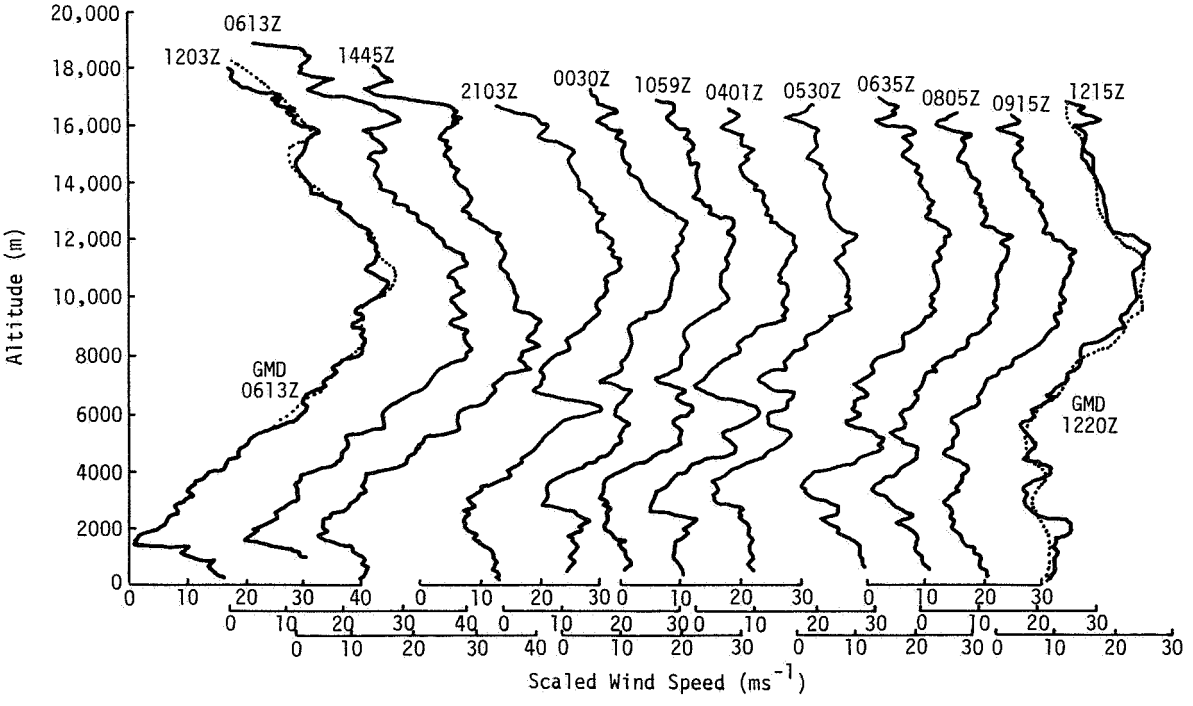

Figure 2. FPS-16 Radar/Jimsphere profile data.

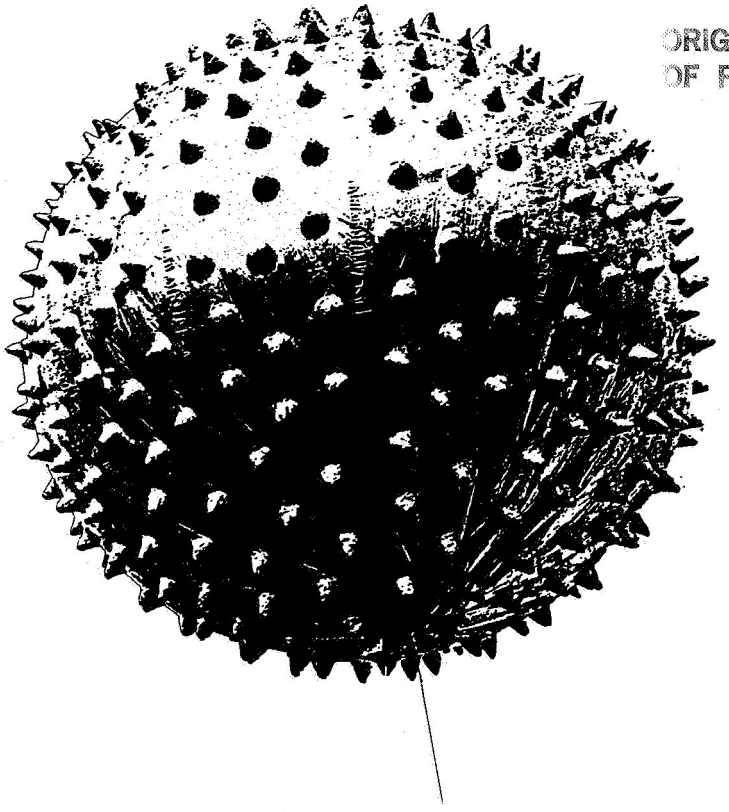

Figure 3. Jimsphere sensor.

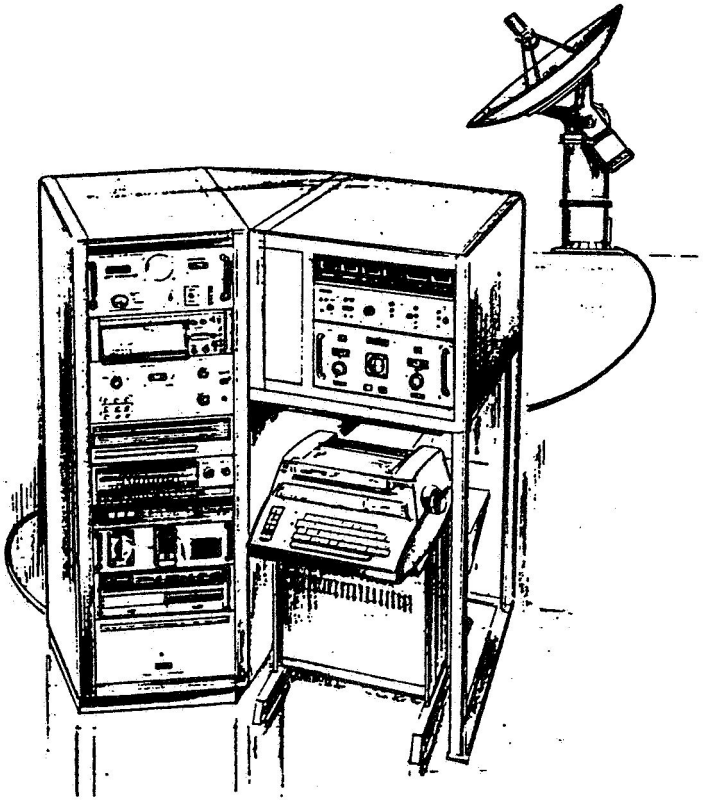

4. Meteorological sounding system tracking and data acquisition system.

If very critical wind conditions exist and the mission requirement dictates a maximum effort to launch with provision for last-minute termination of the operation, then a contingency plan that will provide near real-time wind profile and flight simulation data may be employed. This can be done while the jimsphere is still in flight.

To provide the data for this research, an FPS-16 Radar/Jimsphere Wind Profile Program was conducted to gather 3.5-hr, 7-hr, and 10.5-hr pairs of jimsphere profiles at Kennedy Space Center, Florida. The objectives of this research were to evaluate the accuracy and representativeness of quantitative radar wind profile data, to investigate the data variability of detailed winds aloft containing systems of a scale smaller than that normally detected from rawinsonde data, and to investigate the structure and dynamics of the atmosphere associated with space vehicle (Shuttle) launches.

The data reduction process described in Section II utilizes increased knowledge of parameters, techniques, and improved computational methods. The governing wind equations, their solution procedure, and computations/process are briefly reviewed.

Section III deals with the jimsphere data samples obtained for this investigation and the results of the statistical analysis performed. In-plane and out-of-plane wind profile component data observed during STS missions were used to calculate 3.5-hr component differences. A discussion is presented of how each STS case compares with statistical values calculated from the research sample.

Section IV presents major conclusions from the results of this effort.

II. DATA REDUCTION PROCESS

A. Introductory Remarks

The purpose of the Jimsphere Wind Conversion Program is to compute 1-sec velocity data from 0.1-sec slant range, azimuth, and elevation data as observed while continuously tracking the jimsphere balloon with the FPS-16 radar unit at 0.1-sec time intervals. The equations used in editing the data to obtain the 1-sec Y (altitude), H (rise rate), W_X (zonal), and W_Z (meridional) velocity components are presented. Figures, tables, and discussion of program procedures are also included [10].

The program-generated time is defined as a monotonic increasing array of points in time, equally spaced by 0.1 sec. An analysis of time as recorded by the FPS-16 radar unit while tracking the jimsphere balloon revealed that tracking time recorded erroneously in some cases because of tracking errors or magnetic tape faults. Since possible discontinuities in time could arise from such erroneous recordings of tracking time, the actual tracking time is used only as a reference and the program-generated time array is used in computations to prevent discontinuities. Time, when referred to in this report, should be regarded as program-generated time unless noted otherwise.

The first phase of program development, sometimes called a predicting phase, is concerned with eliminating errors in data that were induced by tracking errors or tape unit faults such as bit-dropping during initial recording of data. These induced errors, characterized as "stray" points and data gaps are thoroughly discussed by DeMandel and Krivo [10].

The raw data are edited by using computed least-squares coefficients in fitting the data through nine values in a floating array. Mid-point estimates and extrapolated look-ahead estimates are computed for replacement of values which are out of tolerance. These values are used to compute 0.1-sec velocities

by transforming slant range, azimuth, and elevation from a spherical coordinate system to a rectangular coordinate system whose origin is at the radar center. The 0.1-sec velocity data are fed through a 55-point Martin-Graham low-pass filter and 1-sec velocity data are output except when a data gap is encountered. The smoothing interval is based on the standard deviation of the data. The altitude data are first differenced to yield the rise rate and then zero-meaned by the use of a second degree least-squares curve fitting procedure. The variance of the resultant values is calculated and is used in determining the smoothing interval with a maximum of 21 points.

The method for smoothing is computing a running mean over the computed NW (smoothing interval) points of the altitude data. This method will cause NW/2 points to be lost in the beginning and end of each file and gaps of greater than 20 sec. If gaps are less than or equal to 20 sec, the gap is filled using the point on each side of the gap and linearly interpolating between them. If gaps are greater than 20 sec, the smoothing interval is computed and data are smoothed up to the gap. The gap is skipped and computation of a new interval begins. This data is converted from time-dependent measurements to space-dependent measurements by computing 5-m and 25-m velocity data from the time-dependent smoothed altitude and unsmoothed velocity data. Using the smoothed 1-sec altitude array, interpolated wind velocity components in 5-m altitude increments are computed from the 5-m data by using a 39-point interval Martin-Graham low-pass filter. The output is printed and written on magnetic tape.

B. Master Reduction Process and Equations

This program is the most important in the data reduction process since it computes winds from the raw radar data. Figure 5 shows the steps of the data reduction process. The meteorological and statistical bases for the developments in this process are given in References 11 and 12.

The equations used in the jimsphere data reduction process along with an appropriate explanation are given. This program is identical to those used by other U.S. government test ranges to process jimsphere data. The equation used in each step of the program is given.

1. Least-Square Linear Curve Fit Computations

Interpolation. (Range, azimuth, elevation):

$$R_{INT} = \frac{\sum_{N=1}^{9} \text{RANGE(N)}}{9} \qquad \text{(average over nine points)} \qquad (1)$$

$$A_{INT} = \frac{\sum_{N=1}^{9} \text{AZIMUTH(N)}}{9} \qquad (2)$$

$$E_{INT} = \frac{\sum_{N=1}^{9} \text{ELEVATION(N)}}{9} \qquad (3)$$

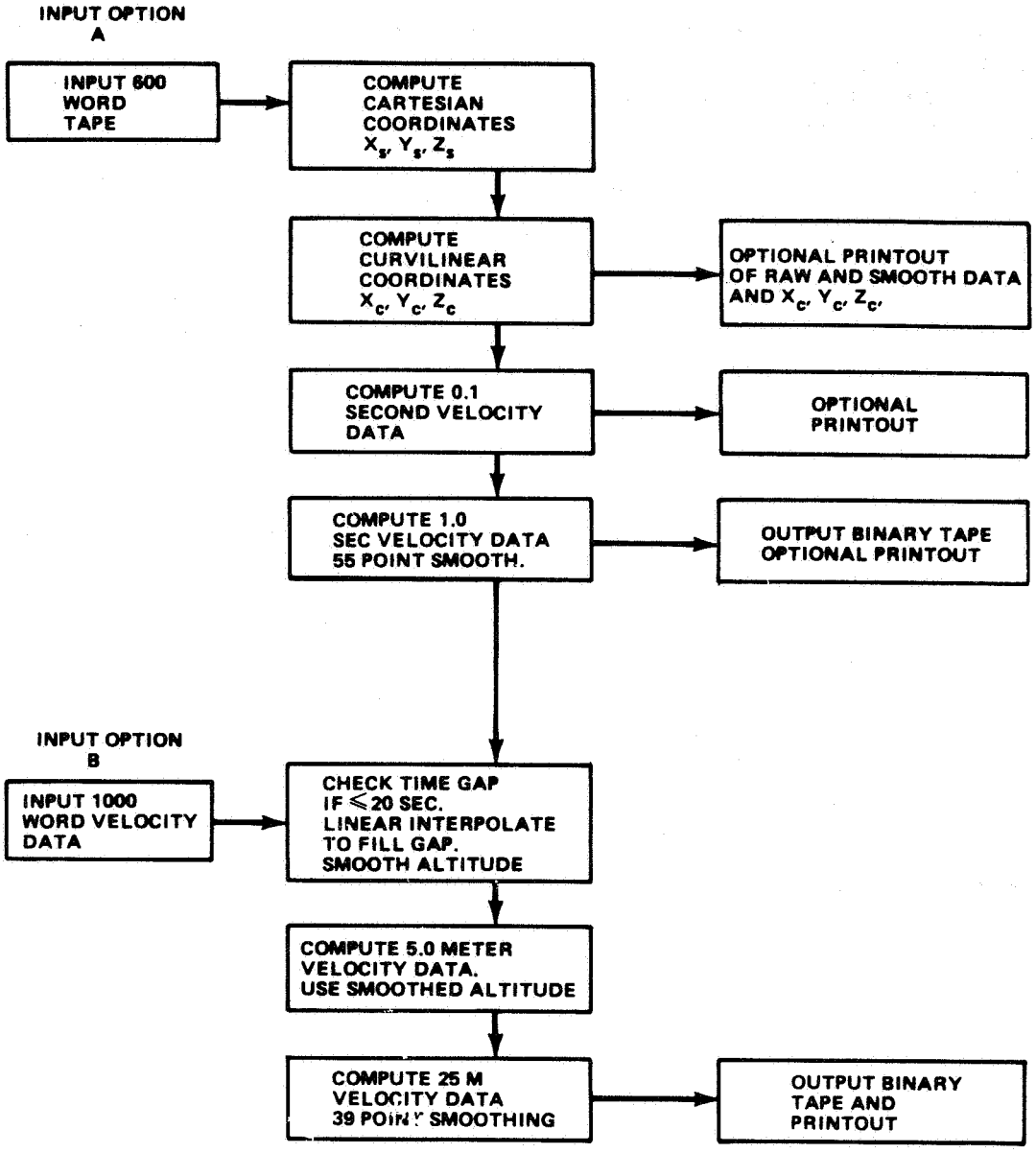

Figure 5. Flowchart of the FPS-16 Radar/Jimsphere master reduction process.

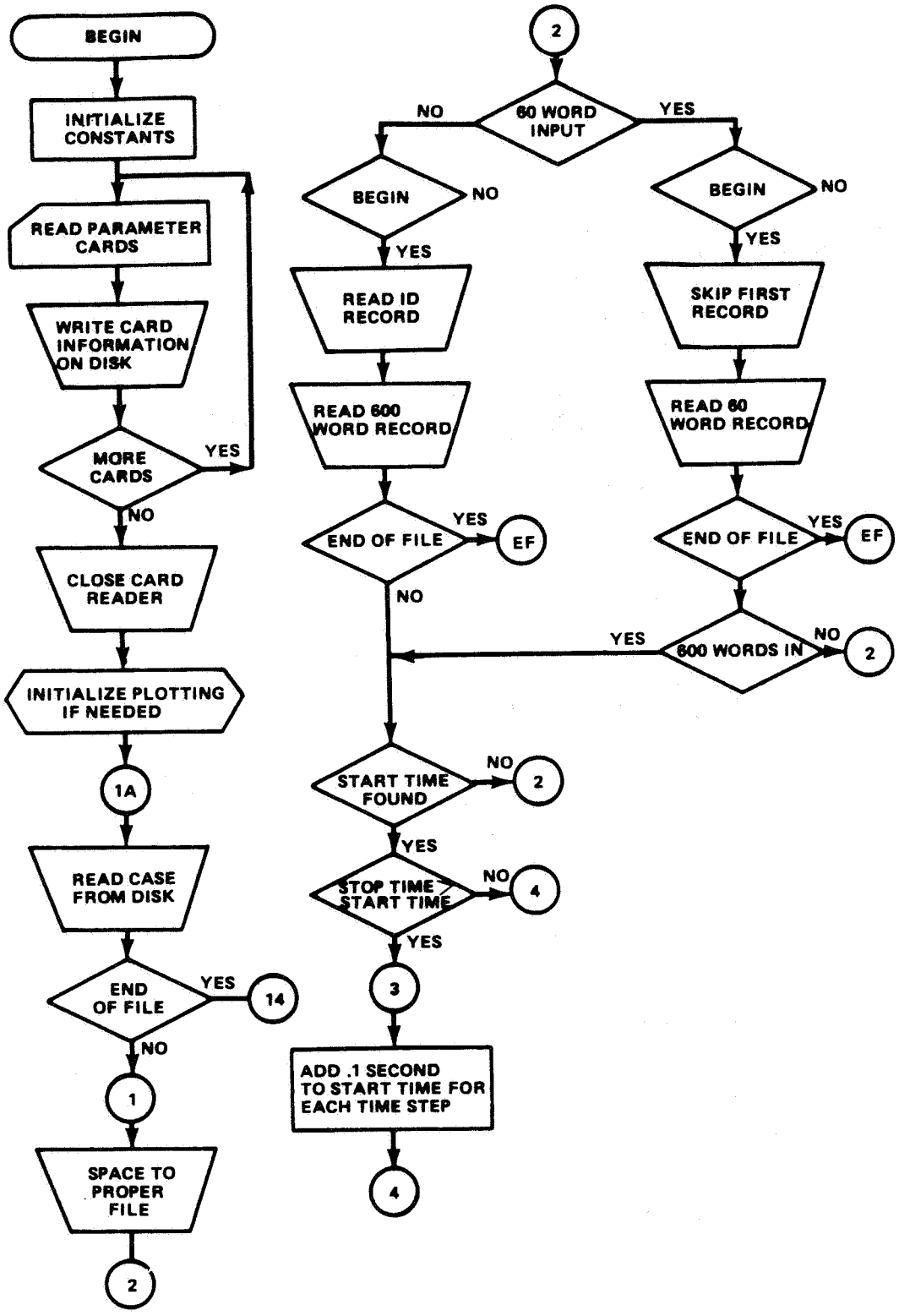

Figure 5. (Continued)

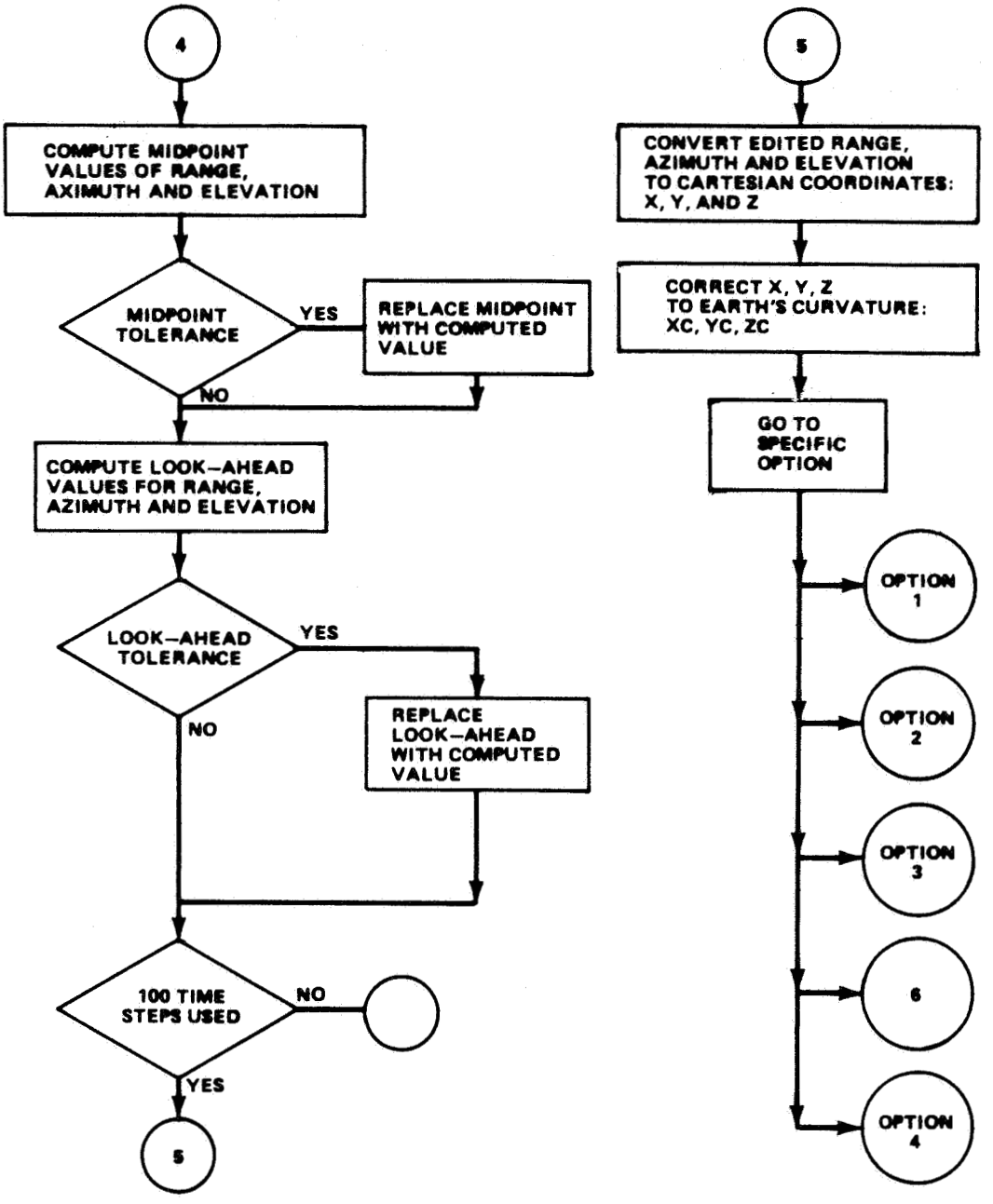

Figure 5. (Continued)

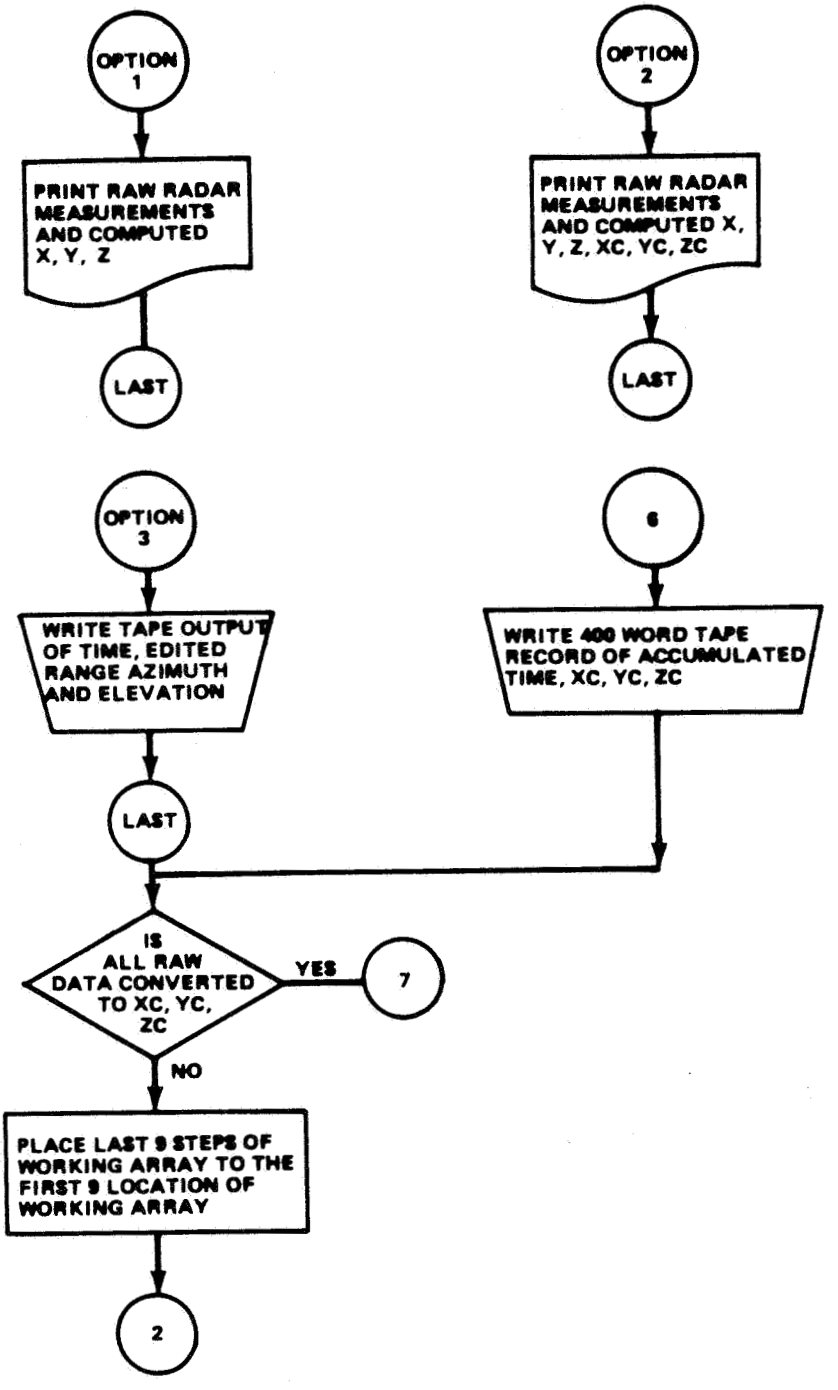

Figure 5. (Continued)

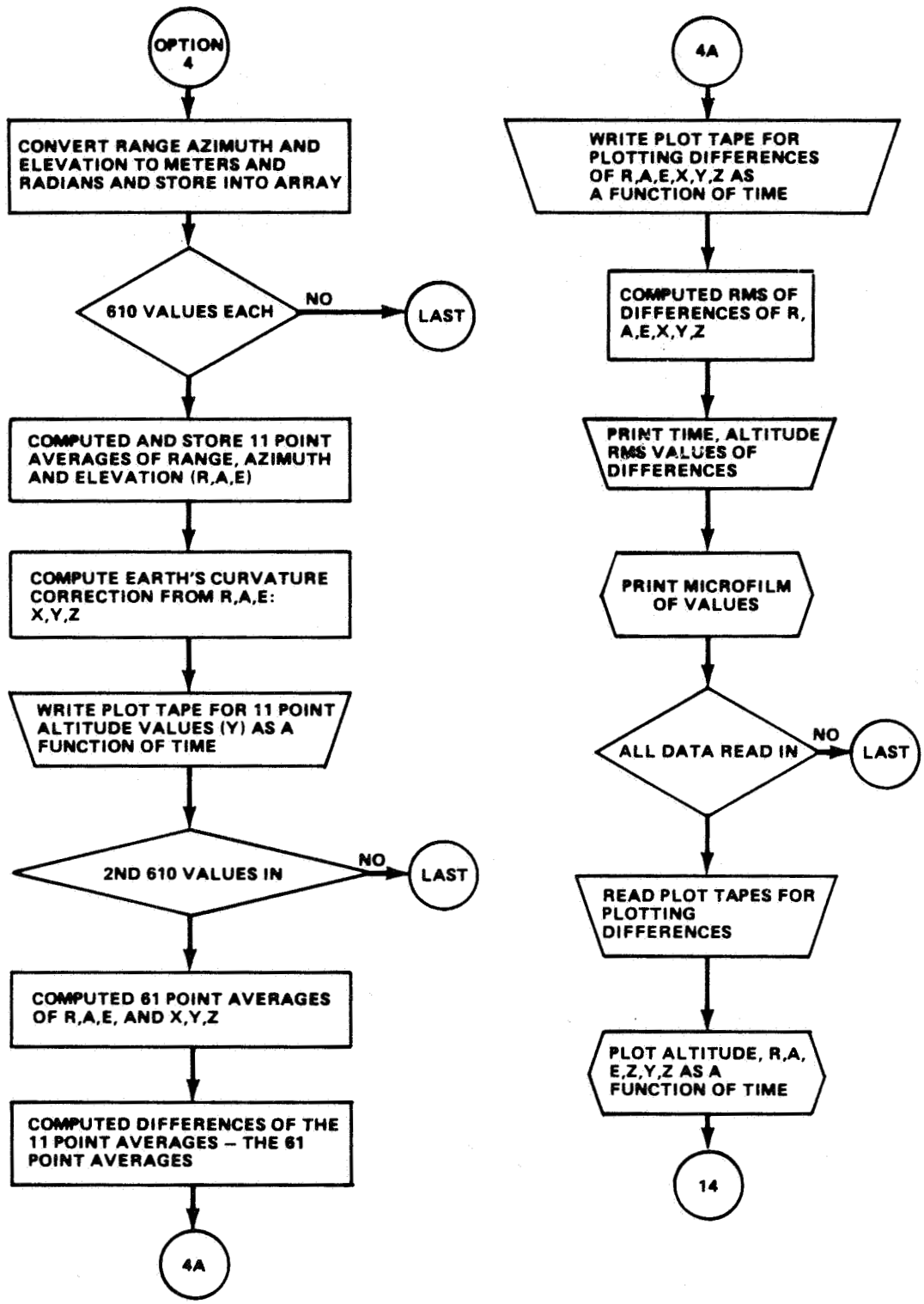

Figure 5. (Continued)

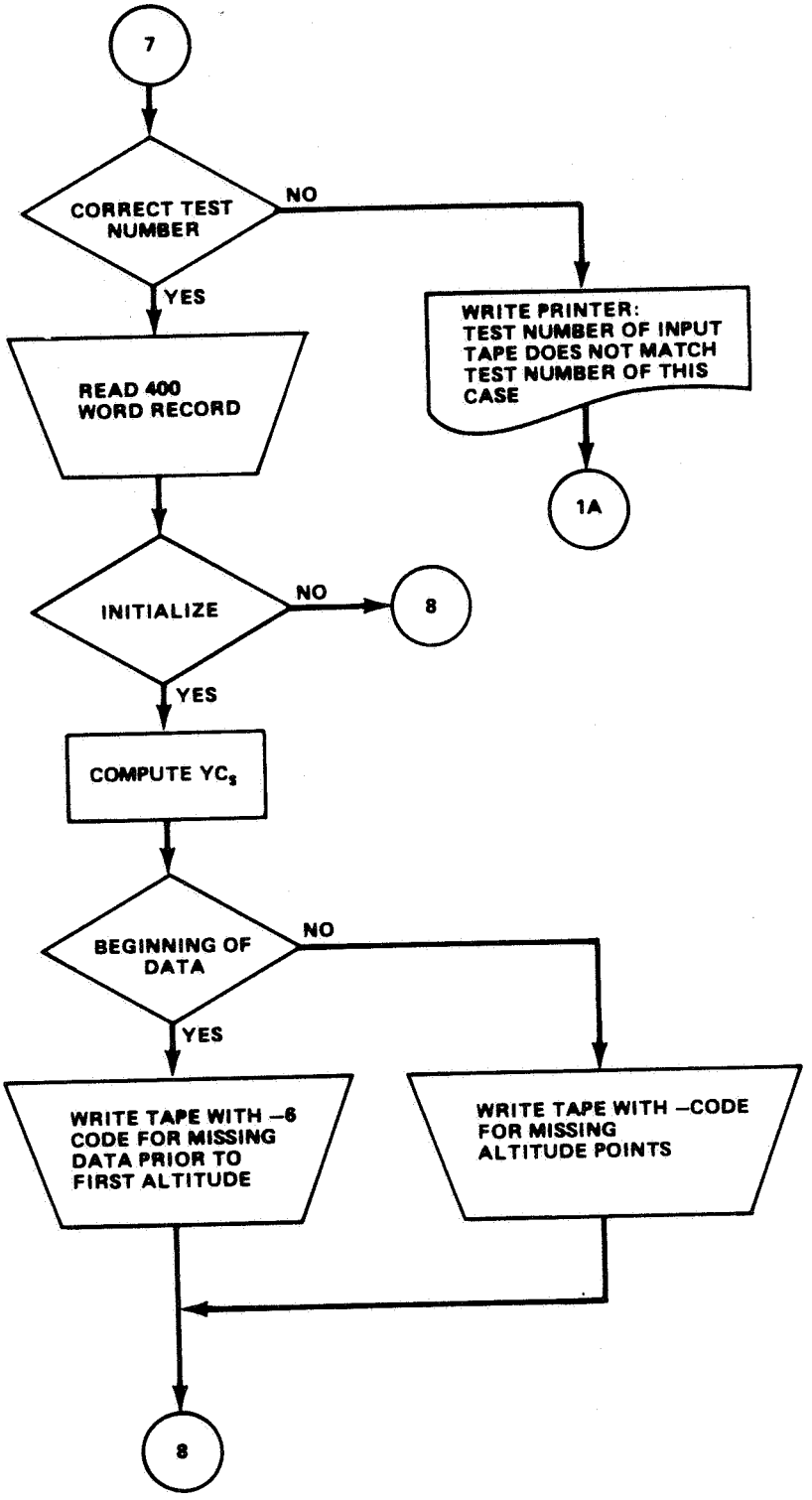

Figure 5. (Continued)

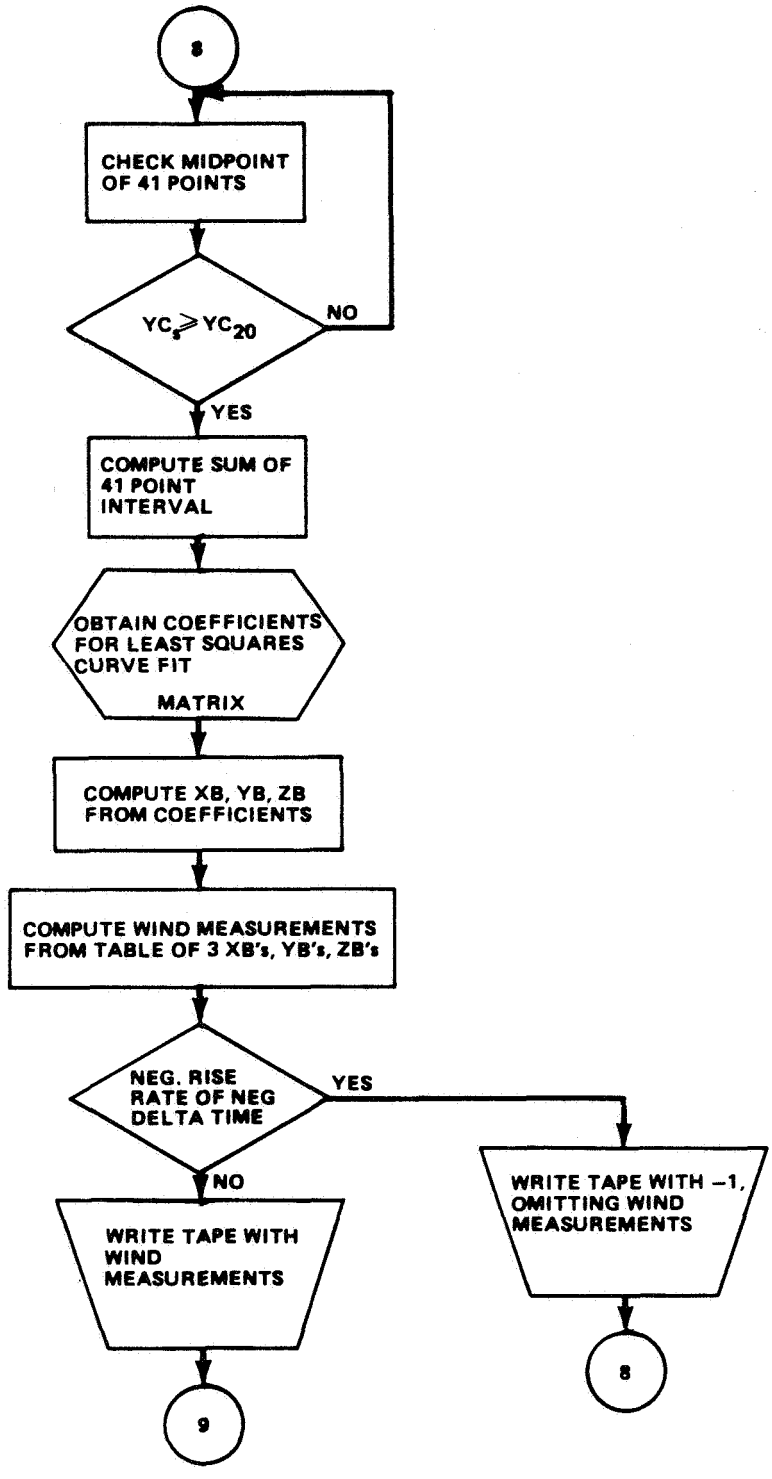

Figure 5. (Continued)

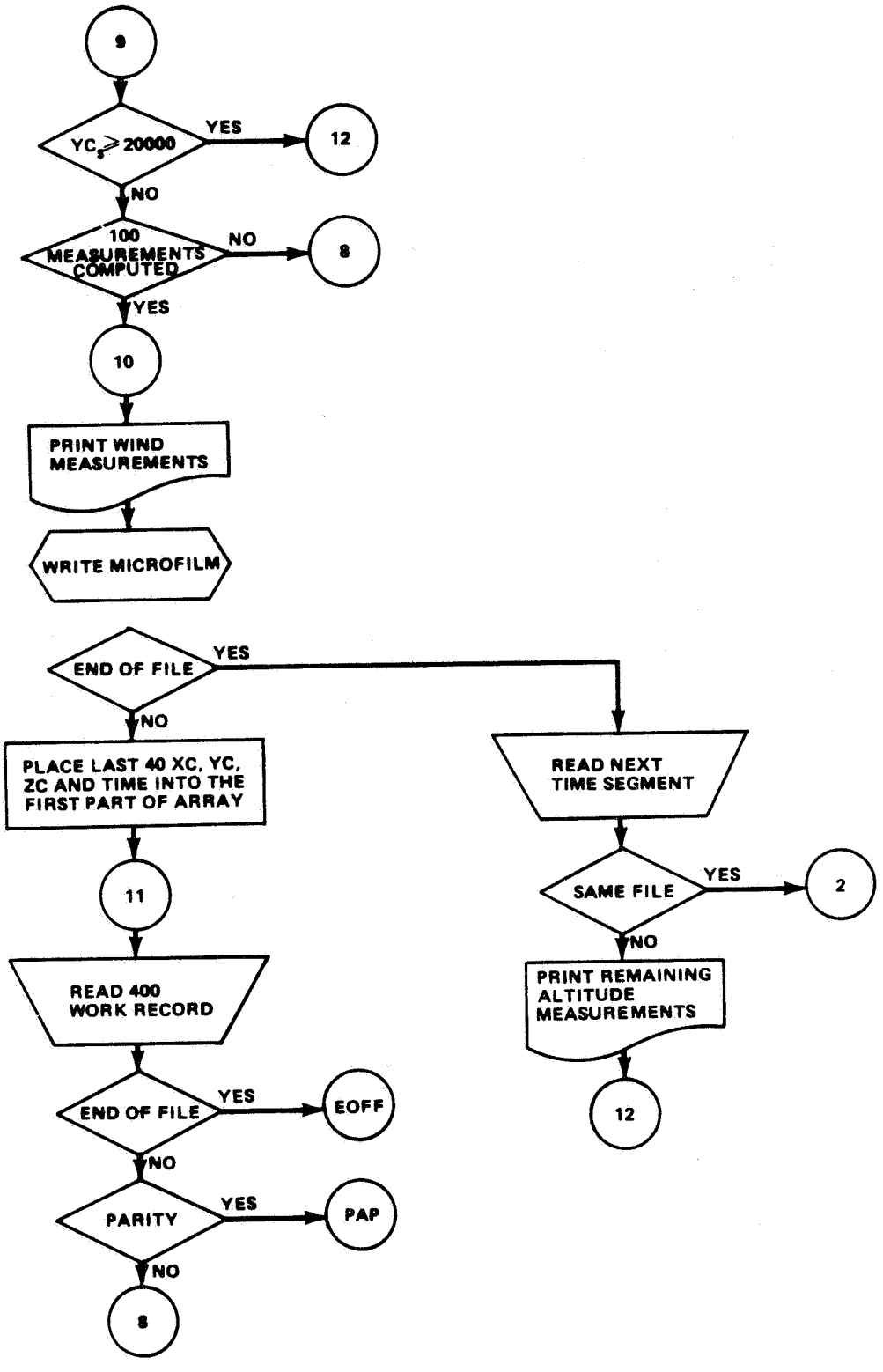

Figure 5. (Continued)

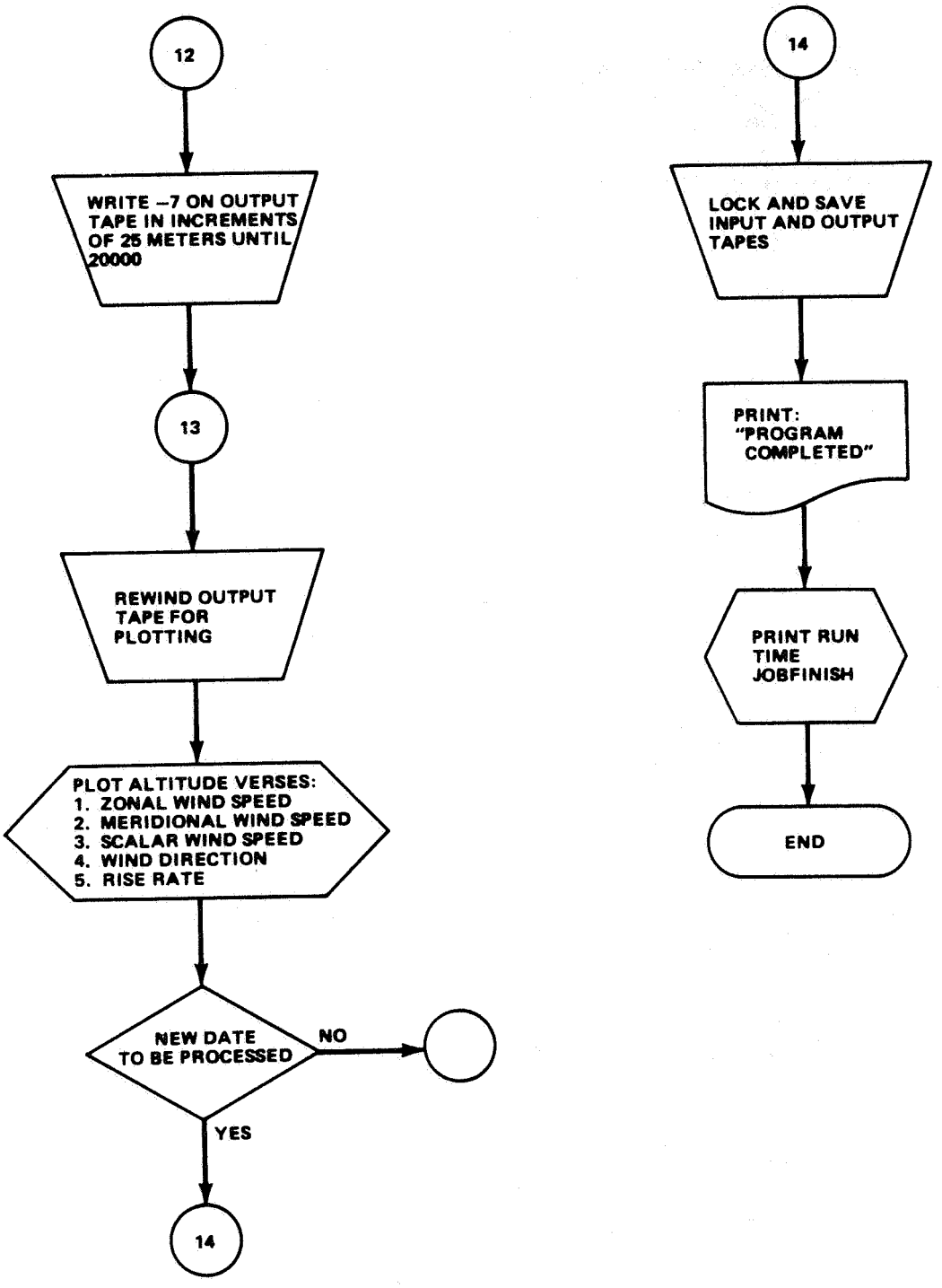

Figure 5. (Continued)

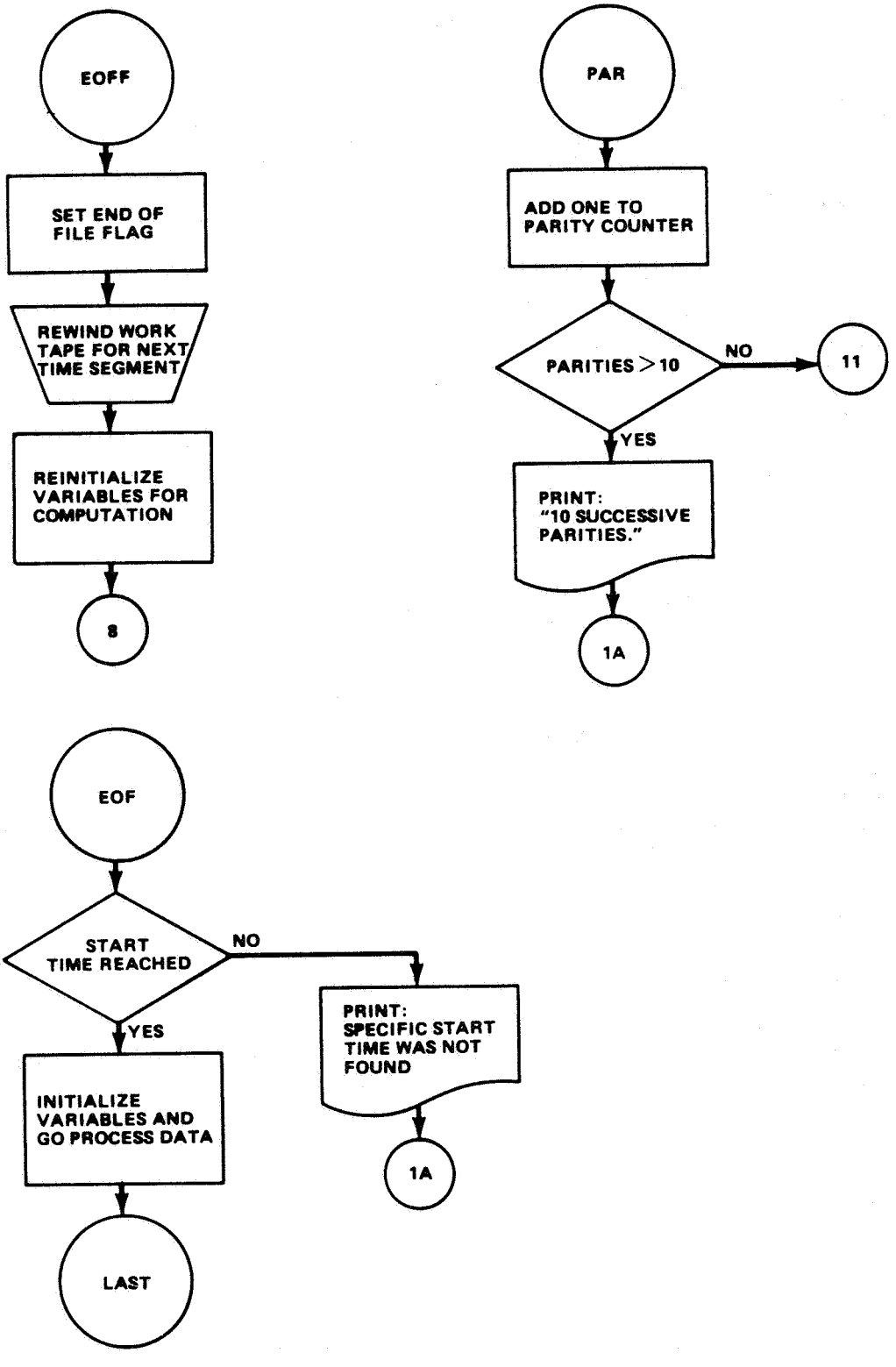

Figure 5. (Concluded)

If values of interpolated R, A, and E are different from the actual midpoint values of R, A, and E by tolerance of 15 yards, 0.03 deg, and 0.03 deg, respectively, then the interpolated value replaces the actual midpoint.

Extrapolation.

$$R,A,E_{EXT} = A_0 + A_1 \tag{4}$$

$$A_0 = \frac{\sum_{N=1}^{9} M_{(N)}}{9} \tag{5}$$

where M is R, A, and E, respectively.

$$A_1 = \frac{1}{T_{INT}} \left[\sum_{N=1}^{9} M_{(N)} \times T_{(N)} \right] \times 1.66666666 \tag{6}$$

where $T_{(N)}$ = -0.4, -0.3, -0.2, -0.1, 0, 0.1, 0.2, 0.3, 0.4, and T_{INT} = 2. If values of extrapolated R, A, and E are different from the tenth point values by 100 yards, 0.15 deg, and 0.15 deg, respectively, then the extrapolated value replaces the actual tenth point. The tolerances of the extrapolated and interpolated phases can be changed. Recycles through 360 deg in azimuth are taken care of automatically.

2. 0.1-Sec Velocity Computations

0.1-sec velocity components W_X (zonal), W_Z (meridional), and H (rise rate) with the associated Y (altitude) are computed from the 0.1-sec R, A, and E data. Transformations of slant range, azimuth, and elevation are made from spherical coordinates to a rectangular coordinate system. The equations for determining X_c, Y_c, and Z_c (subscript c denoting with respect to the Earth curvature) are:

$$X_c = R_E \tan^{-1} \left[\frac{X_s}{Y_s + R_E} \right] \qquad \text{(positive east)} \tag{7}$$

$$Z_c = R_E \tan^{-1} \left[\frac{Z_s}{[X_s^2 + (Y_s + R_E)^2]^{1/2}} \right] \qquad \text{(positive north)} \tag{8}$$

$$Y_c = [X_s^2 + Z_s^2 + (Y_s + R_E)^2]^{1/2} - R_E \qquad \text{(positive upward)} \tag{9}$$

where R_E, the radius of the Earth at the Eastern Test Range, Cape Kennedy (6, 373, 334 m), is considered to be that of a spherical Earth, and:

$$X_s = \rho \cos\theta \sin\phi \qquad \text{(positive east)} \tag{10}$$

$$Z_s = \rho \cos\theta \cos\phi \qquad \text{(positive north)} \tag{11}$$

$$Y_s = \rho \sin\theta \qquad \text{(positive upward)} \tag{12}$$

where ρ is slant range (m), R, θ is elevation (radians) E, and ϕ is azimuth (radians) A.
In the case of elevation angles greater than 90 deg, the following relationship should be used:

$$\sin(180^\circ - \theta) = \sin E \tag{13}$$

$$\cos(180^\circ - \theta) = -\cos E \tag{14}$$

From equations (7), (8), and (9), 0.1-sec velocity components are computed using the following relations:

$$W_{X_K} = \frac{1}{2\Delta t}\left(X_{c_{K+1}} - X_{c_{K-1}}\right) \tag{15}$$

$$H_K = \frac{1}{2\Delta t}\left(Y_{c_{K+1}} - Y_{c_{K-1}}\right) \tag{16}$$

$$Y_K = Y_{c_K} \tag{17}$$

where $\Delta t = 0.1$ since the data are equally spaced by 0.1 sec.

3. 1-Sec Velocity Calculations

1-sec velocity components, W_X (zonal), W_Z (meridional), H (rise rate), and Y (altitude) are computed from the 0.1-sec velocity components using a Martin-Graham low-pass filter. Fifty-five weights are applied over a 55-point interval so that the points are equally weighted on either side of the midpoint to produce a mirror image. For example, the weights for points 1 and 55 are the same, 2 and 54 are the same, etc. These weights were chosen since they provide a desirable frequency response. These weights are presented in Table 1.

TABLE 1. WEIGHTS USED TO OBTAIN SMOOTHED 1-SEC VELOCITY DATA

Points	Weight	Points	Weight
(1.55)	-0.00170115	(15.41)	0.00536330
(2.54)	-0.00335008	(16.40)	0.01109891
(3.53)	-0.00509943	(17.39)	0.01746935
(4.52)	-0.00685550	(18.38)	0.02431932
(5.51)	-0.00850874	(19.37)	0.03146420
(6.50)	-0.00993790	(20.36)	0.03869666
(7.49)	-0.01101528	(21.35)	0.04579480
(8.48)	-0.01161294	(22.34)	0.05253129
(9.47)	-0.01160935	(23.33)	0.05868300
(10.46)	-0.01089632	(24.32)	0.06404076
(11.45)	-0.00938586	(25.31)	0.06841865
(12.44)	-0.00701636	(26.30)	0.07166239
(13.43)	-0.00375300	(27.29)	0.07365641
(14.42)	0.00038329	(28.28)	0.07432916

The equations used to determine the 1-sec Y (altitude) and velocity components W_x (zonal), W_z (meridional), and H (rise rate) are the following:

$$Y_1 = \omega_{28} Y_{i+27} + \sum_{j=1}^{27} \omega_j (Y_{i-j+27} + Y_{i+j+27}) \tag{18}$$

$$Wx_1 = \omega_{28} Wx_{i+27} + \sum_{j=1}^{27} \omega_j (Wx_{i-j+27} + Wx_{i+j+27}) \tag{19}$$

$$Wz_1 = \omega_{28} WZ_{i+27} + \sum_{j=1}^{27} \omega_j (Wz_{i-j+27} + Wz_{i+j+27}) \tag{20}$$

$$H_1 = \omega_{28} H_{i+27} + \sum_{j=1}^{27} \omega_j (H_{i-j+27} + H_{i+j+27}) \tag{21}$$

where ω_j is the weights, j = 1, 2, ... 28 and i = 1, 11, 21 ..., etc.

4. Determination of Smoothing Interval

$$N = [3.56\ \sigma_{W_z}^2] \tag{22}$$

$$NW = 2\left[\frac{N+1}{2}\right] + 1 \tag{23}$$

The brackets indicate the integral portion of the quantity, $\sigma_{W_z}^2$ is the variance, and NW is the number of points in the interval over which the values are smoothed. The smoothing interval is allowed a maximum of 21.

5. Second Degree Least-Squares Curve Fit of Rise Rate

$$W_z = A_0 + A_1 t + A_2 t^2 \tag{24}$$

$$A_0 = \frac{1}{\left[M - \frac{A^2}{B}\right]} \sum_{i=-K}^{K} W_{z_i} \left[1 - i^2 \frac{A}{B}\right] \tag{25}$$

$$A_1 = \frac{1}{\Delta t A} \sum_{i=-K}^{K} i W_{z_i} \tag{26}$$

$$A_2 = \frac{1}{\Delta t^2 \left[M - \frac{A^2}{B}\right]} \sum_{i=-K}^{K} \left[i^2 \frac{M}{B} - \frac{A}{B}\right] W_{z_i} \tag{27}$$

where

$$M = 201$$

$$K = \frac{M-1}{2} = 100$$

$$AF = 2 \sum_{i=1}^{100} i^2 = 676{,}700$$

$$BF = 2 \sum_{i=1}^{100} i^4 = 4,\ 100,\ 666,\ 660$$

$$\frac{M}{B} = 0.490,\ 164,\ 2{,}017 \times 10^{-7}$$

$$\frac{A}{B} = 0.165,\ 021,\ 9{,}479 \times 10^{-7}$$

$$\left[M - \frac{A^2}{B} \right] = 89.329,\ 647,\ 84 \quad .$$

6. Smoothing of Altitude

1. Fit 200 consecutive values of W_Z to a second-degree polynomial.

2. Compute the variance of $W_Z (\sigma_{W_Z}{}^2)$ from

$$\sigma_{W_Z}{}^2 = \frac{1}{200} \sum_{i=1}^{200} (W_{Z_{iRAW}} - W_{Z_{icurvefit}})^2 \tag{28}$$

3. Compute $N = [3.56\ \sigma_{W_Z}{}^2]$ (brackets [ ] denote integer portion):

$$NW = 2\left[\frac{N+1}{2}\right] + 1 \qquad 3 \leqslant NW \leqslant 21 \tag{29}$$

4. Use NW to determine the size of the smoothing span for the next 201 – (NW – 1)/2 consecutive points. Then use the next 201 consecutive points to determine a new NW.

7. 5-m Velocity Computations

The procedure for deriving velocity data values as a function of height requires the use of interpolation. Accordingly, an initial value of altitude (which is a multiple of 5 m) is determined using the first smoothed 1-sec altitude value, and from that initial value the corresponding velocity components (zonal, meridional, rise rate) are computed using linear interpolation as a function of the time at which the altitude was reached. Similarly, the next altitude value is the previous value plus 5 m, etc. until 5-m velocity data have been computed from all the 1-sec velocity data.

A criterion for determining the first value of altitude used in computing 5-m data was developed to enable the 25-m data to be computed from the 5-m velocity data at integral multiples of 25 m. Once the initial 5-m altitude value has been determined, a table is made within the 1-sec data to find the nearest 1-sec altitude measurements surrounding the 5-m altitude value. The time of occurrence of the 5-m altitude is then computed using the relation:

$$T_5 = \frac{1}{Y1_n - Y1_{n-1}} \begin{vmatrix} t_{n-1} & Y1_{n-1} - Y1_5 \\ T_n & Y1_n - Y1_5 \end{vmatrix} \tag{30}$$

where $t_n = t_{n-1} + 1$ and $Z_{n-1} < Z_5 \leqslant Z_n$. Using T_5, the zonal, meridional, and vertical components associated with T_5 are computed from the following general relation:

$$f_5 = \frac{1}{t_n - T_{n-1}} \begin{vmatrix} f_{n-1} & t_{n-1} - T_5 \\ f_n & t_n - T_5 \end{vmatrix} \tag{31}$$

which reduces to:

$$f_5 = (f_n - f_{n-1})\,(T_5 - t_{n-1}) + f_{n-1} \tag{32}$$

since $t_n = t_{n-1} + 1$. The quantities f_n and f_{n-1} are values of the $\bar{W}_{x_1}$, $\bar{W}_{z_1}$, and H_1 1-second components surrounding f_5.

8. 25-m Velocity Calculations

Using 5-m wind velocity data as previously described, the 25-m velocity data may be computed. Thirty-nine weights are used to obtain 25-m velocity data using the Martin-Graham low-pass filter technique where points 1 and 39, points 2 and 38, etc., are equally weighted (Table 2). The general equations used in the Martin-Graham low-pass filter technique for the 25-m computations are as follows:

$$W_{z_{25}} = \sum_{j=1}^{m} \omega_j (W_{z_{5_{i-j+m}}} + W_{z_{5_{i+j1m}}}) + \omega_{m+1} W_{z_{5_{i+m}}} \tag{33}$$

$$H_{25} = \sum_{j=1}^{m} \omega_j (H_{5_{i-j+m}} + H_{5_{i+j+m}}) + \omega_{m+1} H_{5_{i+m}} \tag{34}$$

$$W_{x_{25}} = \sum_{j=1}^{m} \omega_j (\bar{W}_{x_{5_{i-j+m}}} + W_{x_{5_{i+j+m}}}) + \omega_{m+1} W_{x_{5_{i+m}}} \tag{35}$$

where ω_j is the weights j = 1, 2, ..., m+1 and where m = (number of weights/2) and [ ] denotes integral portion.

TABLE 2. WEIGHTS USED OVER A 39-POINT INTERVAL TO COMPUTE 25-m VELOCITY DATA

Points	Weight	Points	Weight
(1.39)	$0.31609500E^{-02}$	(11.29)	$-0.19400450E^{-01}$
(2.38)	$0.46590200E^{-02}$	(12.28)	$-0.11719670E^{-01}$
(3.37)	$0.54903200E^{-02}$	(13.27)	$0.24096200E^{-02}$
(4.36)	$0.50246700E^{-02}$	(14.26)	$0.22573790E^{-01}$
(5.35)	$0.27815200E^{-02}$	(15.25)	$0.47256220E^{-01}$
(6.34)	$-0.13689400E^{-02}$	(16.24)	$0.73969890E^{-01}$
(7.33)	$-0.70447600E^{-02}$	(17.23)	$0.99595700E^{-01}$
(8.32)	$-0.13284600E^{-01}$	(18.22)	$0.12087210E^{-00}$
(9.31)	$-0.18611820E^{-01}$	(19.21)	$0.13494444E^{00}$
(10.30)	$-0.21240690E^{-01}$	(20.20)	$0.13986549E^{00}$

9. Scalar Velocity Equations

Scalar velocity is computed by:

$$V_{25} = (W_{x_{25}}{}^2 + W_{z_{25}}{}^2)^{1/2} \tag{36}$$

Wind direction is computed by:

$$\phi \tan^{-1} \frac{W_x}{W_z} + \text{quadrant correction} \quad . \tag{37}$$

The quadrant correction is determined from the signs of W_x and W_z:

W_x+ W_z-	360 - 0	W_x- W_z+	180 - 0
W_x+ W_z+	0 + 180	W_x- W_z-	0 .

III. DATA ANALYSIS PROCESS

A. Introductory Remarks

For years the problem of wind (gust and turbulence) measurements for use in establishing design inputs for airplanes has been well-known and accepted. This continues to be a significant problem area for the airborne or cruise-type vehicles which do not change altitude very fast. However, for vertically or near vertically rising vehicles, the wind shear or wind profile, which defines the gross change in wind speed with altitude, is also of considerable importance in addition to the turbulence influence. Therefore, the problem is to measure and define the physical and statistical properties of wind profiles, wind shear, and turbulence for use as inputs to structural and control system design for aerospace vehicles and missiles. Although not simple, this problem for the larger aerospace vehicles, like the Space Shuttle, limits itself to a relatively few geographic locations. However, for military missiles and smaller research rockets, the design must take into account expected conditions at various potential launch sites.

The objective of this work was to develop a data base of paired detailed wind profiles for use in evaluating STS ascent capability. To insure Shuttle ascent capability through the winds aloft present on the day of launch, flight is simulated through a sequence of measured detailed wind profiles. Detailed profiles are required because the Shuttle responds to small-scale wind features that are not present in rawinsonde data. From the simulations, the wind effects on loads and performance can be predicted. However, wind measurement and simulation time requirements dictate that the launch decision be based on a wind measured about 3.5 hr before launch. It is to account for possible load increases due to wind profile changes during these last 3.5 hr before launch that the data base of paired detailed profiles is needed.

Inflight winds constitute the major atmospheric forcing function in space vehicle and missile design and operations. A frequency content of the wind profile near the bending mode frequencies or wind shear with the characteristics of a step input may exceed the vehicle structural capabilities (especially on forward stations for the small-scale variations of the wind profiles). Wind profiles with high speeds and shears exert high structural loads at all stations on a large space vehicle, and when the influences of bending dynamics are high, even a profile with low speeds and high shears can create large loads [13].

Because of the possibility of launch into unknown winds, operational missile systems must accept some inflight risk loss in exchange for a rapid-launch capability. But research and development missiles, and space vehicles in particular, cost so much that the overall success of a flight outweighs the considerations of launch delays caused by excessive inflight wind loads. If the exact wind profile could be known in advance, it would be a relatively simple task to decide upon the launch date and time. However, there is little hope of accurately forecasting the detailed wind profile very much into the future.

Over the years, therefore, emphasis has been placed increasingly on prelaunch monitoring of inflight winds. Now, finally, prelaunch profile monitoring techniques essentially preclude the risk of launching a space vehicle or research and development missile into an inflight wind condition that would cause it to fail. The potential variability of the wind profile up to 12 hr prior to launch plays an important role in assessments relative to launch decisions.

The FPS-16 Radar/Jimsphere System is routinely used in the prelaunch wind monitoring of NASA Space Shuttle missions. The accuracy of the highly detailed profile data provided by this system is discussed by Susko and Vaughan [14]. The resolution of these data permits calculating the structural

loads associated with the first bending mode and generally the second mode of missiles and space vehicles during the critical high dynamic pressure phase of flight. This provides better than an order of magnitude accuracy improvement over the conventional rawinsonde wind profile measuring system.

Beginning about 12 hr before each STS launch, an intensive wind monitoring activity is begun. During this prelaunch period, load calculations are made at about 3.5-hr intervals for all critical vehicle structures by means of ascent simulations using an updated wind profile for each case. These calculated loads are then compared against red-line (upper limit) load values to insure ascent capability. It is in the establishment of the red-line values that the pairs of detailed profiles come into play. The not-to-be-exceeded load of each structure must be reduced by some factor, depending upon wind variability, to account for possible wind profile changes during the time between the last ascent simulation and launch. At present, this time is 3.5 hr. To determine the amount of reduction required (called "knockdown load"), each structural load is calculated at frequency altitude intervals from each profile of each pair. The 99 percent change in load from all pairs has been used as the knockdown load for that structure.

B. System Description

The FPS-16 Radar/Jimsphere System winds data are obtained by a method of tracking a super-pressure aluminized mylar sphere with the FPS-16 radar. The sphere is a passive target and contains no instrumentation. The position of the sphere is obtained in space at intervals of 0.1 sec and processed to obtain wind speeds averaged over approximately 50 m in altitude and given at 25 m altitude intervals.

Because of the low inertia of the balloon (weight of the balloon excluding gas is approximately 400 grams) and high drag characteristics, it responds readily to changes in the small-scale features of the wind field. This rapid response of the sensor combined with the superior tracking capabilities of the FPS-16 radar provide wind speeds with an RMS vector error of generally less than 0.5 $msec^{-1}$. This was determined from simultaneous radar tracks of the same balloon. Rawinsonde (GMD-1) measured wind speeds are averaged over approximately 600 m in the vertical direction and have an RMS vector error ranging between approximately 2 and 15 $msec^{-1}$ depending upon the wind speed. Thus, the altitude resolution and accuracy of the wind velocity profile as measured by the FPS-16 radar/jimsphere method are an order of magnitude better than those measured by the rawinsonde system.

The jimsphere wind sensor was used in measuring the detailed wind profiles presented in this document. The jimsphere (Fig. 3) is a 2-m diameter super-pressure aluminized mylar sphere with 398 conical roughness elements, which are approximately 7.62 cm in diameter at the base and 7.62 cm high, randomly spaced over the surface of the sphere. The roughness elements, combined with a mass of 100 grams is sewed into the load patch to provide a displacement of the center of mass, aerodynamic stability, and large drag. Although this design eliminated a large part of the aerodynamically induced motions, the jimsphere still contains a spiral mode of oscillations with a period of approximately 4.5 sec as revealed by Doppler radar. The oscillation is not believed to be of significance in measuring winds for two reasons: (1) the FPS-16 radar does not measure these motions accurately, and (2) the radar position coordinates are smoothed over 4 sec in time, which would eliminate the spiral motion.

C. Analysis

While the main concern was to develop a data base for the 3.5-hr knockdown loads, it was considered desirable to develop 7-hr and 10.5-hr pairs since load simulations are performed at those times, also.

The following guidelines used in selecting the pairs of profiles were established to insure a valid and representative data base:

Step 1. Each pair must be separated by greater than 24 hr (to eliminate light or strong wind bias).

Step 2. Each profile must reach greater than 15 km altitude.

Step 3. Eliminate profiles exhibiting excessive noise and wind points.

Step 4. Distribute the number of profiles evenly over months and years.

Step 5. Times between profiles of a pair must be within ±1 hr of the specified pair time.

It was immediately apparent that there were not enough profiles to provide a reasonable data base for each month. All jimsphere profiles are listed in NASA CR-161664 [15]. Consequently, months exhibiting similar wind profile statistics were grouped according to seasons. Winter included December 15 through April 15, summer extended from June through September, and transition season included all other months.

The vector wind value at each 25-m interval on each profile was converted to component values (u and v). Differences (Δu and Δv) in 3.5-, 7-, and 10.5-hr components were determined, and from these data standard deviations of the differences (σu and σv) were calculated.

Any particular value of σu and σv may have evolved from several different possible changes in the profile. Two obvious changes are an increase or a decrease in the wind speed, and/or a change in the wind direction. To a certain degree, these types of changes, if occurring over a broad enough layer (several km), may lend themselves to being predicted from analysis of synoptic data. However, predicting the trend and not the detail is the best that can be expected. Another frequently noted profile change occurs when a small-scale feature, less than 1 km in thickness, appears to move up or down in location on a profile thereby creating the effect at a specific location of a decrease or increase in speed and/or a change in wind direction.

Figure 6 presents σu profiles for the three defined seasons for 3.5-, 7-, and 10.5-hr time changes. Figure 7 presents σv profiles for the same set of conditions. The curves have been necessarily smoothed to eliminate profile variations resulting from the sample size. The effect of smoothing is to accentuate the most important features of the profiles. For example, on Figure 6 the σu values for 3.5-hr changes are greatest in the winter and smallest in the summer. Also, σu increases in magnitude from about 1 km altitude to about 12 km and decreases above the peak σu altitude.

σu values for 3.5 hr at 12 km, for example, show an 8 percent increase from the transition case to the winter case and about an 18 percent decrease from the transition case to the summer case. The variation is even larger at some other altitudes. The general profile trends and shapes discussed above can also be applied to σu for 7 to 10.5 hr. In all cases shown, the peak in the σu profile correlates well with the altitude of the maximum wind speed, and this effect becomes more pronounced as the time interval increases to 10.5 hr.

σv data shown on Figure 7 reflect similar relationships relative to the seasons and time intervals as have already been noted for σu. An analysis of σv for 3.5-hr changes, for example, shows that this standard deviation increases about 12 percent between the transition and winter cases at 12 km altitude while the change in σv from the transition to the summer season shows a decrease of 17 percent. A special feature of Figure 7 for the 7- and 10.5-hr cases is that σv increases by as much as 30 percent from the transition to the winter profile. This is particularly true for altitudes below 12 km. This large increase does not appear in the σu data.

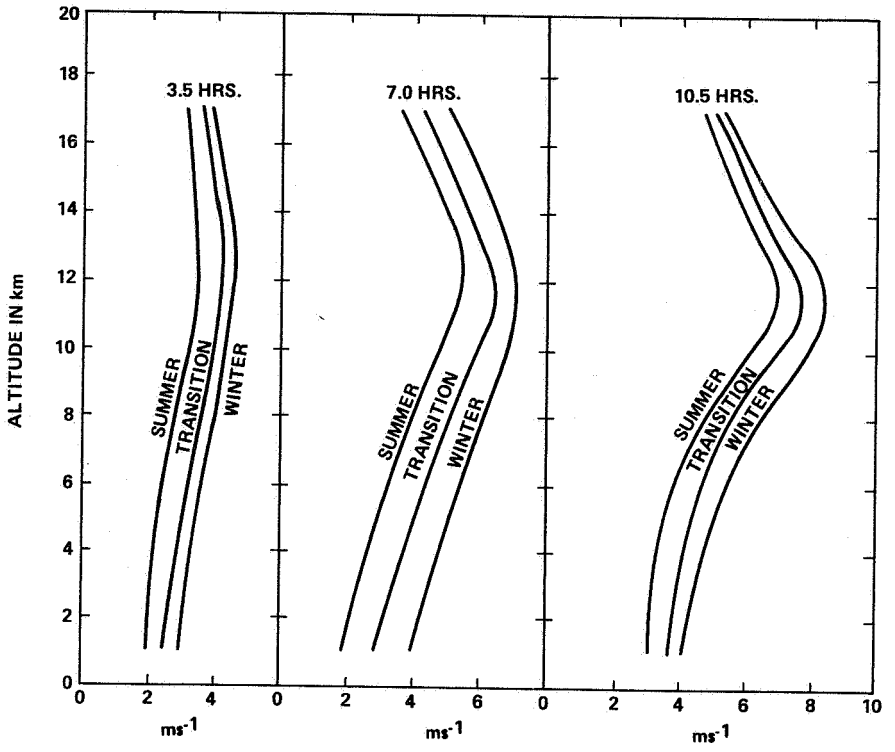

Figure 6. Standard deviation of the u component from paired profile differences for given seasons and time intervals.

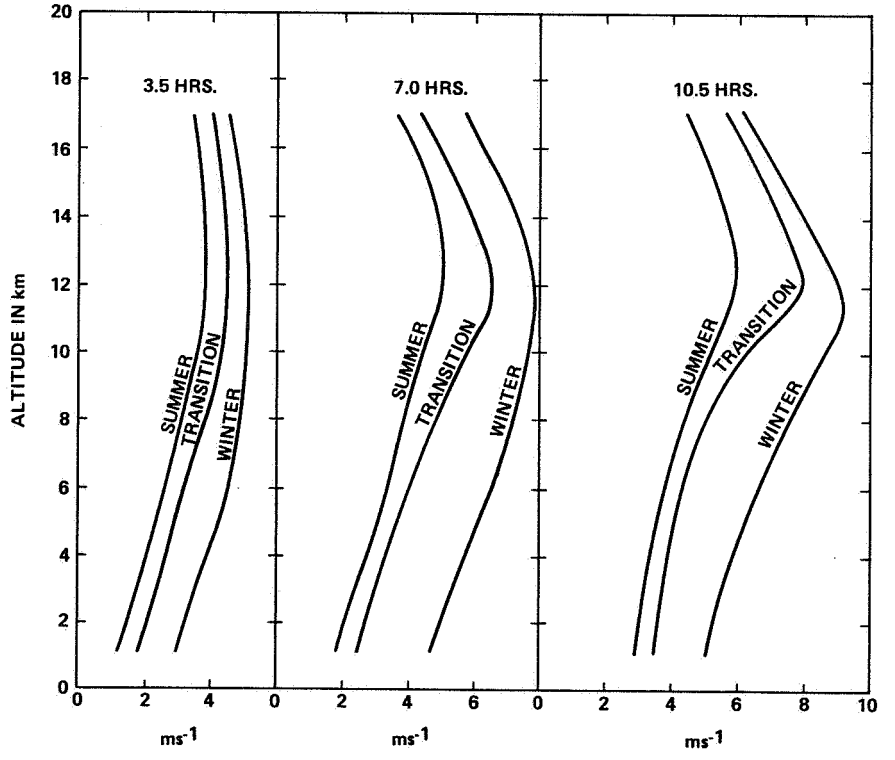

Figure 7. Standard deviation of the v component from paired profile differences for given seasons and time intervals.

A comparison has been made between the calculated 99 percent 3.5-hr changes in wind speed components and the 3.5-hr component changes actually observed during the final 12 hr prior to launch for 10 Space Shuttle missions (STS-2, -3, -4, -5, -6, -7, -8, -9, -11, and -13). An example of jimsphere data used is presented in Figure 8 as obtained at 0200 GMT, November 12, 1981, during the STS-2 pre-launch period. Wind speed, wind direction, and in-plane and out-of-plane component profiles utilized in this research were also used in post-flight evaluations fo all STS missions [16-25].

The in-plane wind component is defined as a wind vector in either the same direction (+) as the vehicle launch azimuth or in the opposite (–) direction. The out-of-plane component is defined as a wind component directed either from the right (+) or from the left (–) with respect to the launch azimuth. The ±in-plane or ±out-of-plane terms are interchangeable with head (+) or tail (–) wind and left (–) or right (+) crosswinds, respectively.

The wind component differences (±u or ±v) associated with the referenced STS data set for Δ3.5-hr intervals were determined from the appropriate in-plane (±u) and out-of-plane (±v) data. Figure 9 is an example of a plot of a basic data set. The u and v components are normally defined as east/west and north/south, respectively. However, operationally the component u is along the flight azimuth and the v component is perpendicular to the flight path. Seven of the launch studies had a flight azimuth of approximately 90 deg east of north; however, STS-2 and STS-3 were launched on a 60 deg east of north launch azimuth and STS-9 was launched 35 deg east of north. Therefore, in only three cases was it necessary to recompute u and v from the standard meteorological coordinates to take into account the actual flight azimuth of the vehicle.

Although only the 3.5-hr component differences are of concern to the launch decision process, the 7- and 10.5-hr differences are also considered because they correspond to important operational decision points in the countdown. The temporal character of mesoscale perturbations in the troposphere has been investigated by Vaughan [26]. The 99 percent wind component changes for u and v over periods greater than 3.5 hr are presented on Figures 10 and 11 to illustrate the rapid increase which can occur in the wind. These data were calculated from the 1σ values of u and v for the 12 km altitude during the three defined seasons as presented on Figures 6 and 7. Because the wind component changes can almost double, as seen from a comparison of the 3.5- and 10.5-hr 1σ values, it is essential that the final launch decision relative to ascent loads calculations is made as close as possible to the liftoff time. This requirement attempts to minimize the load uncertainties due to wind variability. The magnitude of this wind variability is presented on Figure 11 for the v component during the winter which shows that at the 1 percent risk level the increase in the 3.5-hr change and 10.5-hr change amounts to almost 78 percent. Vector wind changes over periods greater than or equal to 12 hr have been studied by Adelfang [27-29]. Vector wind models have been developed which discuss wind shear statistics for both Cape Kennedy, Florida, and Vandenberg Air Force Base, California [7].

An example of the u and v differences over 3.5 hr given in Figure 9 were compared to the calculated 99 percent values calculated from values in Figures 6 and 7. This particular case, STS-2, shows the largest 3.5-hr Δu component exceedence observed in the 10 cases studied. This STS-2 mission data case from the transition season produced a 3.5-hr change of 22 m/s in the u component compared to the calculated 99 percent value in Figure 6 of 9.3 m/s at an altitude of 10,500 m. The v component change of 11 m/s at 9,500 m for this same case only slightly exceeded the 99 percent value of 10 m/s from Figure 7. The other 22 observed u and v difference profiles given in the appendix were compared with calculated 99 percent values from the appropriate seasonal data, i.e., summer, winter, or transition.

A discussion of the actual operational implications of these data is needed. Several factors affect whether the wind component change is critical to a go/no-go recommendation relative to launch. First, wind changes are only of critical importance to the Space Shuttle loads calculations in the 6 to 14 km

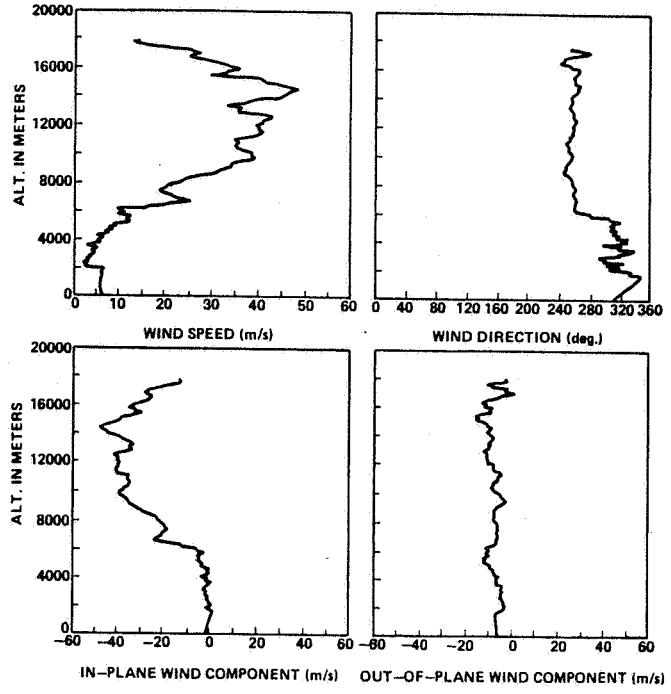

Figure 8. STS-2 prelaunch/launch jimsphere profiles of wind speed, wind direction, in-plane and out-of-plane wind components, 0200 GMT November 12, 1981.

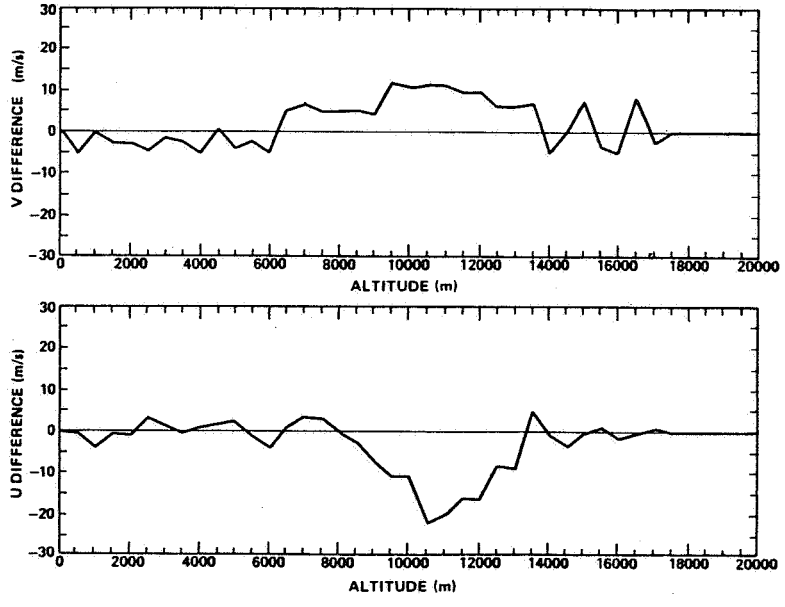

Figure 9. Jimsphere-measured wind component changes (u,v) observed at Kennedy Space Center, Florida, between 1130 GMT and 1558 GMT November 12, 1981, during NASA's STS-2 countdown.

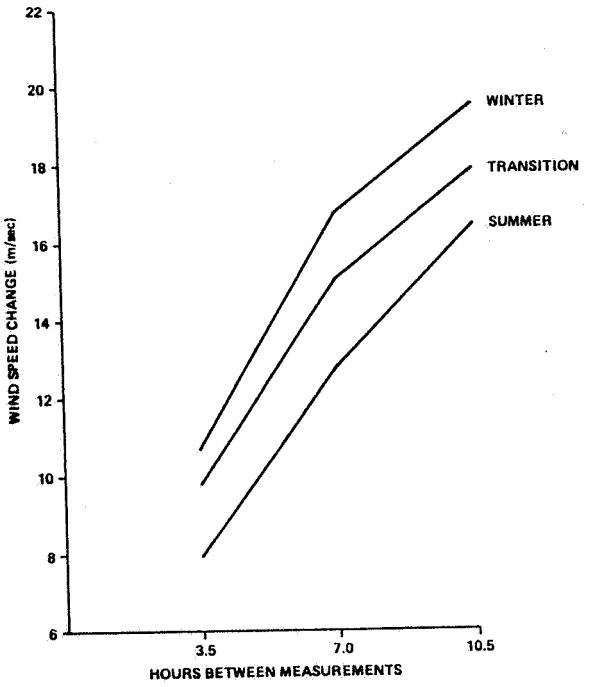

Figure 10. One percent risk of u wind component change at 12 km altitude for Kennedy Space Center, Florida.

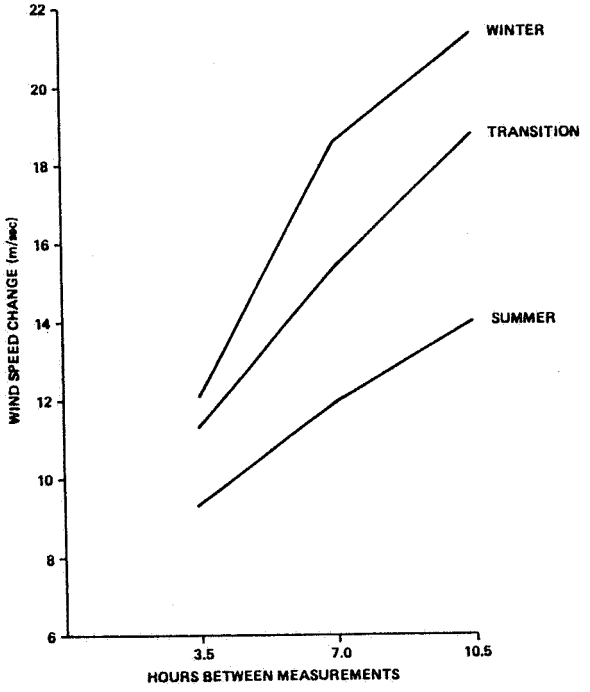

Figure 11. One percent risk of v wind component change at 12 km altitude for Kennedy Space Center, Florida.

layer. Second, a particular wind component change may be important to loads depending on the exact altitude of occurrence and the severity of the wind speed and shear profiles which existed prior to the change. Third, if the Δ change amounts to a large reduction in shear, then the effect may be a relief in loads rather than an increase. Further, if the large change observed in Figure 9 occurred at an altitude where the vehicle was not sensitive to this change, then the change will not be a critical factor. Also, if the change occurs in conjunction with overall wind speed and wind shear profiles which are less severe than expected, then the effect of a component change greater than the 99 percent value may be minimized relative to load measurements. It is also possible that a wind component change over a relatively small layer, for example 150 m, may not be important if the vehicle does not respond critically to wavelengths of this size.

There are 23 cases of u and v profile differences presented; however, it is of value in this study to concentrate on only the 8 cases which qualify as independent as defined by criteria discussed earlier. The remaining 15 cases verify data on Figures 10 and 11 relative to time periods greater than 2.5 hr. It is also seen that small perturbations or gusts which affect one measurement period may ge gone the next. Gust characteristics have been studied by Adelfang, Evans, and Smith [30,31].

Since the knockdown loads discussed earlier are directly related to wind changes over 3.5-hr periods immediately prior to launch, it is of importance to choose the L-3.5 to L-0 hr data for analysis. An example of the knockdown load effects is presented on Figure 12. The effect of wind change on the overall load calculations for a particular element on a vehicle is considered along with other effects unrelated to wind. The value of each individual effect is evaluated with many other effects using the root-sum-square procedure. Therefore, an increase of 60 percent, for instance, in the wind component effect in this example, results in only a 19 percent increase in total loads in this example. However, the wind variability is still the only real-time change affecting loads calculations and is, therefore, of great importance to the launch decision process.

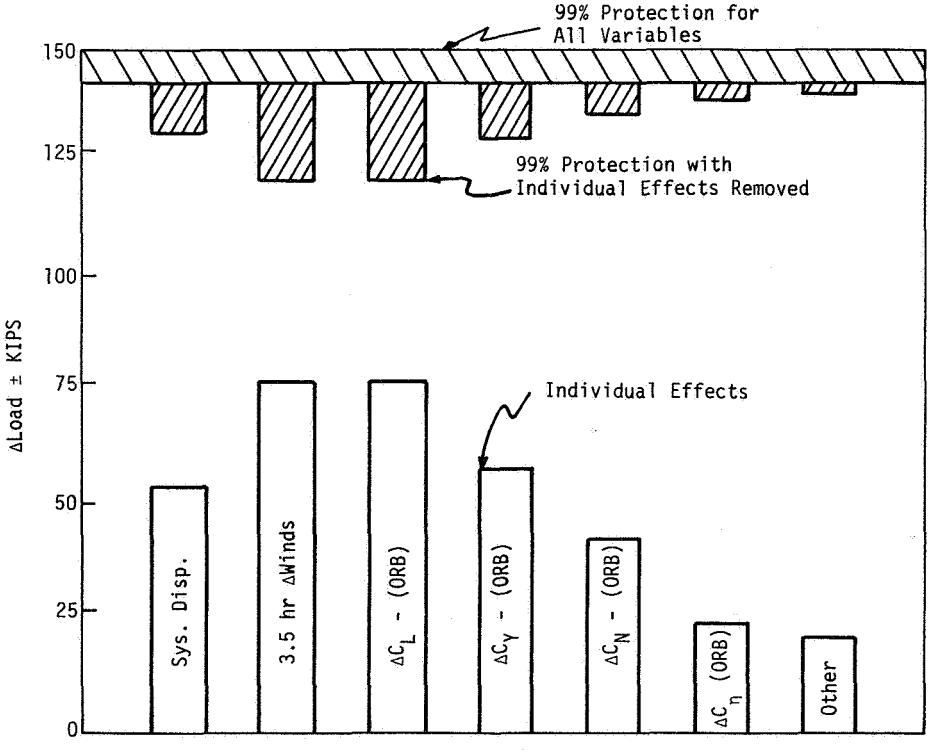

Figure 12. Knockdown load effects example.

An analysis has been conducted in which the appropriate 99 percent values were compared with individual 3.5-hr differences of u and v components. Results indicate that exceedence of the 99 percent values occurred in STS-2, -5, and -11. However, only in the Δu component was the exceedence considered significant. Both the STS-5 and STS-11 cases were examples of relaxation or relief in shear, thereby, producing potential load relief. Diminishing shear magnitudes, however, caused by either wind speed or direction changes from one time period to the next do not always produce potential relief of ascent loads. Sometimes a reduction in the component profile at one altitude produces greater shear values in the layer immediately above or below by adding to existing shears. No significance can be attached to a find that only one exceedence in the Δu component and none in the Δv occurred in the 10 shuttle cases. Overall confidence in the values selected for calculating knockdown loads may improve when either the 50 sample per season statistical base is increased and/or the statistical sample of actual launch cases increases significantly.

This research effort will be expanded to cover the Vandenberg Air Force Base, California, Space Shuttle launch site. Comparisons will be made between the Kennedy Space Center and Vandenberg Air Force Base wind component changes determined from comparable wind profile pairs of data sets.

IV. CONCLUSIONS

1) Jimsphere/FPS-16 radar high resolution data used for this research contain the detail and accuracy required to determine wind component change statistics which can be used in space vehicle ascent capability studies.

2) There is significant variability in the u and v wind components observed at intervals of 3.5 hr, 7 hr, and 10.5 hr for the defined seasons at Kennedy Space Center, Florida.

3) The u and v wind components can vary during a period of 3.5 hr by more than 20 percent when comparing the transition season to the winter season. Somewhat smaller changes occur between the transition season and the summer season.

4) The largest component wind changes occur where the strongest wind magnitudes are present in the winter at approximately the 12-km altitude. At that altitude, for example, there is a 1 percent risk that the u wind component speed will exceed approximately 10 $msec^{-1}$ in 3.5 hr.

5) At the 1 percent risk level the difference between the 3.5-hr and 10.5-hr winter v component change is almost 80 percent.

6) Only one of ten STS launch cases studied produced a significant wind component exceedence at the 1 percent risk level.

7) Since current Space Shuttle knockdown loads calculations are based on transition season data, the seasonal differences shown by this research should be further assessed for potential impact to knockdown loads and prelaunch loads simulation results.

REFERENCES

1. Secretariat, Range Commanders Council: Range Reference Atmosphere Documents. IRIG Document No. 104-63, White Sands Missile Range, New Mexico, 1963.

2. Vaughan, William W.: Interlevel and Intralevel Correlations of Wind Components for Six Geographical Locations. NASA TN D-561, December 1960.

3. Turner, Robert E., and Hill, Charles K.: Terrestrial Environment (Climatic) Criteria Guidelines for Use in Aerospace Vehicle Development, 1982 Revision. NASA TM 82473, June 1982.

4. West, George, and Smith, R. E.: Shuttle and Planetary Environment Criteria Guidelines for Use in Space Vehicle Development. Volume I, NASA TM 82478, January 1983.

5. West, George, and Smith, R. E.: Space and Planetary Environment Criteria Guidelines for Use in Space Vehicle Development. Volume II, NASA TM 82501, June 1983.

6. Newberry, C. W., and Eaton, K. J.: Wind Loading Handbook. Building Research Establishment Report, Her Majesty's Stationary Office, 1974.

7. Smith, O. E.: Vector Wind and Vector Wind Shear Model 0 to 27 km Altitude for Cape Kennedy, Florida, and Vandenberg AFB, California. NASA TM X-73319, July 1976.

8. Etkin, Bernard: Dynamics of Atmospheric Flight. New York: John Wiley and Sons, Inc., 1972.

9. Barr, N. M., Gangsaas, Daginn, and Schaeffer, D. R.: Wind Models for Flight Simulator Certification of Landing and Approach Guidance and Control Systems. Report No. FAA-RD-74-206, U.S. Department of Transportation, Federal Aviation Administration, Washington, D.C., December 1974.

10. DeMandel, R. E., and Krivo, S. J.: Characteristics and Processing of FPS-16/Jimsphere Raw Radar Data. NASA CR 61290, May 1969.

11. Scoggins, James R.: An Evaluation of Detailed Wind Data as Measured by the FPS-16 Radar/Spherical Balloon Technique. NASA TN D-1572, May 1963.

12. DeMandel, R. E., and Krivo, S. J.: Capability of the FPS-16 Radar/Jimsphere System for Direct Measurement of Vertical Air Motions. NASA CR 61232, June 1968.

13. Ryan, Robert S., Scoggins, James R., and King, Alberta W.: Use of Wind Shears in the Design of Aerospace Vehicles. Journal of Spacecraft and Rockets, 4(11):1526-1532, November 1967.

14. Susko, Michael, and Vaughan, William W.: Accuracy of Wind Data Obtained by Tracking a Jimsphere Wind Sensor Simultaneously with Two FPS-16 Radars. NASA TM X-53752, July 1968.

15. Willett, J. A.: Summary of Jimsphere Wind Profiles–Programs, Data, Comments. NASA CR 161664, March 1979.

16. Johnson, D. L., and Brown, S. C.: Atmospheric Environment for Space Shuttle (STS-2) Launch. NASA TM 82463, December 1981.

17. Johnson, D. L., and Brown, S. C.: Atmospheric Environment for Space Shuttle (STS-3) Launch. NASA TM 82480, April 1982.

18. Johnson, D. L., Hill, C. K., and Batts, G. W.: Atmospheric Environment for Space Shuttle (STS-4) Launch. NASA TM 82498, July 1982.

19. Johnson, D. L., Hill, C. K., and Batts, G. W.: Atmospheric Environment for Space Shuttle (STS-5) Launch. NASA TM 82515, March 1983.

20. Johnson, D. L., Hill, C. K., and Batts, G. W.: Atmospheric Environment for Space Shuttle (STS-6) Launch. NASA TM 82529, May 1983.

21. Johnson, D. L., Hill, C. K., and Batts, G. W.: Atmospheric Environment for Space Shuttle (STS-7) Launch. NASA TM 82542, July 1983.

22. Johnson, D. L., Hill, C. K., and Batts, G. W.: Atmospheric Environment for Space Shuttle (STS-8) Launch. NASA TM 82560, October 1983.

23. Johnson, D. L., Hill, C. K., and Batts, G. W.: Atmospheric Environment for Space Shuttle (STS-9) Launch. NASA TM 82572, January 1984.

24. Johnson, D. L., Hill, C. K., and Batts, G. W.: Atmospheric Environment for Space Shuttle (STS-11) Launch. NASA TM 82580, March 1984.

25. Johnson, D. L., Hill, C. K., Jasper, G., and Batts, G. W.: Atmospheric Environment for Space Shuttle (STS-13) Launch. NASA TM 82588, May 1984.

26. Vaughan, William W.: An Investigation of the Temporal Character of Mesoscale Perturbation in the Troposphere and Stratosphere. NASA TN D-8445, March 1977.

27. Adelfang, Stanley I.: Analysis of Vector Wind Change with Respect to Time for Cape Kennedy, Florida. NASA CR 150779, August 1978.

28. Adelfang, Stanley I.: Analysis of Vector Wind Change with Respect to Time for Vandenberg Air Force Base, California. NASA CR 150776, August 1978.

29. Adelfang, Stanley I.: Analysis of Wind Bias Change with Respect to Time at Cape Kennedy, Florida, and Vandenberg AFB, California. NASA CR 150777, August 1978.

30. Adelfang, Stanley I., and Evans, Beverly: Vector Wind Profile Gust Model. CSC Contractor Report for NASA Marshall Space Flight Center, Alabama, April 1980.

31. Adelfang, Stanley I., and Smith, O. E.: Vector Wind Profile Gust Model. NASA TM-32441, August 1981.

APPENDIX

Figures A-1 through A-66 are additional data used in the analyses of wind profile pairs in this investigation.

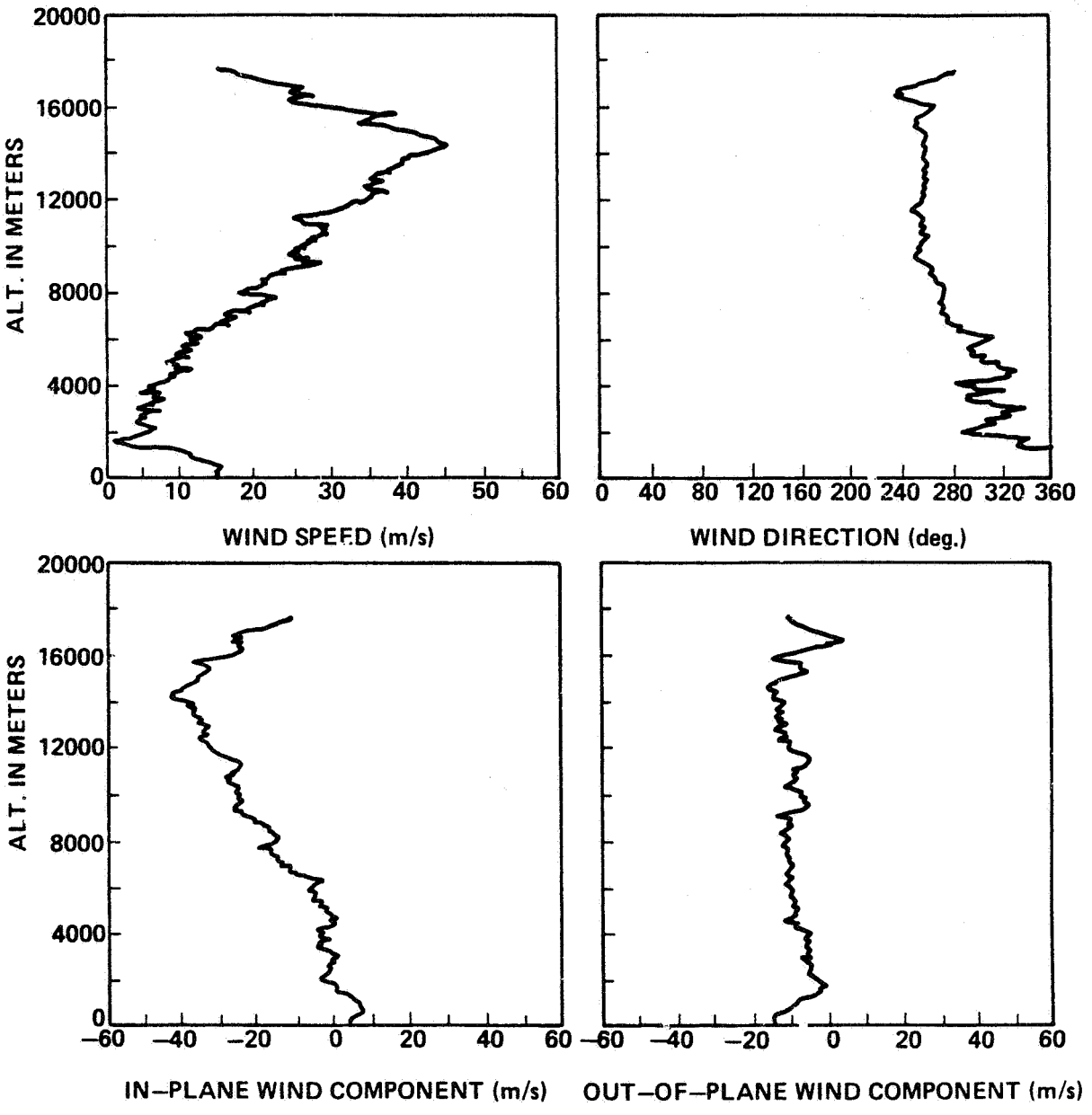

Figure A-1. STS-2 prelaunch/launch jimsphere profiles of wind speed, wind direction, in-plane and out-of-plane wind components, 0430 GMT November 12, 1981.

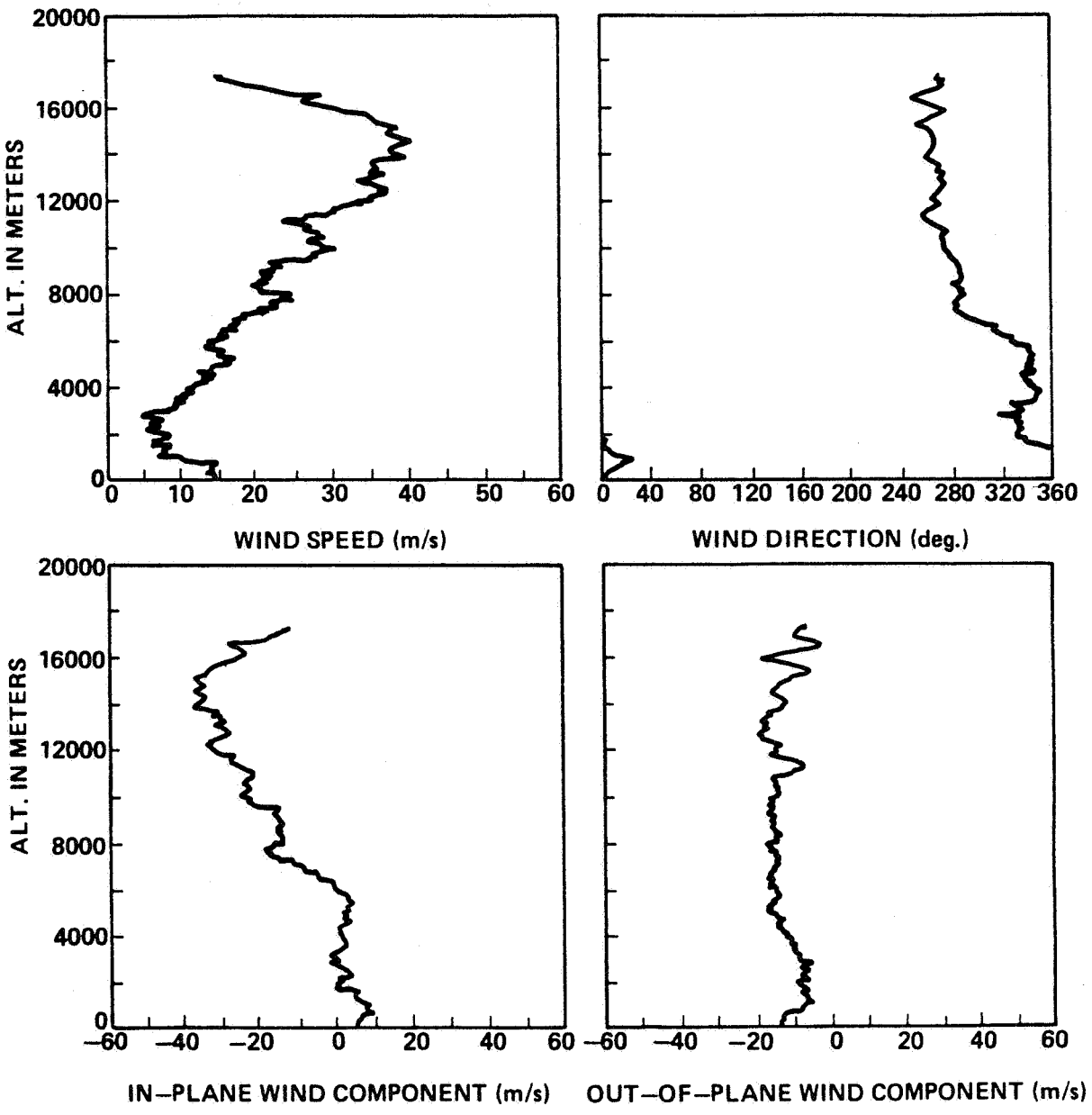

Figure A-2. STS-2 prelaunch/launch jimsphere profiles of wind speed, wind direction, in-plane and out-of-plane wind components, 0800 GMT November 12, 1981.

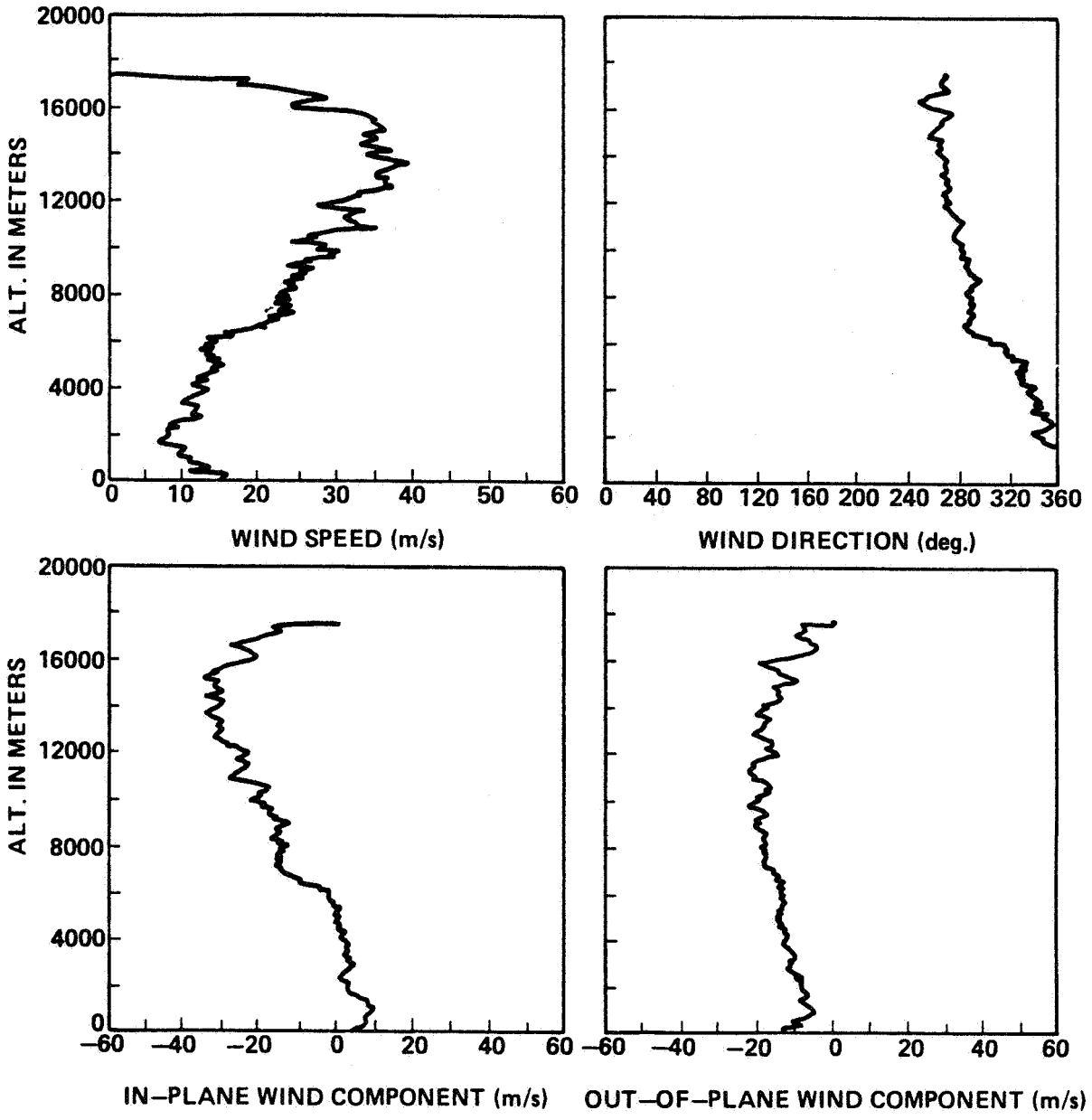

Figure A-3. STS-2 prelaunch/launch jimsphere profiles of wind speed, wind direction, in-plane and out-of-plane wind components, 1130 GMT November 12, 1981.

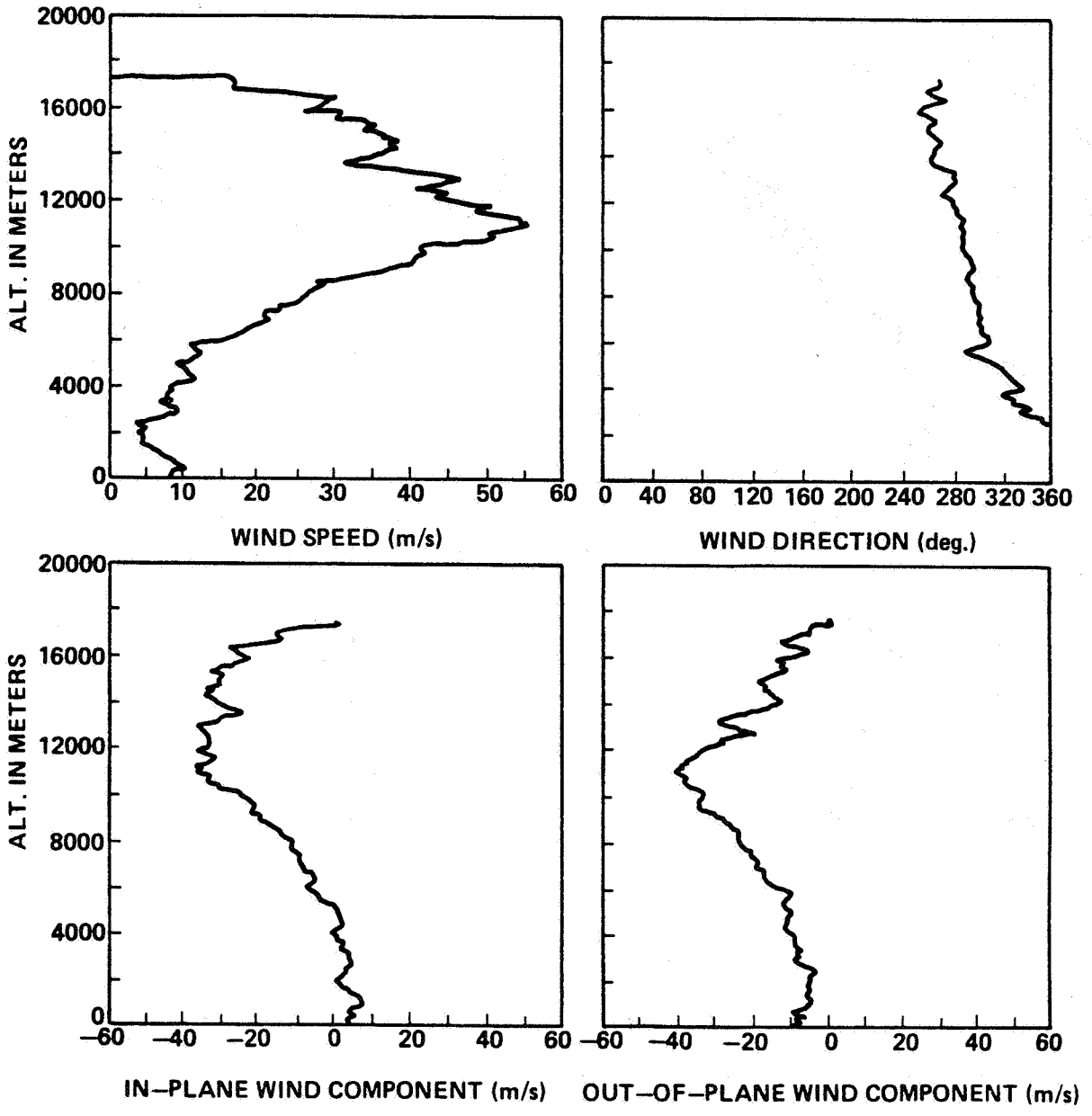

Figure A-4. STS-2 prelaunch/launch jimsphere profiles of wind speed, wind direction, in-plane and out-of-plane wind components, 1558 GMT November 12, 1981.

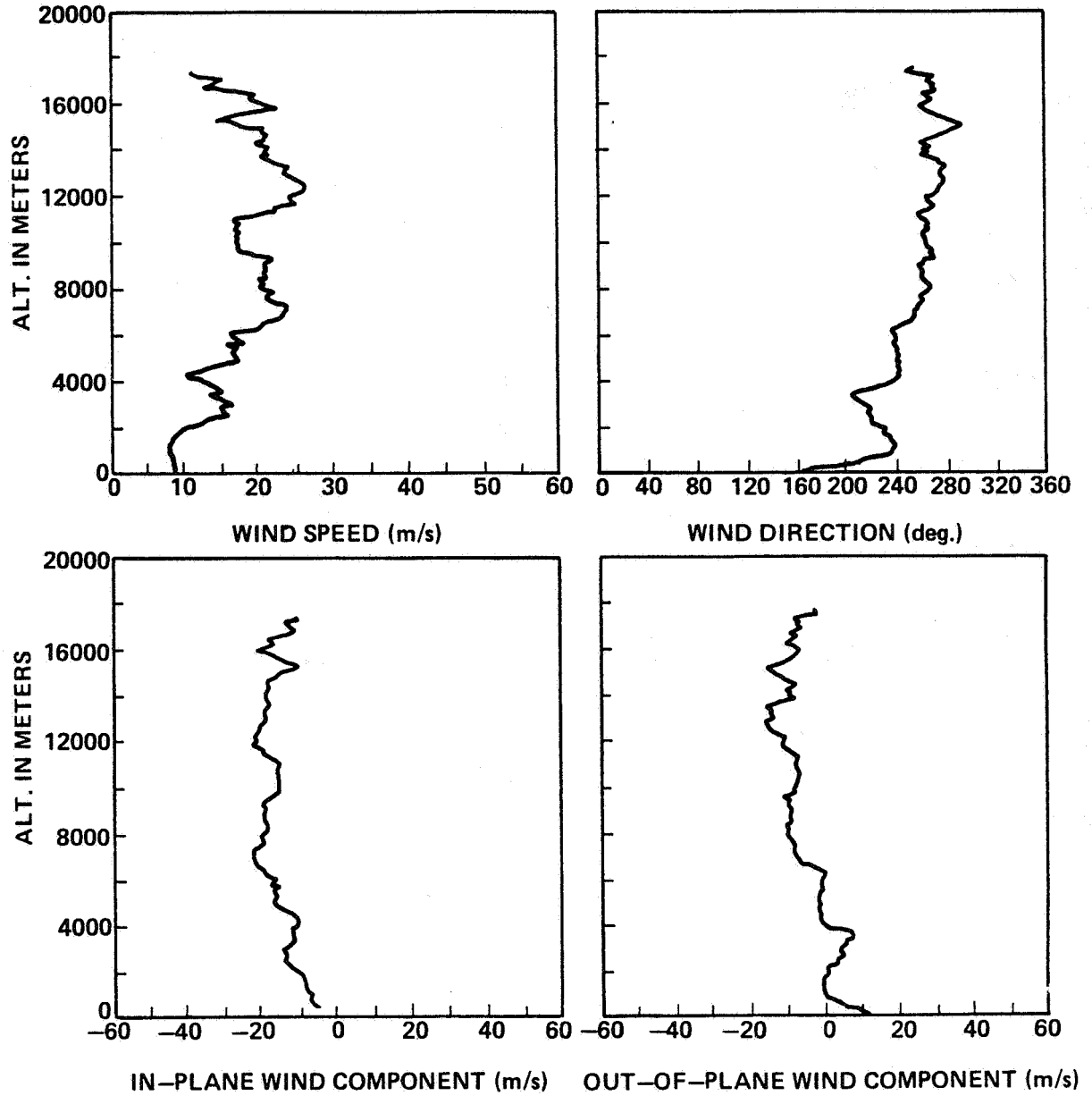

Figure A-5. STS-3 prelaunch/launch jimsphere profiles of wind speed, wind direction, in-plane and out-of-plane wind components, 0200 GMT March 22, 1982.

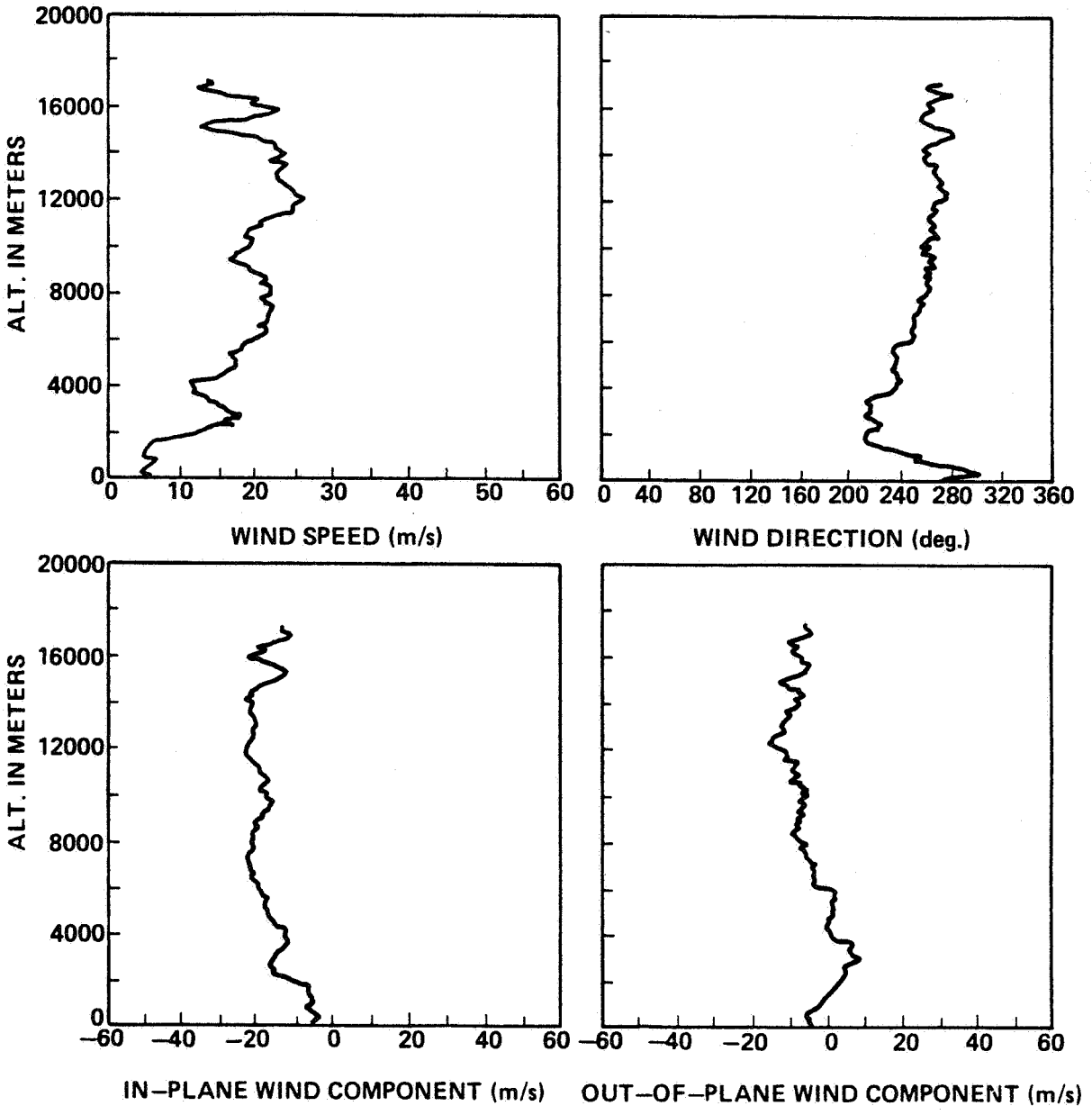

Figure A-6. STS-3 prelaunch/launch jimsphere profiles of wind speed, wind direction, in-plane and out-of-plane wind components, 0430 GMT March 22, 1982.

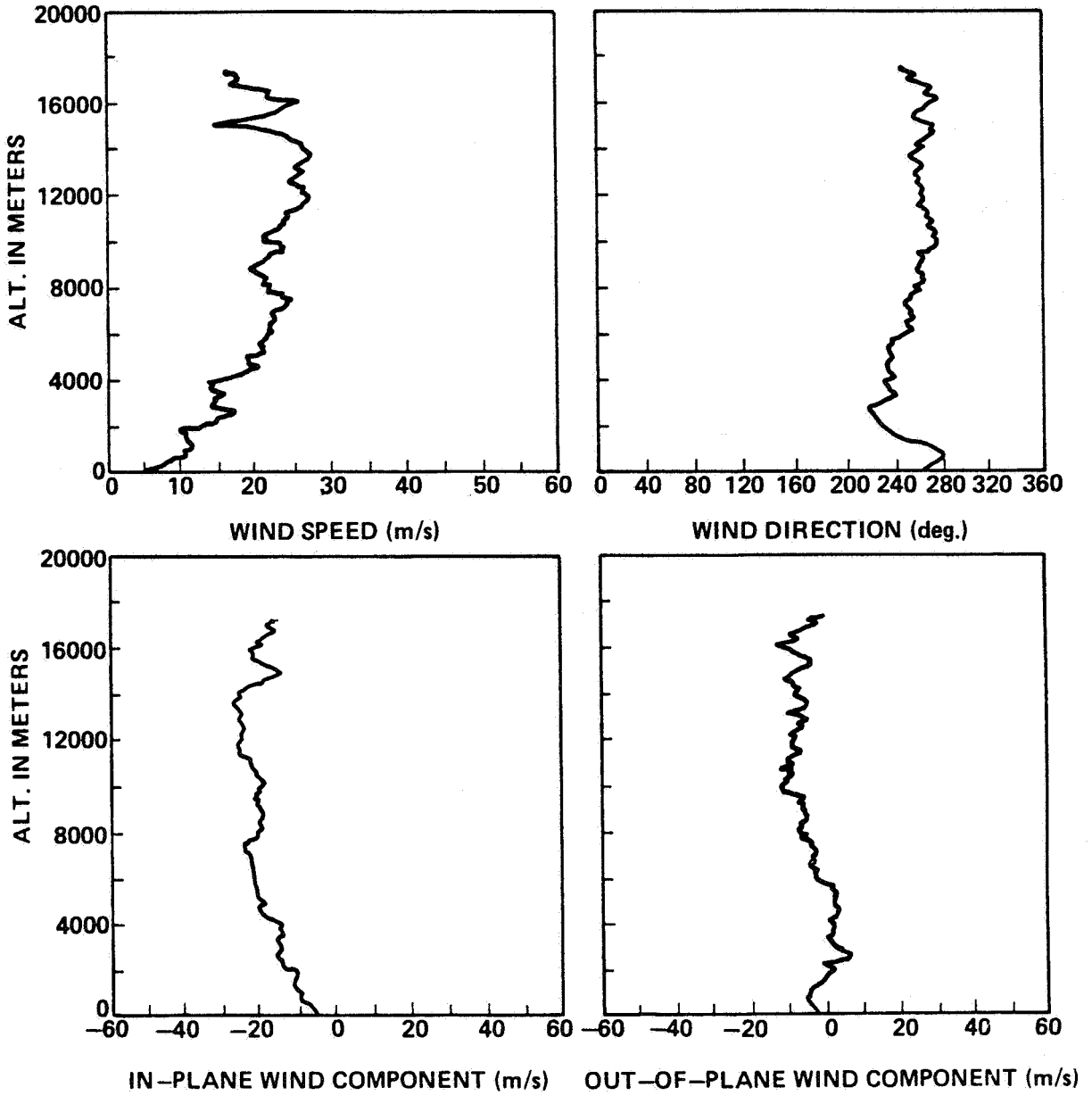

Figure A-7. STS-3 prelaunch/launch jimsphere profiles of wind speed, wind direction, in-plane and out-of-plane wind components, 0800 GMT March 22, 1982.

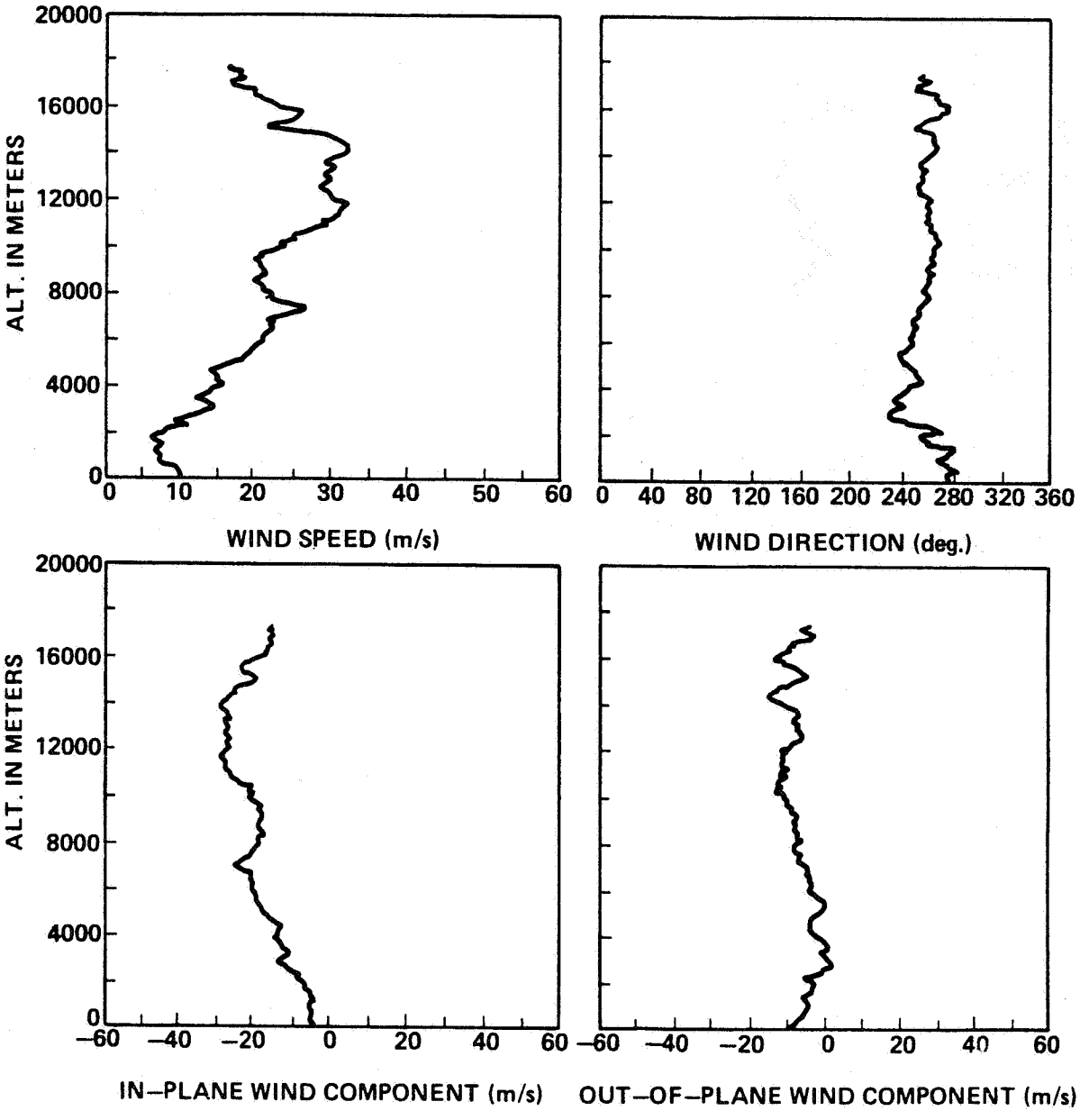

Figure A-8. STS-3 prelaunch/launch jimsphere profiles of wind speed, wind direction, in-plane and out-of-plane wind components, 1230 GMT March 22, 1982.

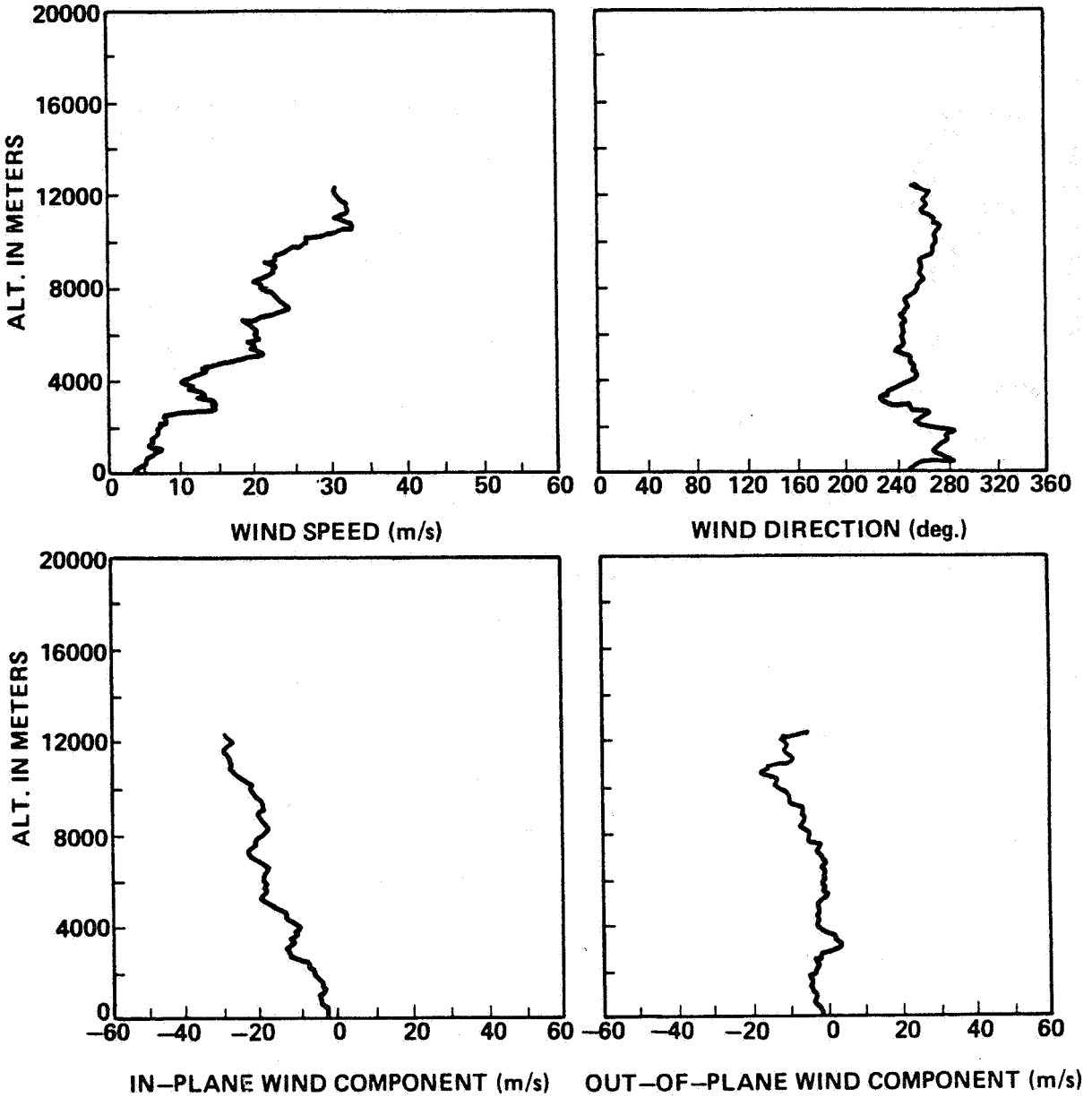

Figure A-9. STS-3 prelaunch/launch jimsphere profiles of wind speed, wind direction, in-plane and out-of-plane wind components, 1417 GMT March 22, 1982.

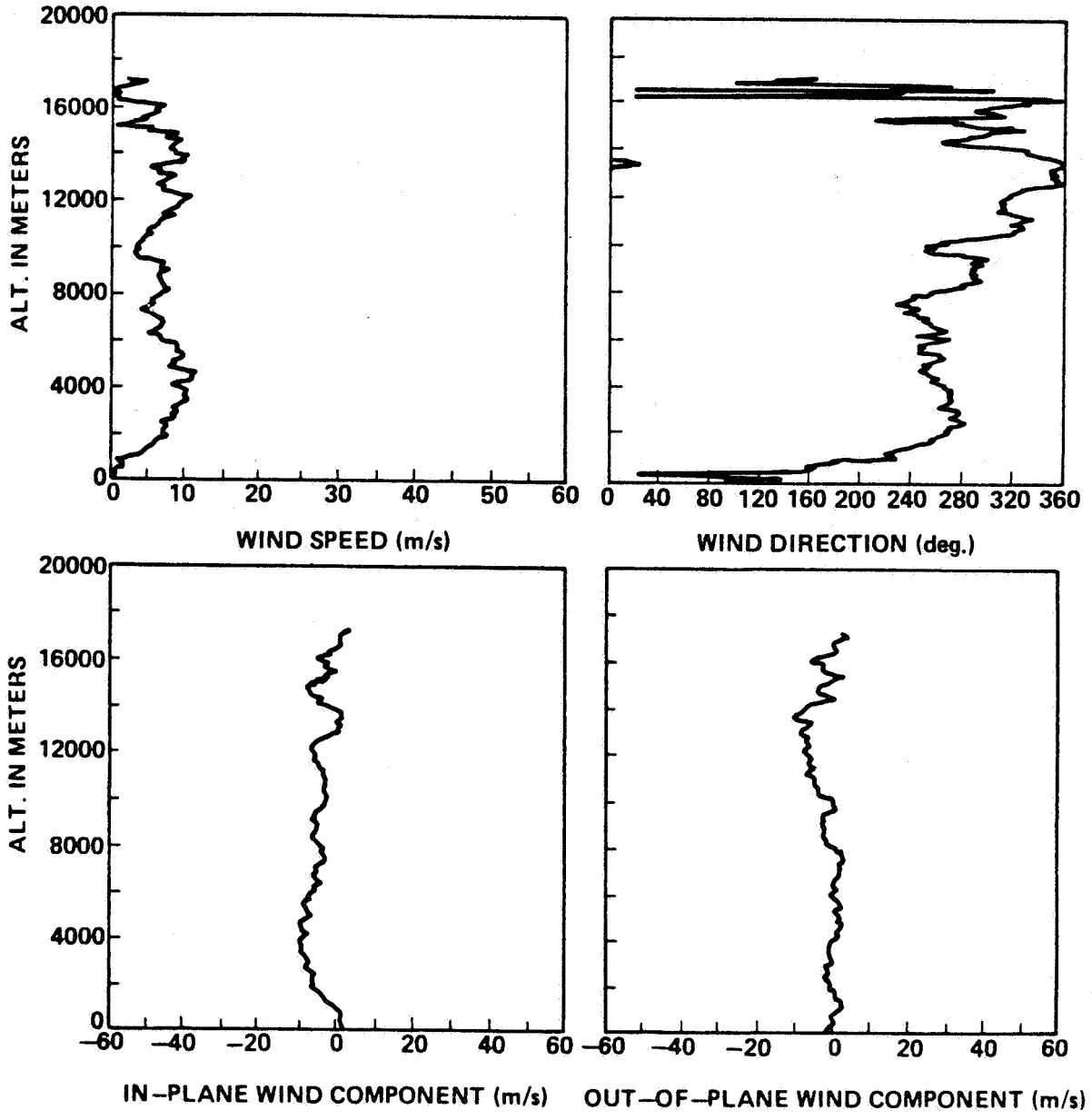

Figure A-10. STS-4 prelaunch/launch jimsphere profiles of wind speed, wind direction, in-plane and out-of-plane wind components, 0100 GMT June 27, 1982.

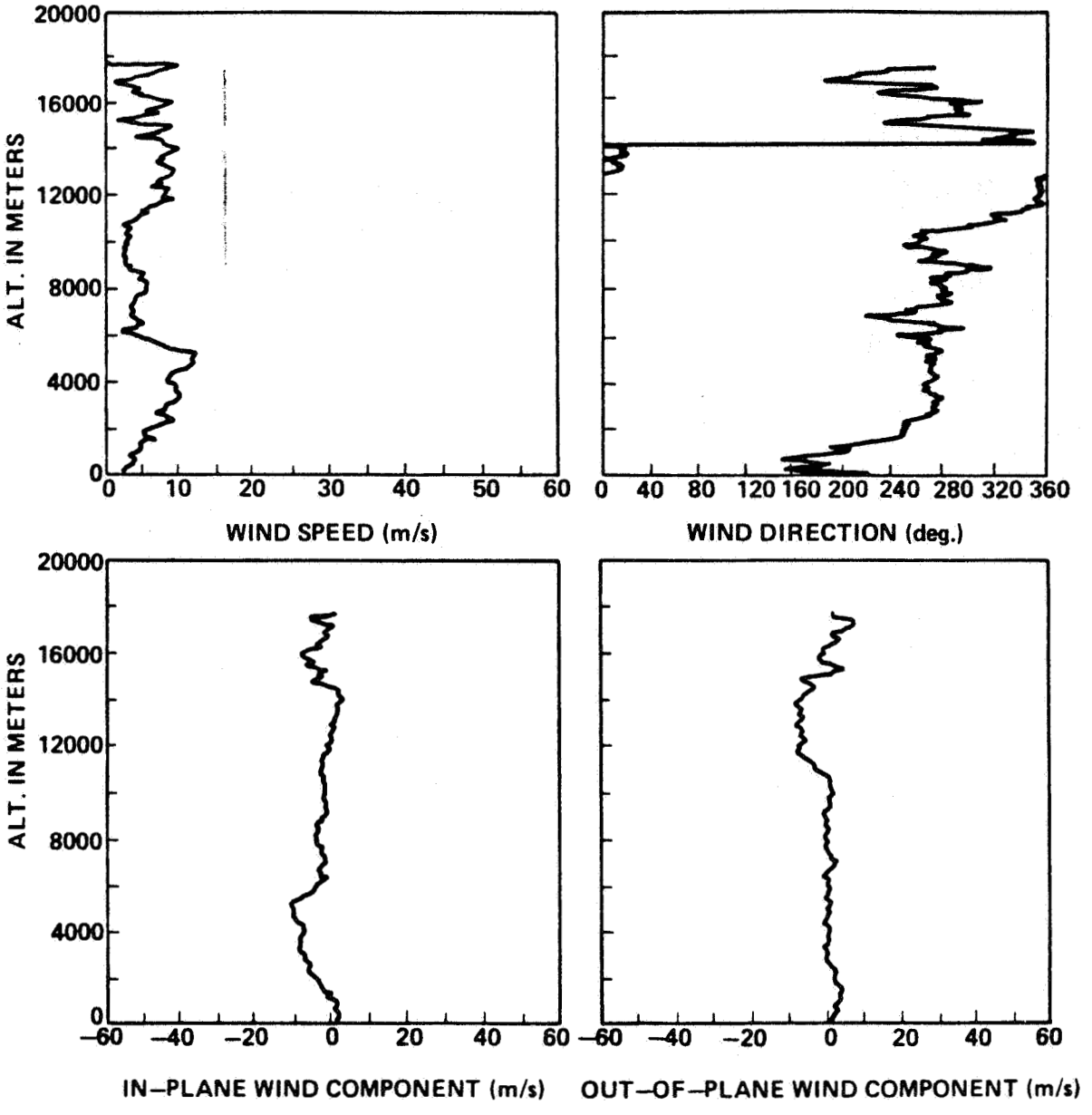

Figure A-11. STS-4 prelaunch/launch Jimsphere profiles of wind speed, wind direction, in-plane and out-of-plane wind components, 0330 GMT June 27, 1982.

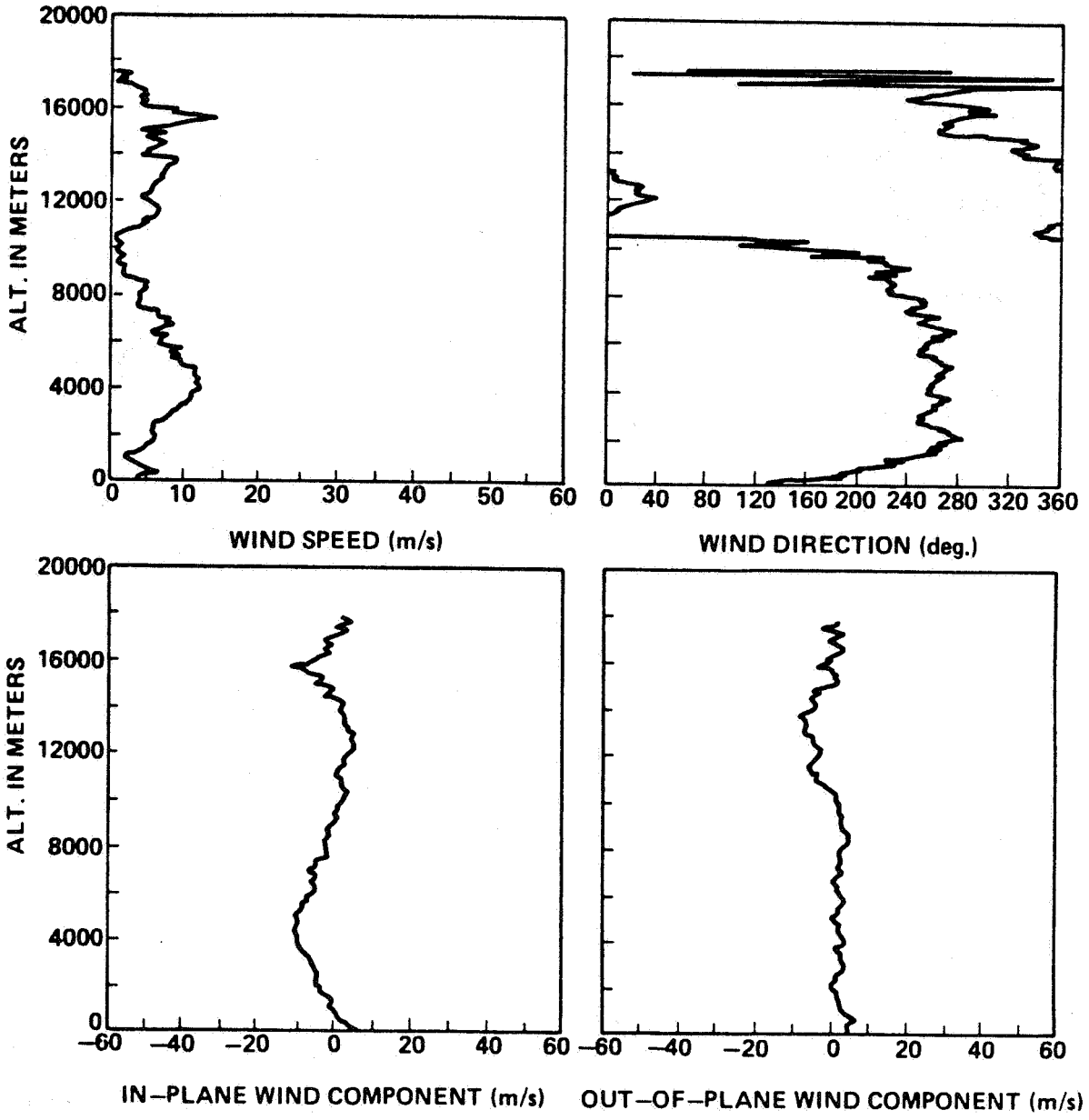

Figure A-12. STS-4 prelaunch/launch jimsphere profiles of wind speed, wind direction, in-plane and out-of-plane wind components, 0745 GMT June 27, 1982.

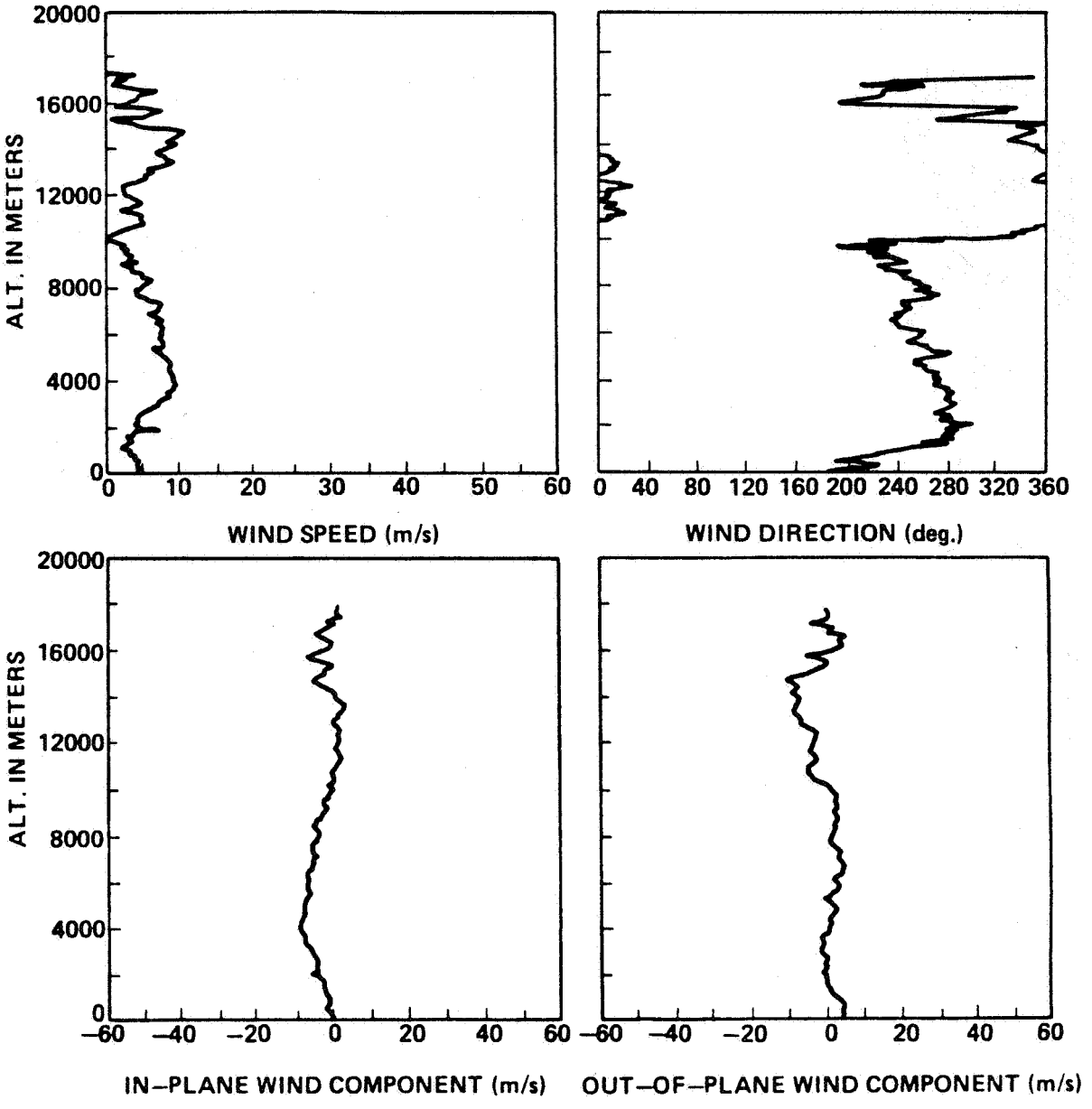

Figure A-13. STS-4 prelaunch/launch jimsphere profiles of wind speed, wind direction, in-plane and out-of-plane wind components, 1130 GMT June 27, 1982.

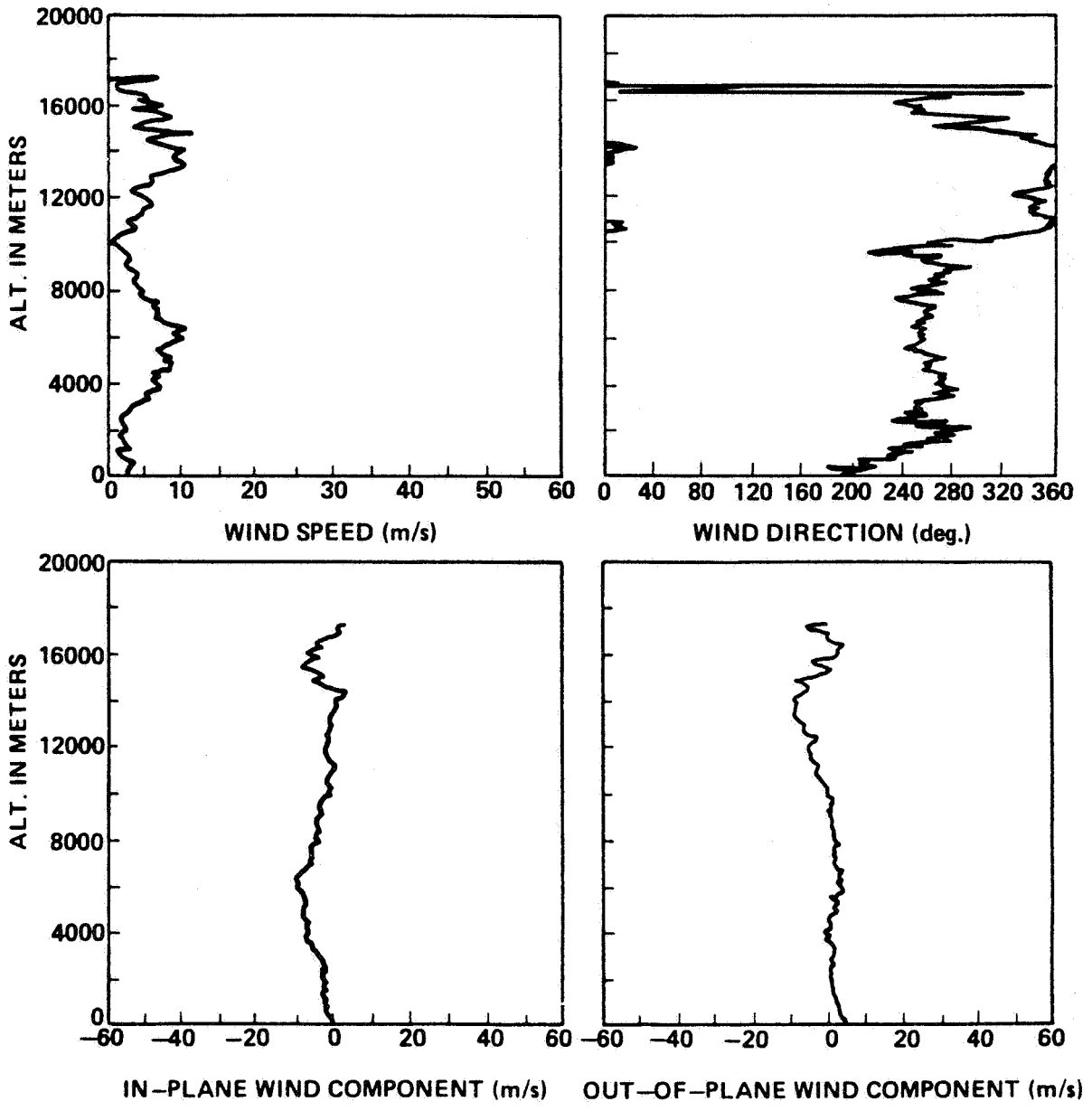

Figure A-14. STS-4 prelaunch/launch jimsphere profiles of wind speed, wind direction, in-plane and out-of-plane wind components, 1515 GMT June 27, 1982.

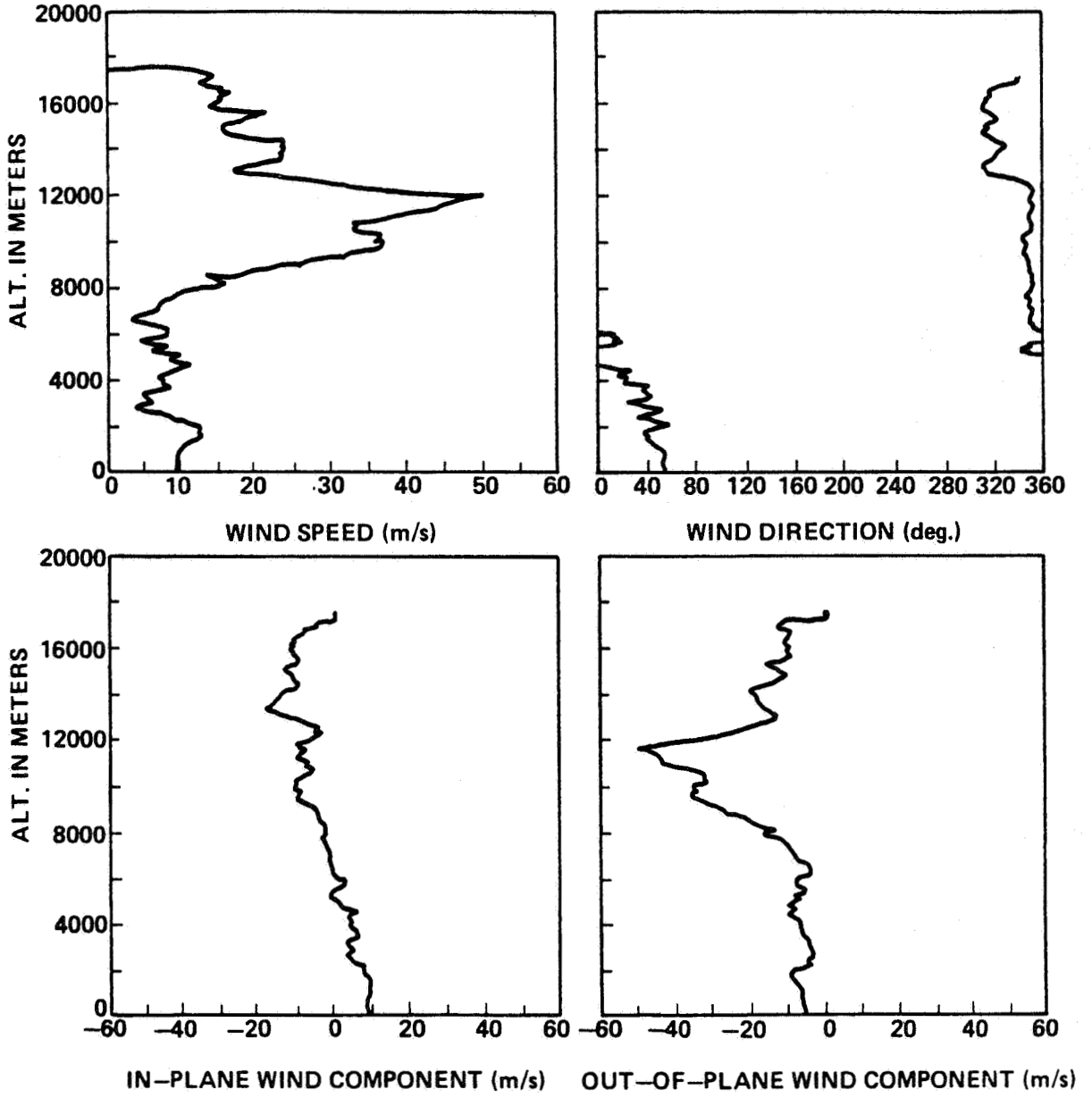

Figure A-15. STS-5 prelaunch/launch jimsphere profiles of wind speed, wind direction, in-plane and out-of-plane wind components, 2219 GMT November 10, 1982.

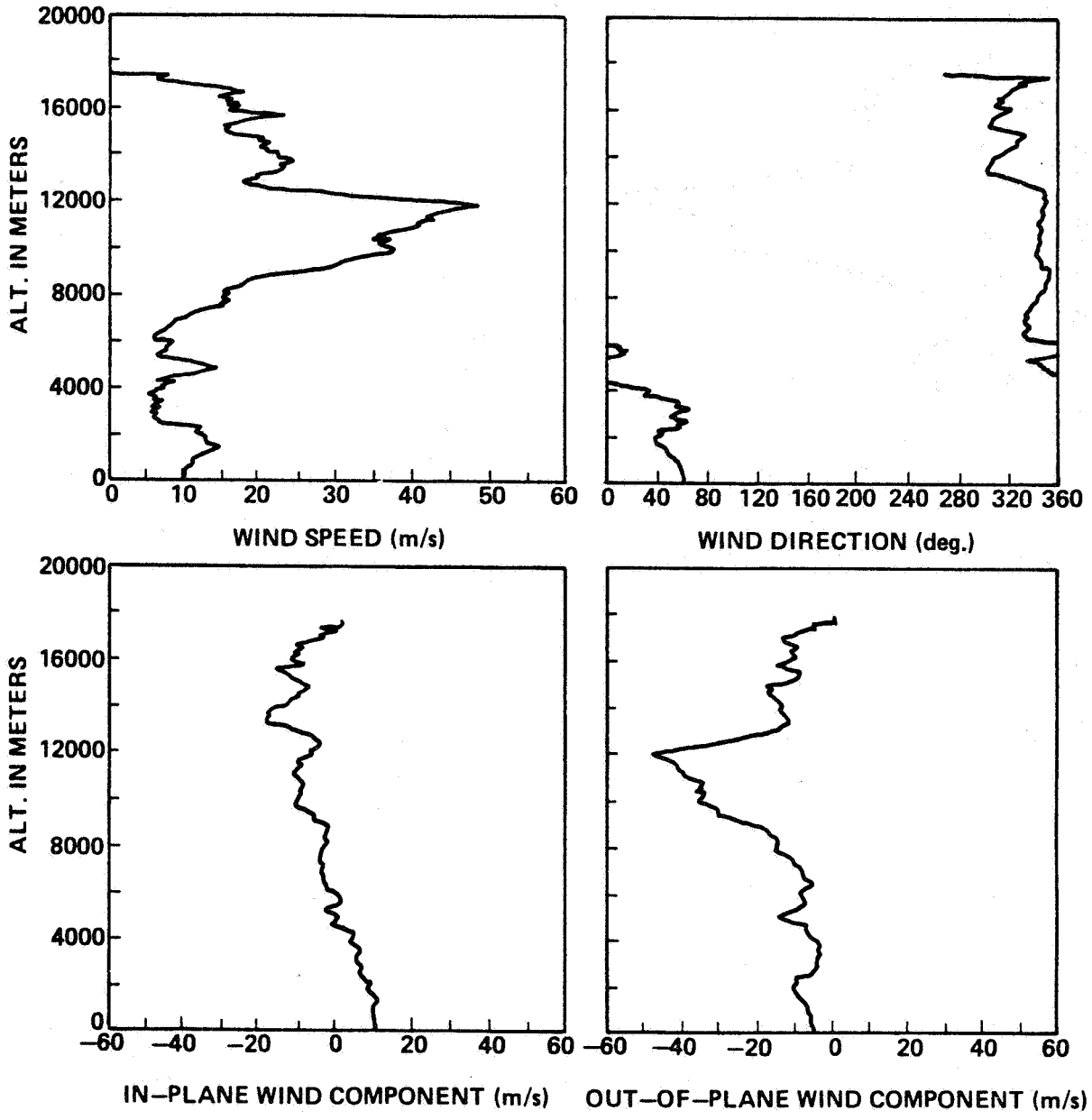

Figure A-16. STS-5 prelaunch/launch jimsphere profiles of wind speed, wind direction, in-plane and out-of-plane wind components, 0019 GMT November 11, 1982.

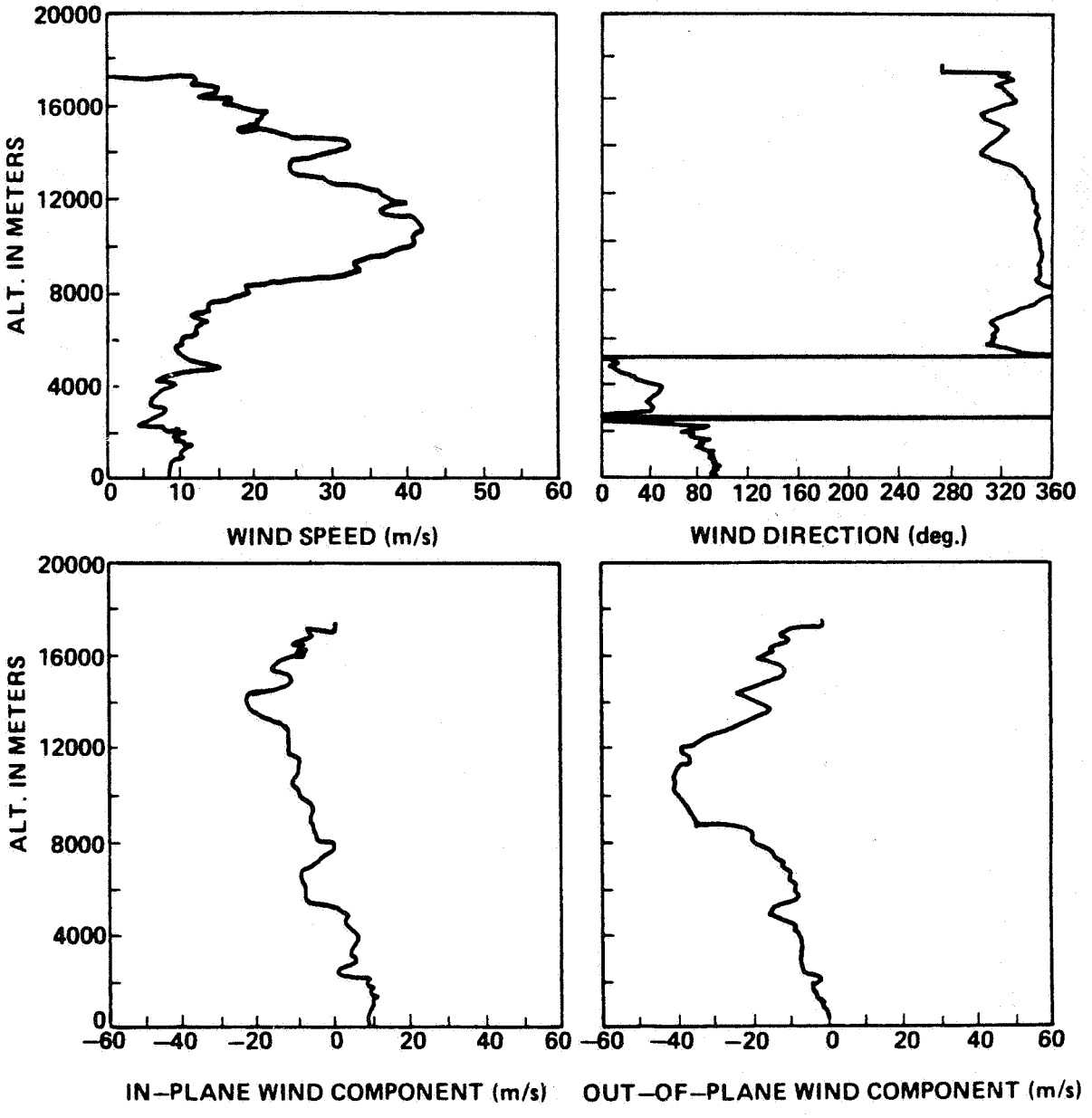

Figure A-17. STS-5 prelaunch/launch jimsphere profiles of wind speed, wind direction, in-plane and out-of-plane wind components, 0504 GMT November 11, 1982.

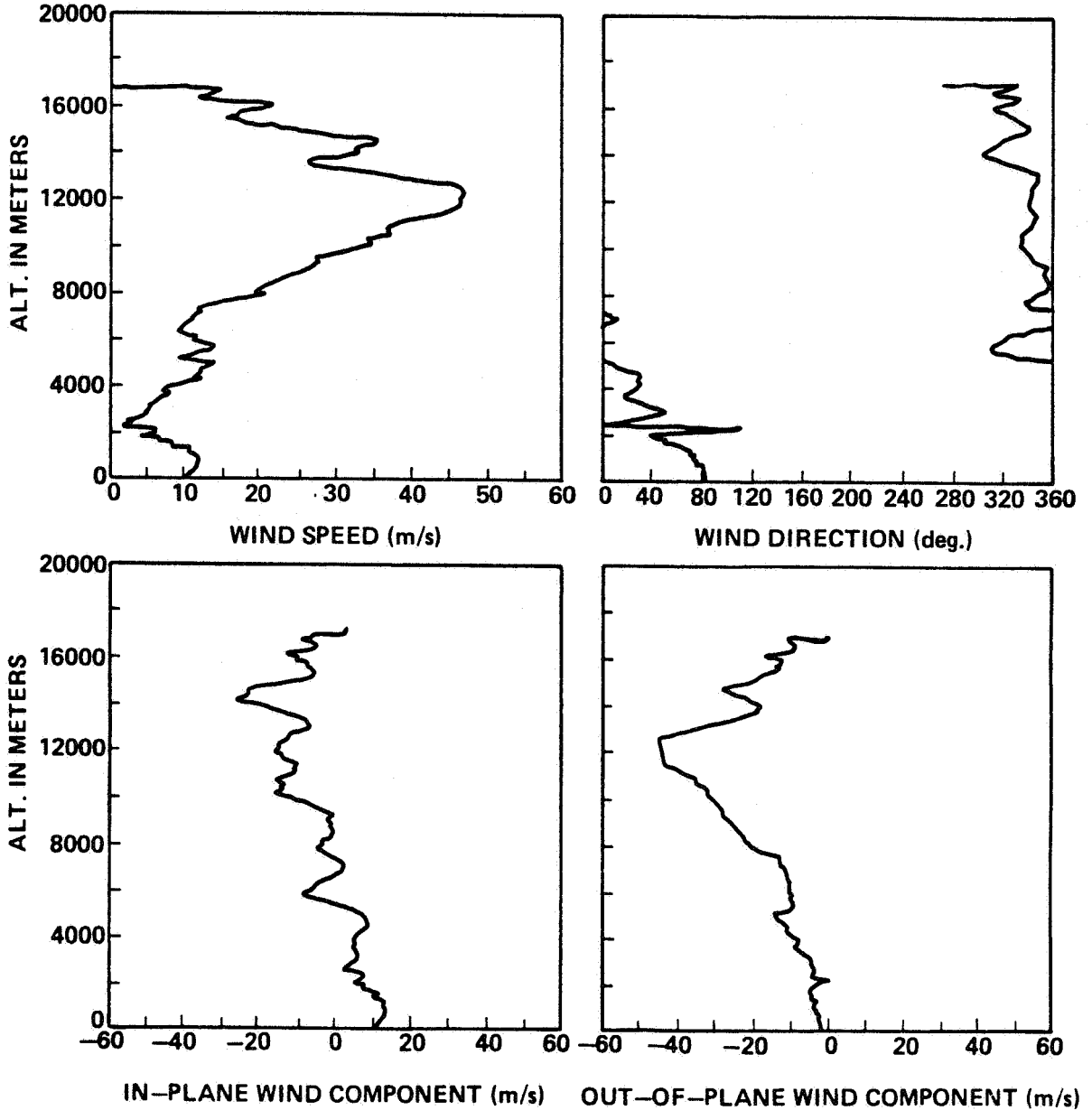

Figure A-18. STS-5 prelaunch/launch jimsphere profiles of wind speed, wind direction, in-plane and out-of-plane wind components, 0849 GMT November 11, 1982.

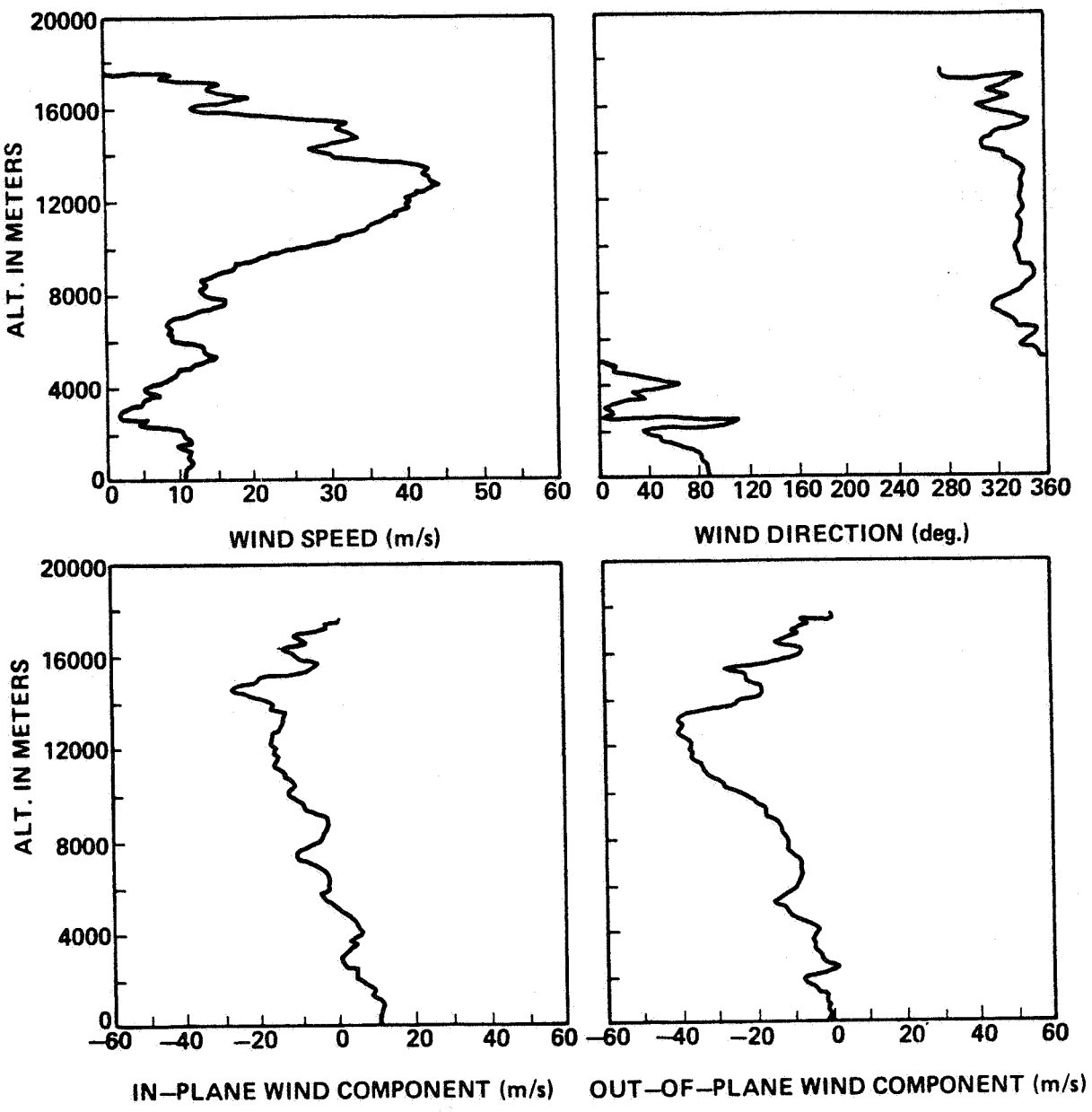

Figure A-19. STS-5 prelaunch/launch jimsphere profiles of wind speed, wind direction, in-plane and out-of-plane wind components, 1235 GMT November 11, 1982.

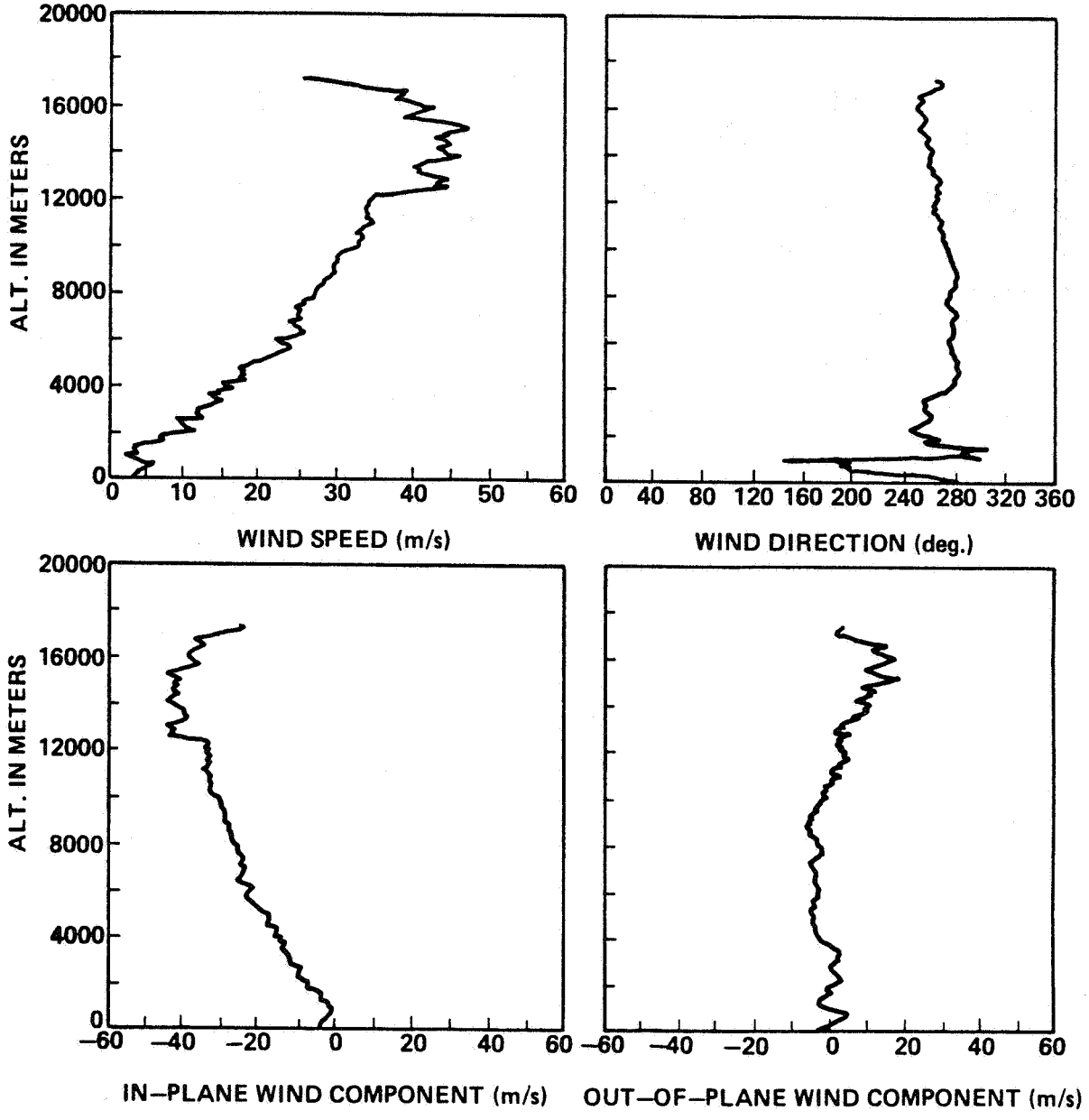

Figure A-20. STS-6 prelaunch/launch jimsphere profiles of wind speed, wind direction, in-plane and out-of-plane wind components, 0430 GMT April 4, 1983.

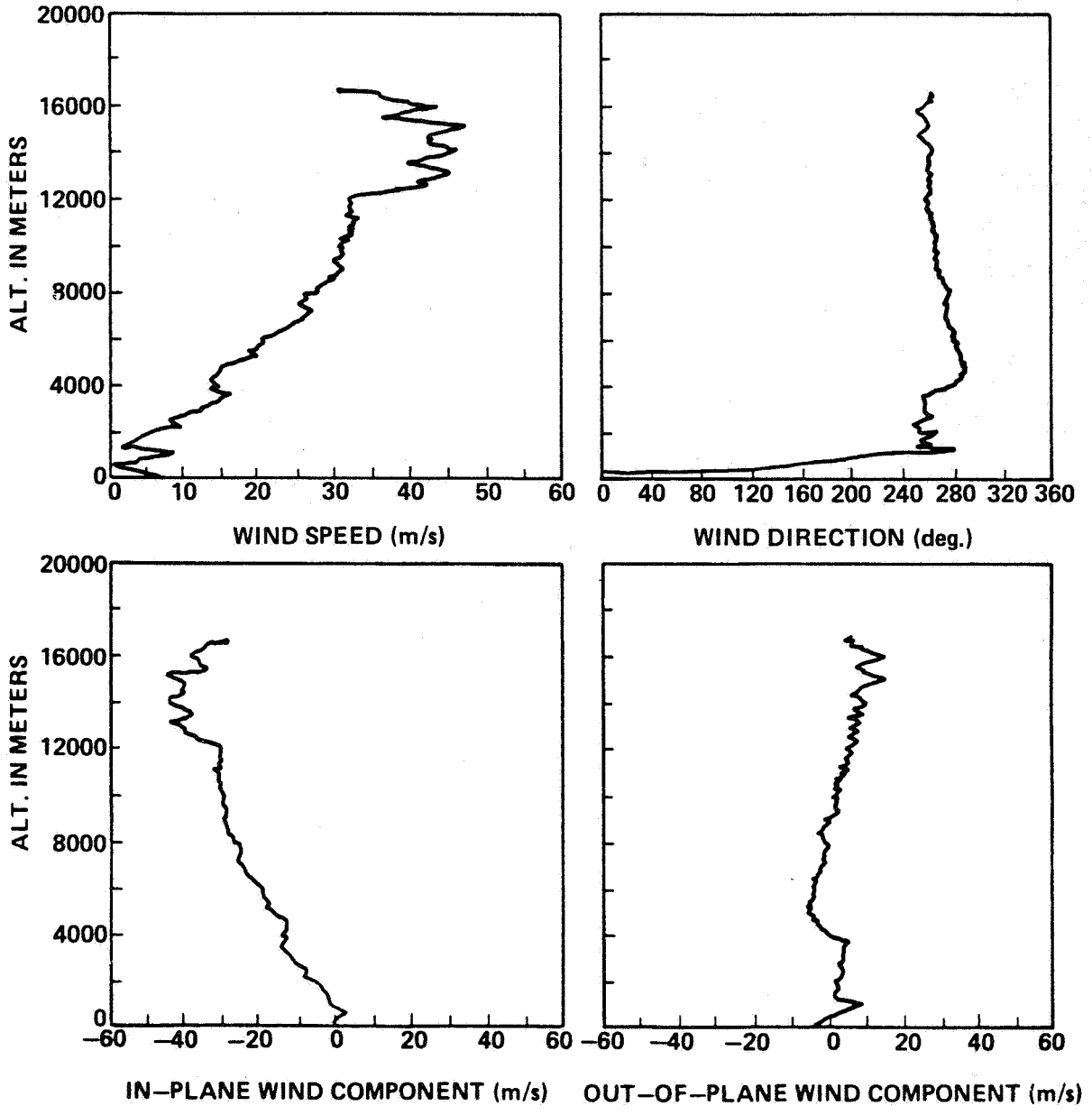

Figure A-21. STS-6 prelaunch/launch jimsphere profiles of wind speed, wind direction, in-plane and out-of-plane wind components, 0630 GMT April 4, 1983.

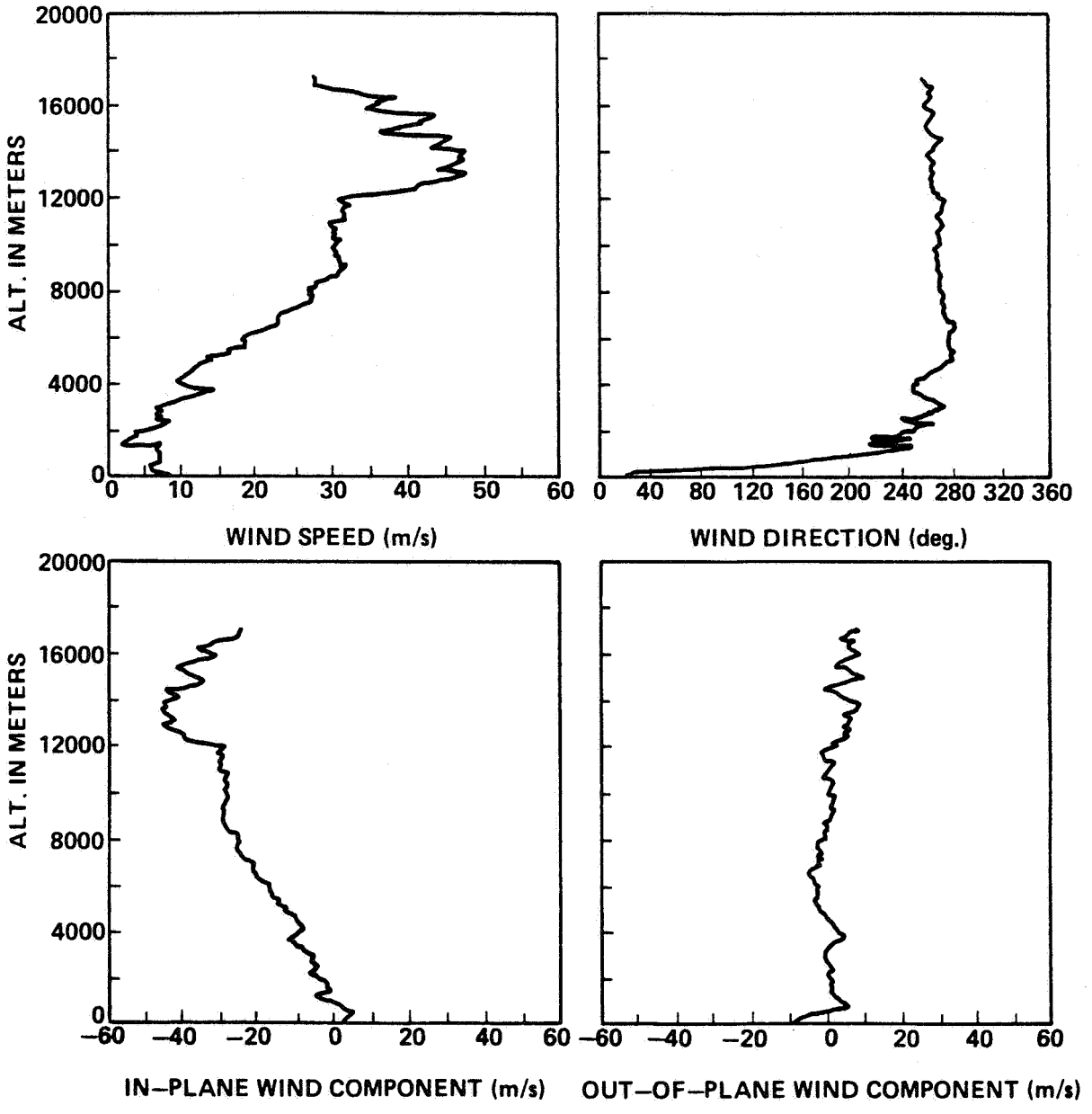

Figure A-22. STS-6 prelaunch/launch jimsphere profiles of wind speed, wind direction, in-plane and out-of-plane wind components, 1145 GMT April 4, 1983.

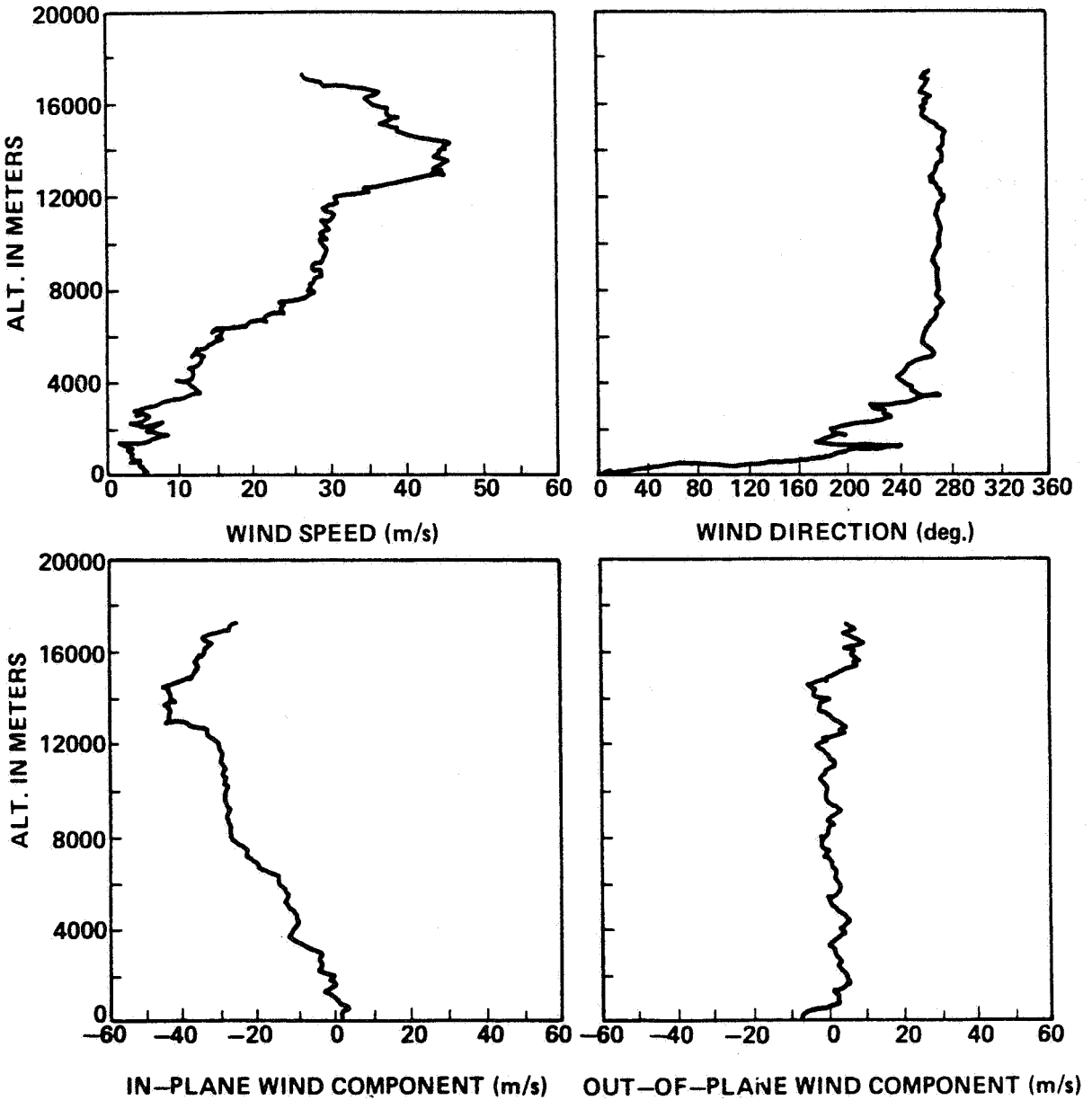

Figure A-23. STS-6 prelaunch/launch jimsphere profiles of wind speed, wind direction, in-plane and out-of-plane wind components, 1515 GMT April 4, 1983.

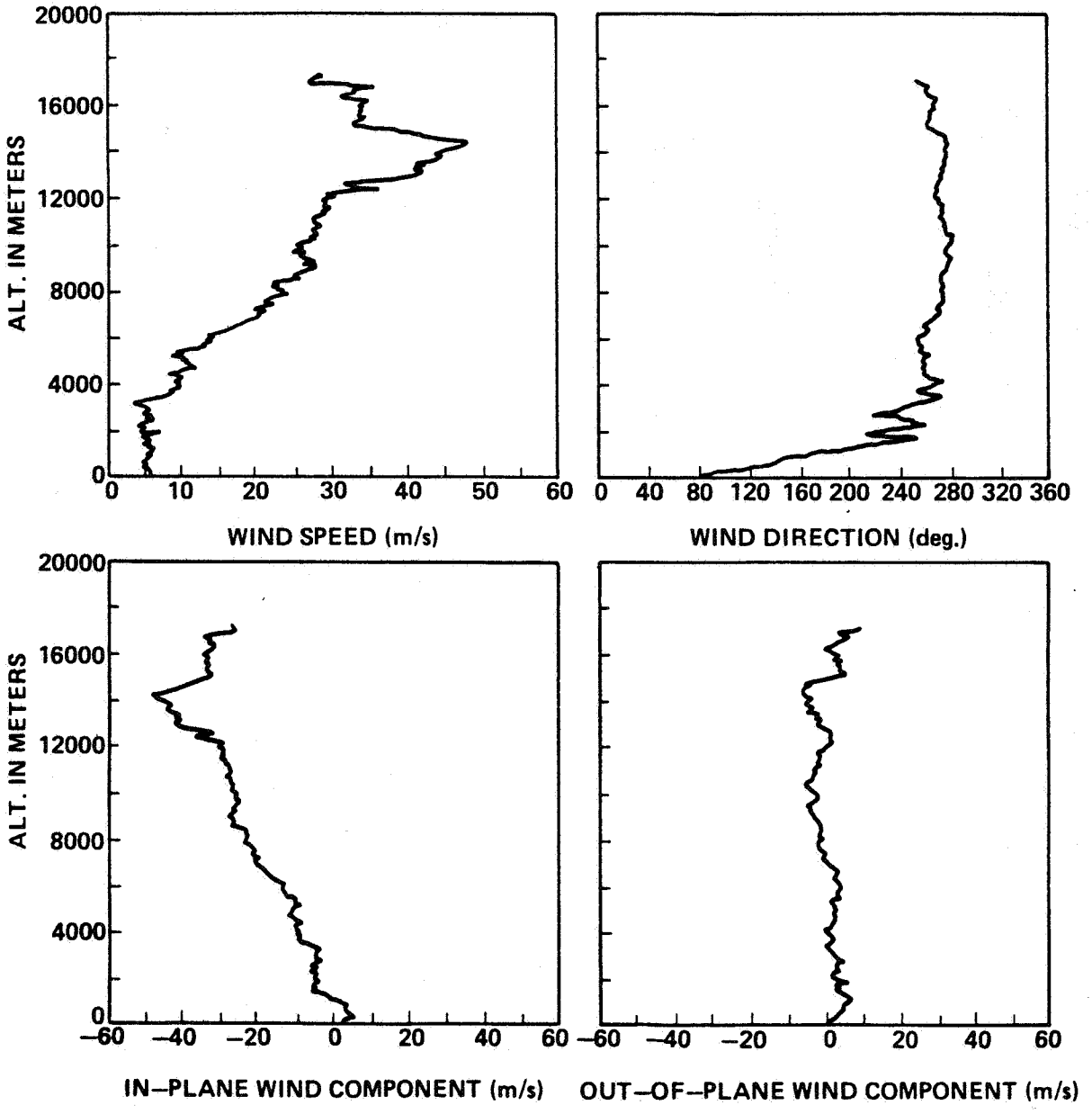

Figure A-24. STS-6 prelaunch/launch jimsphere profiles of wind speed, wind direction, in-plane and out-of-plane wind components, 1845 GMT April 4, 1983.

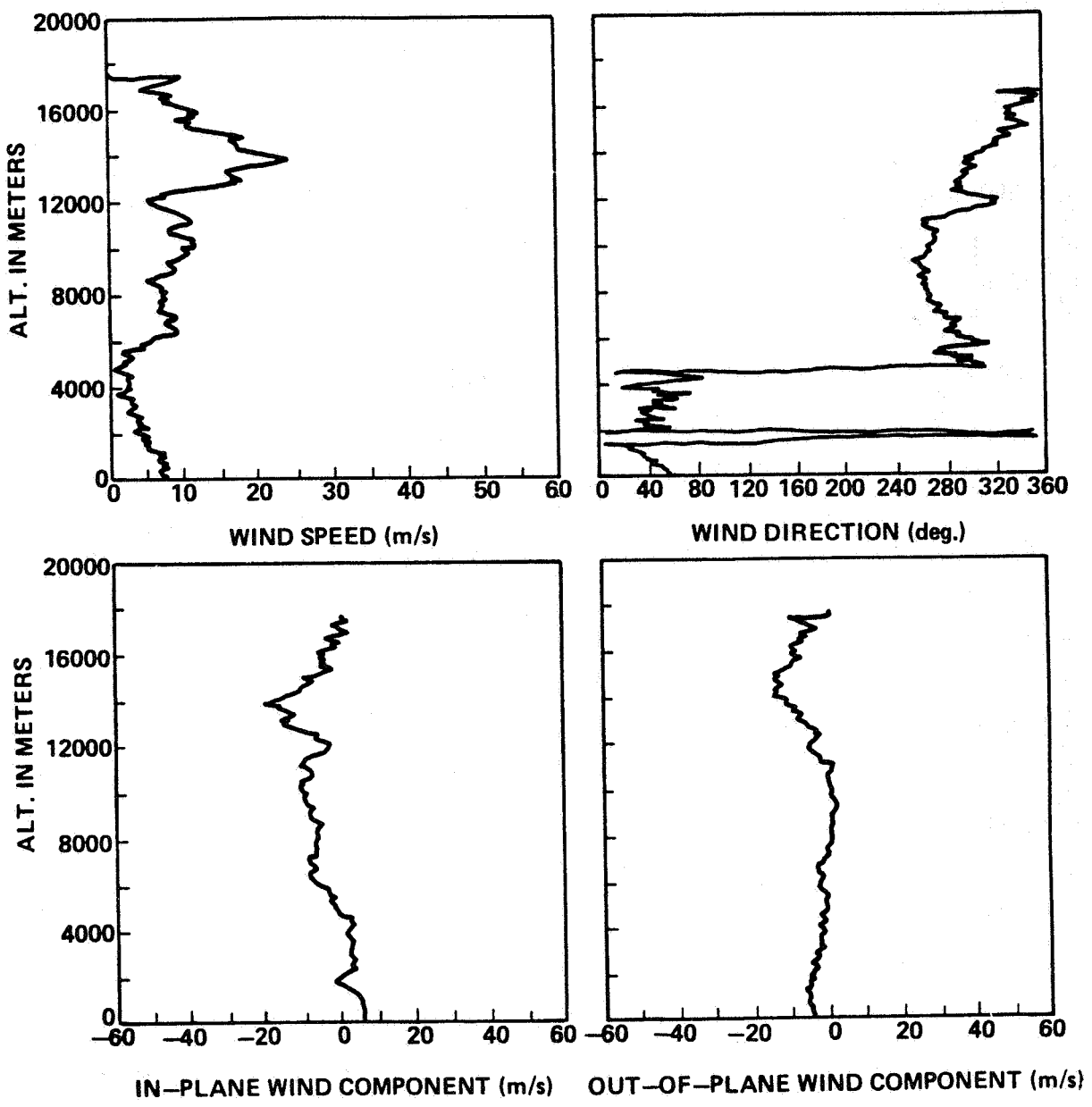

Figure A-25. STS-7 prelaunch/launch jimsphere profiles of wind speed, wind direction, in-plane and out-of-plane wind components, 2133 GMT June 17, 1983.

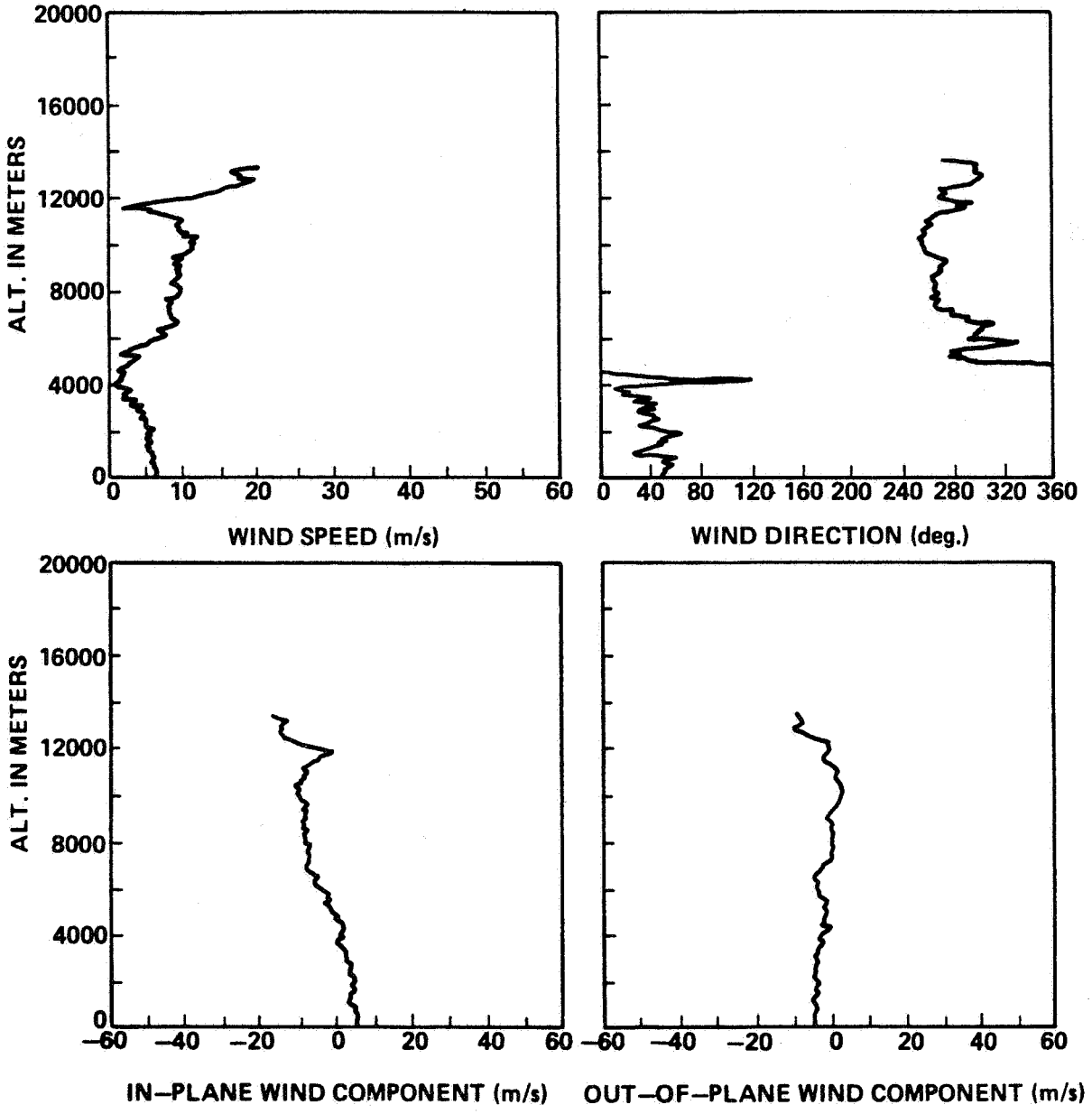

Figure A-26. STS-7 prelaunch/launch jimsphere profiles of wind speed, wind direction, in-plane and out-of-plane wind components, 2333 GMT June 17, 1983.

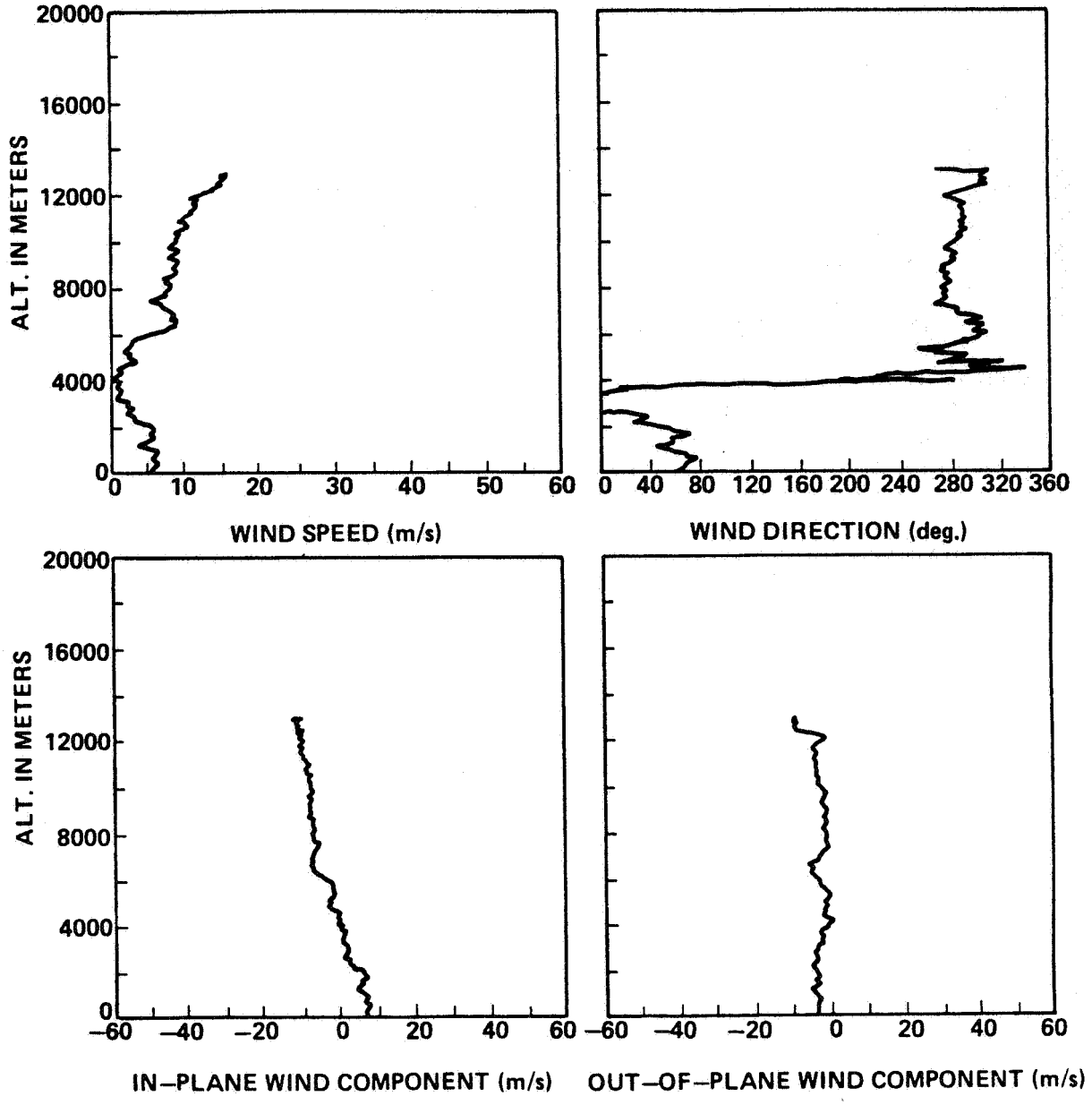

Figure A-27. STS-7 prelaunch/launch jimsphere profiles of wind speed, wind direction, in-plane and out-of-plane wind components, 0418 GMT June 18, 1983.

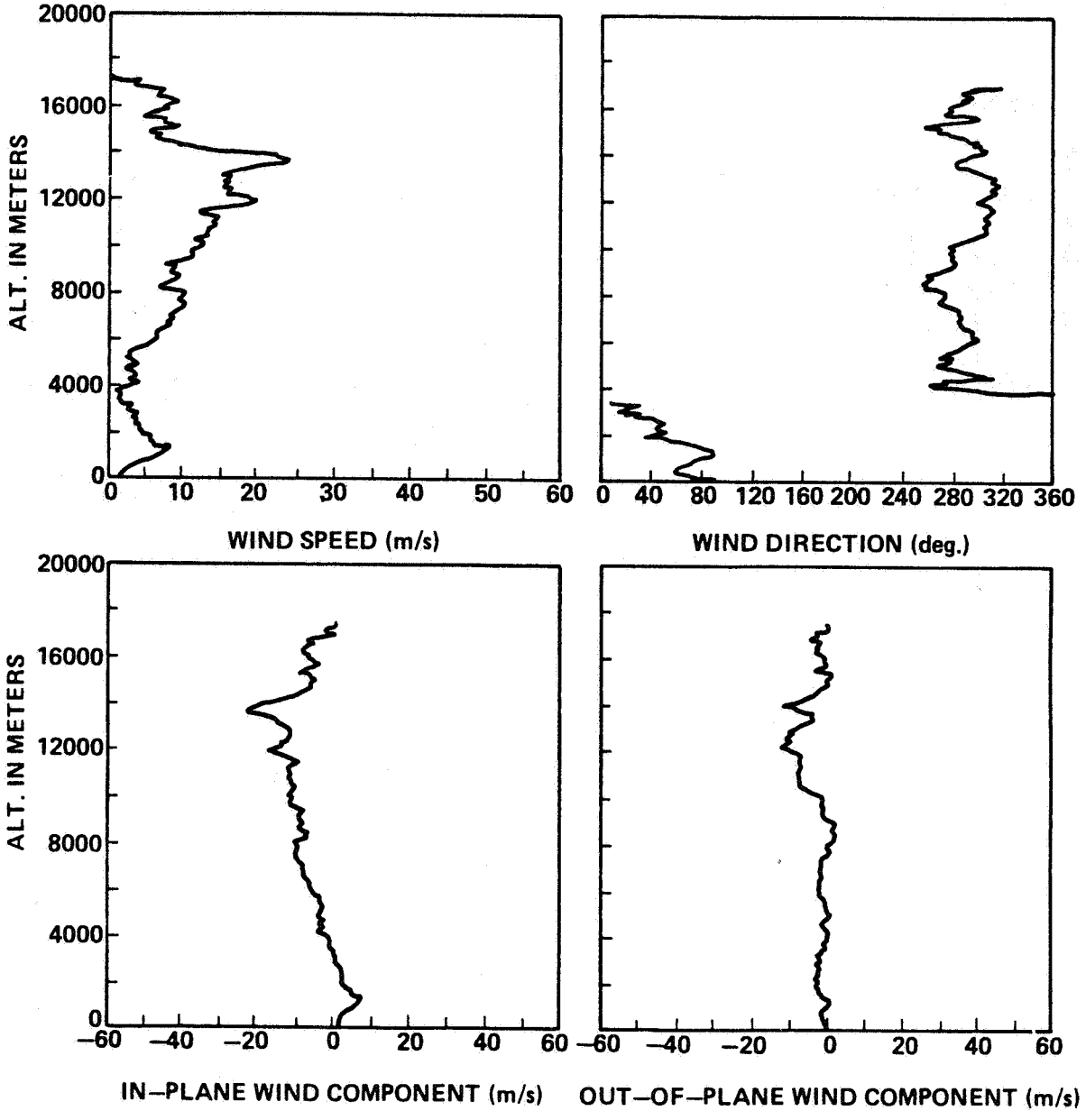

Figure A-28. STS-7 prelaunch/launch jimsphere profiles of wind speed, wind direction, in-plane and out-of-plane wind components, 0803 GMT June 18, 1983.

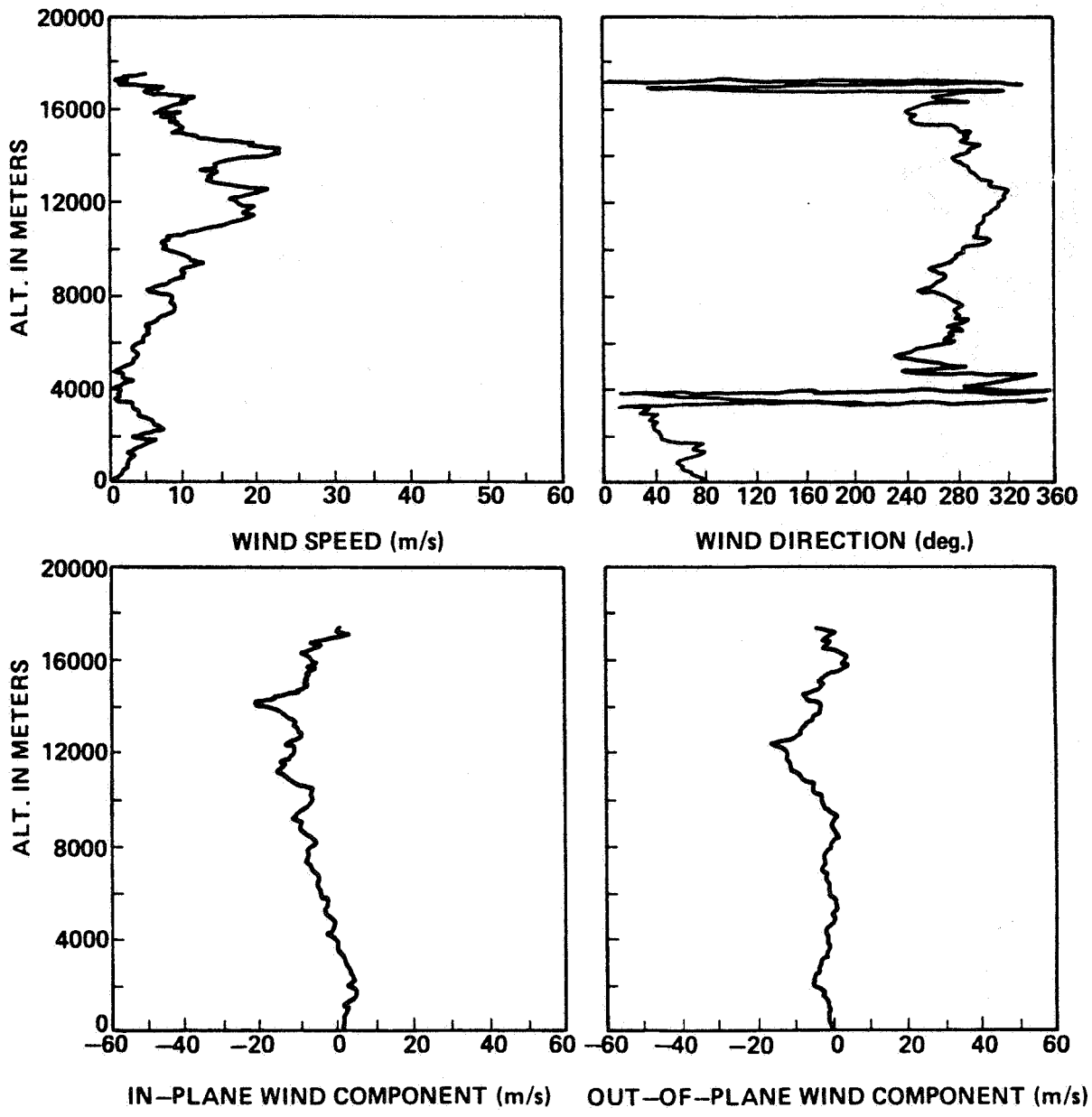

Figure A-29. STS-7 prelaunch/launch jimsphere profiles of wind speed, wind direction, in-plane and out-of-plane wind components, 1150 GMT June 18, 1983.

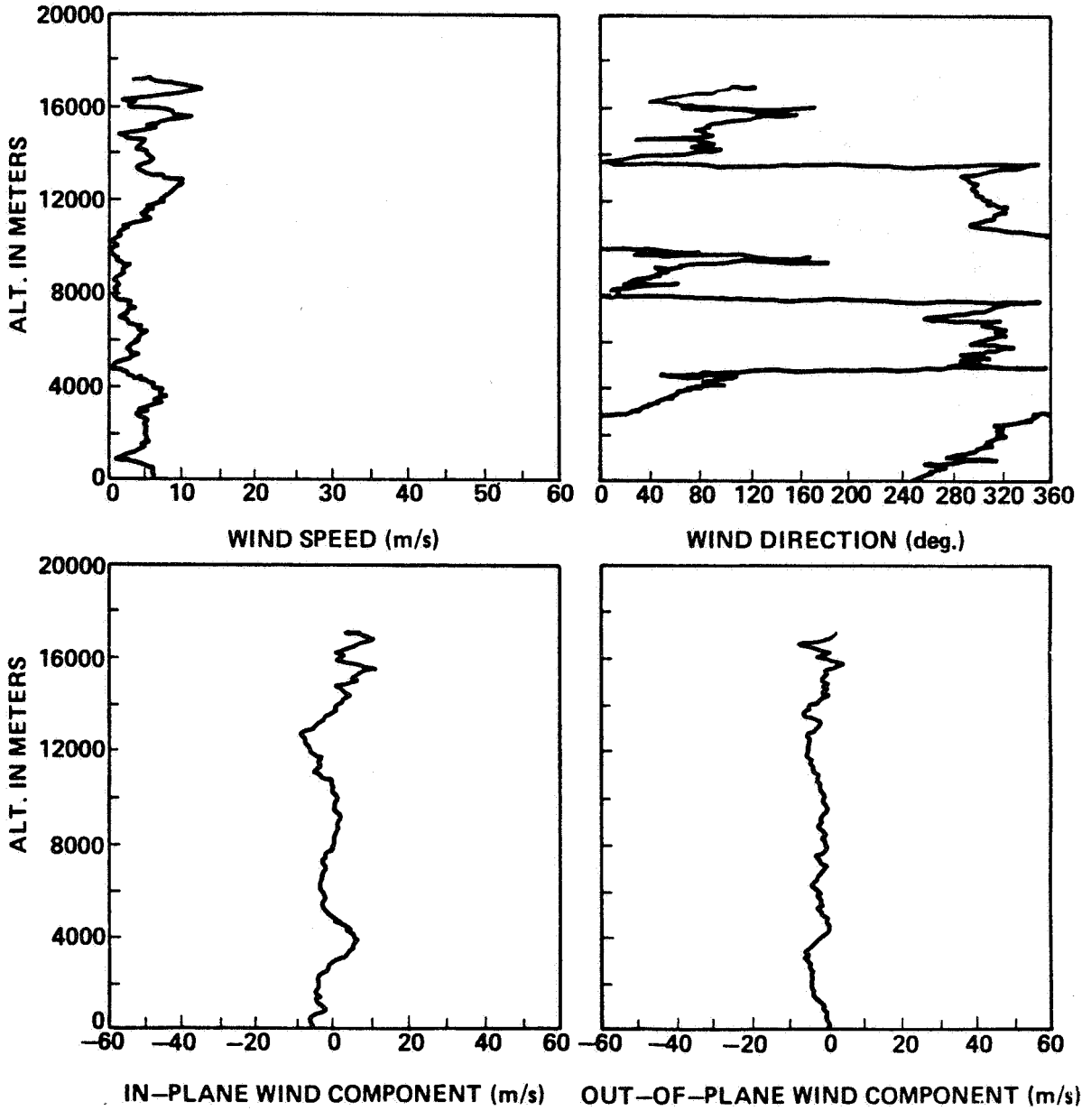

Figure A-30. STS-8 prelaunch/launch Jimsphere profiles of wind speed, wind direction, in-plane and out-of-plane wind components, 1750 GMT August 29, 1983.

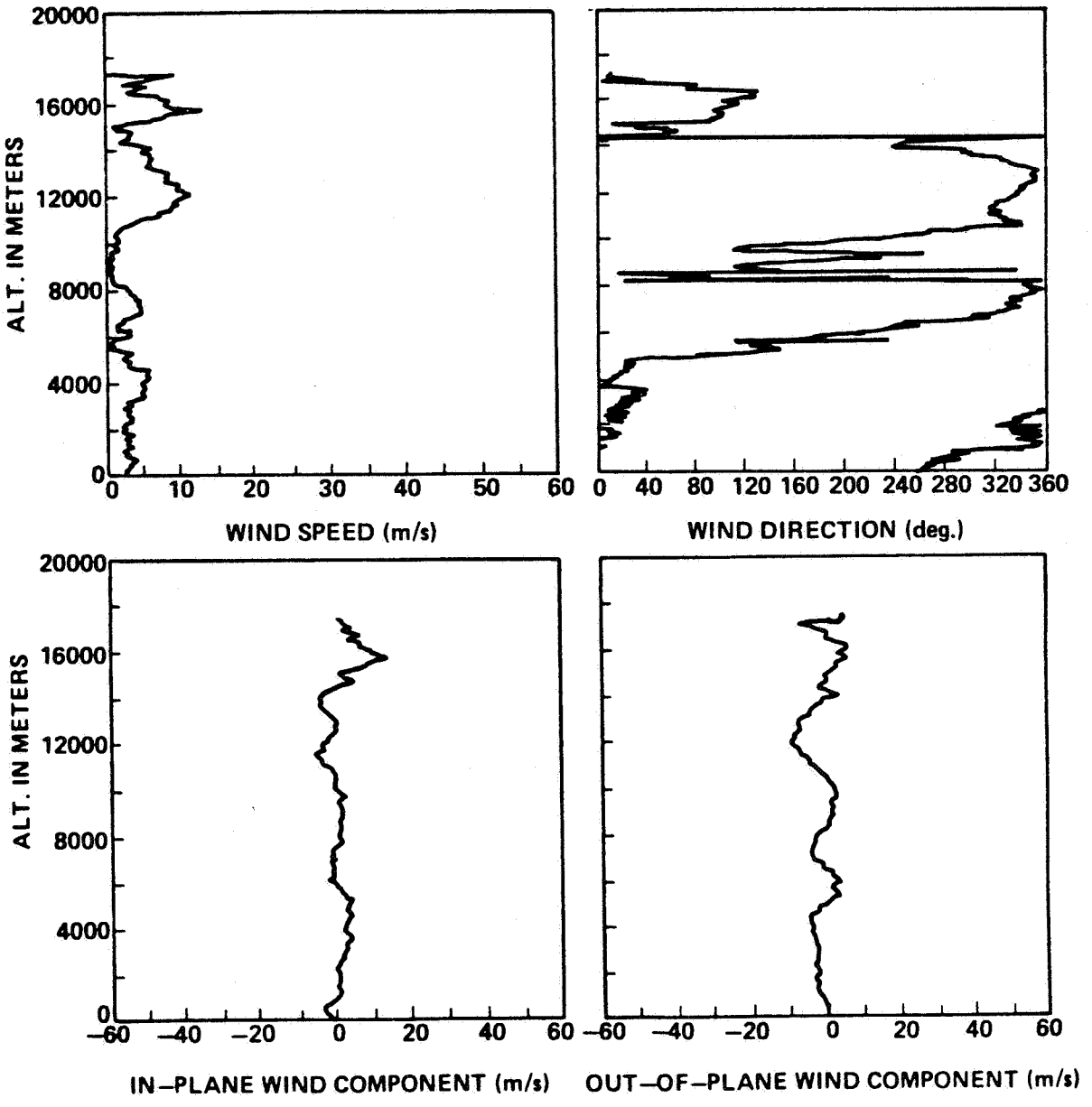

Figure A-31. STS-8 prelaunch/launch jimsphere profiles of wind speed, wind direction, in-plane and out-of-plane wind components, 2300 GMT August 29, 1983.

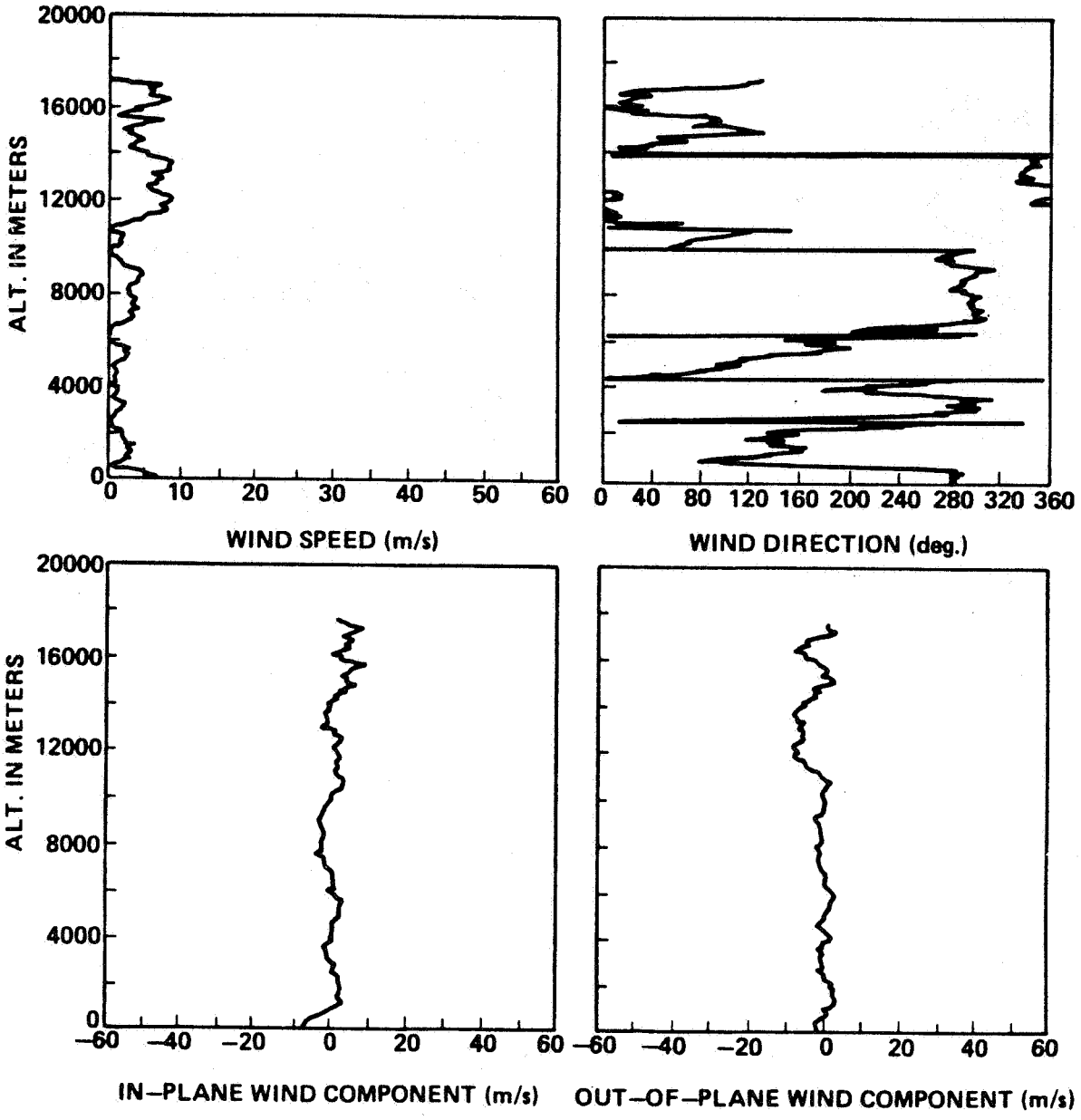

Figure A-32. STS-8 prelaunch/launch jimsphere profiles of wind speed, wind direction, in-plane and out-of-plane wind components, 0702 GMT August 30, 1983.

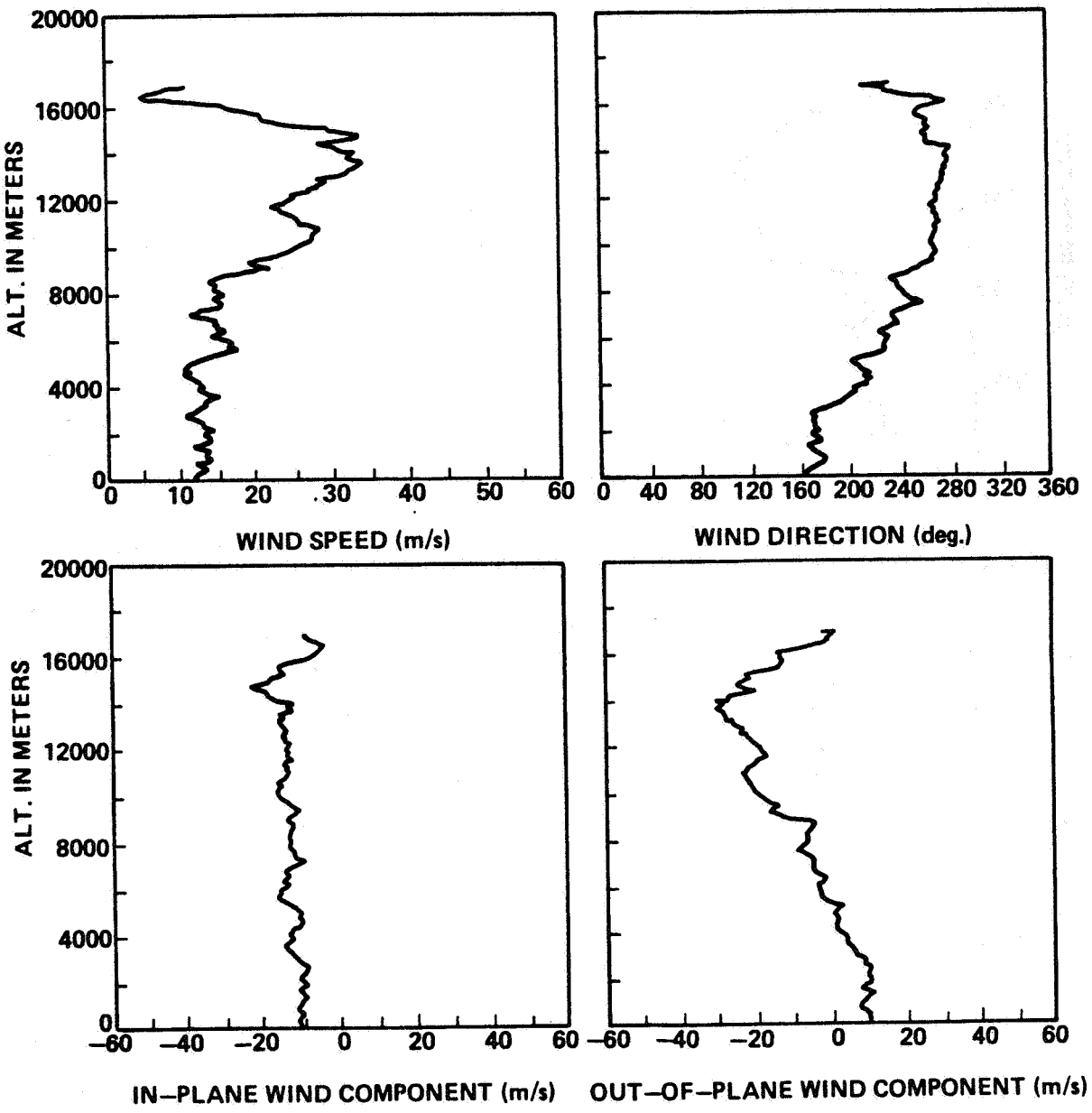

Figure A-33. STS-9 prelaunch/launch jimsphere profiles of wind speed, wind direction, in-plane and out-of-plane wind components, 0300 GMT November 28, 1983.

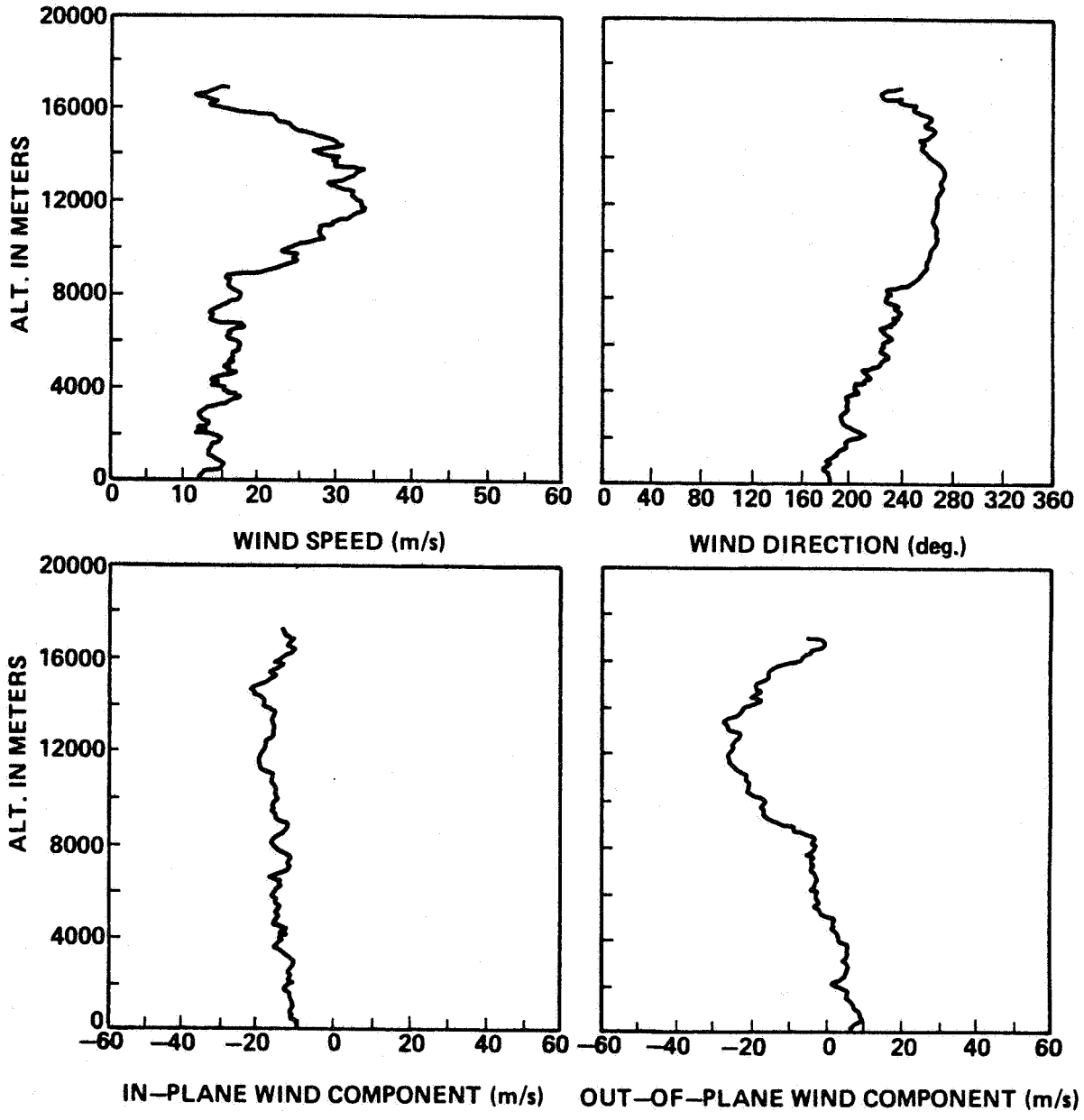

Figure A-34. STS-9 prelaunch/launch jimsphere profiles of wind speed, wind direction, in-plane and out-of-plane wind components, 0845 GMT November 28, 1983.

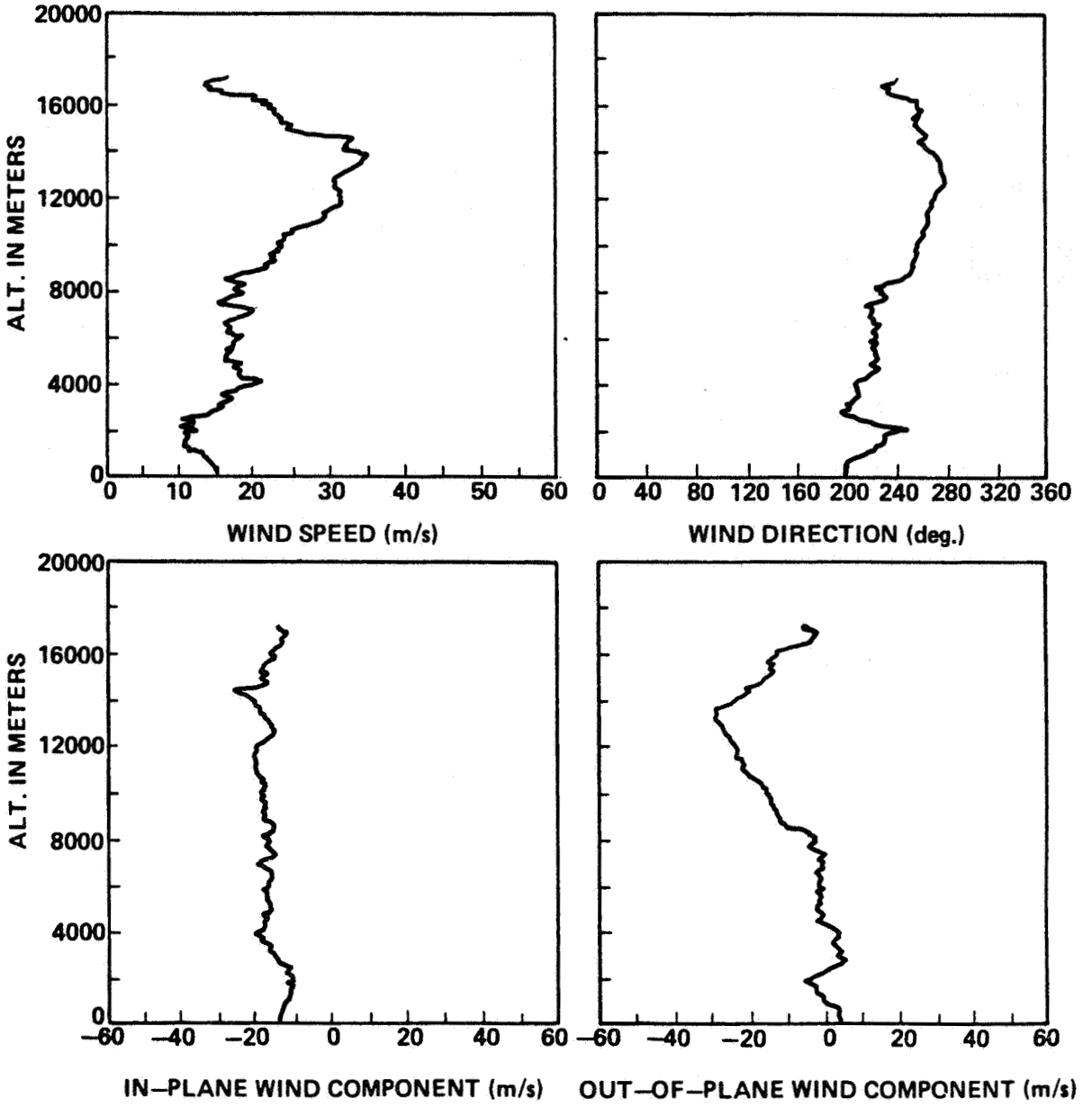

Figure A-35. STS-9 prelaunch/launch jimsphere profiles of wind speed, wind direction, in-plane and out-of-plane wind components, 1230 GMT November 28, 1983.

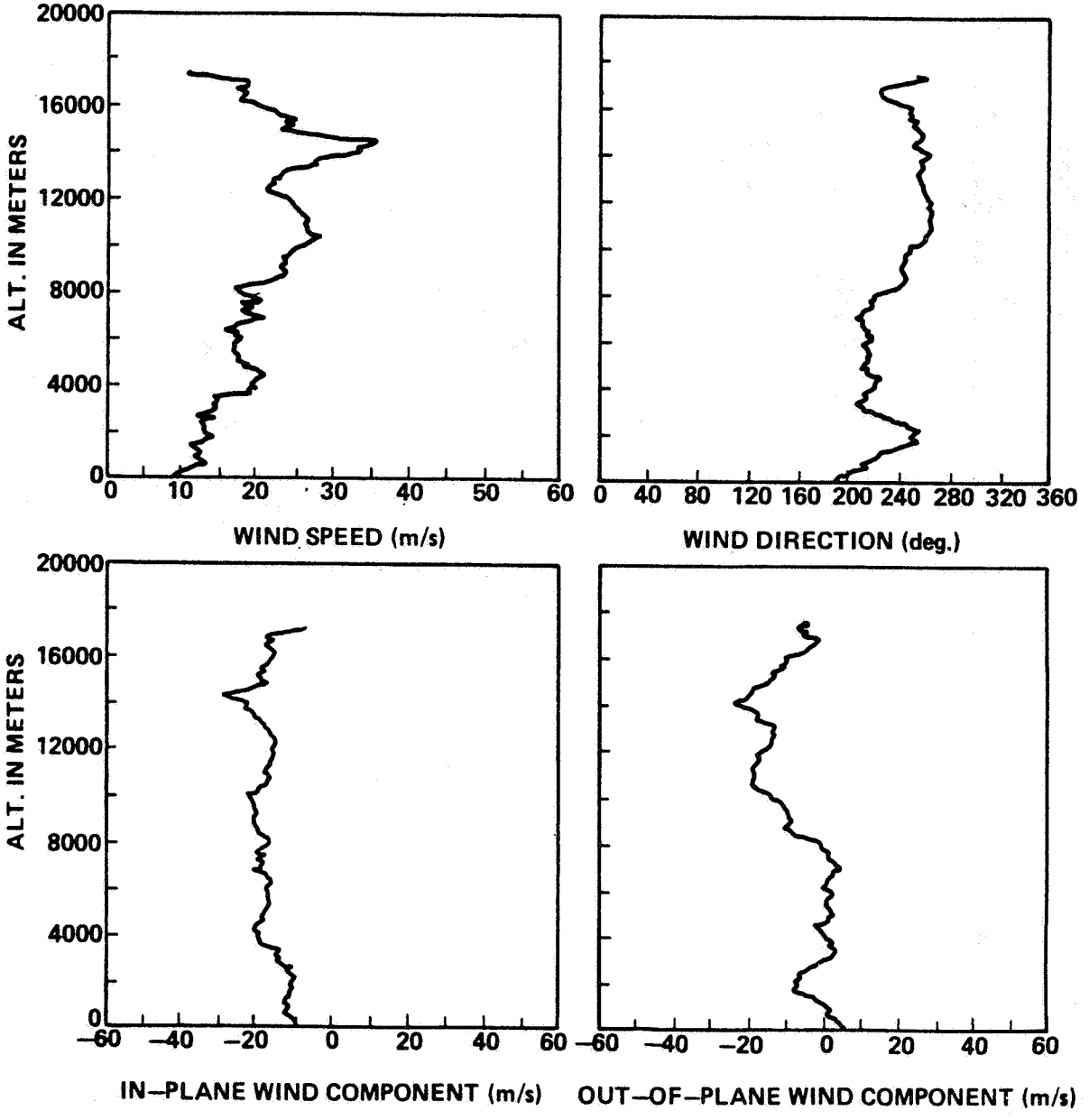

Figure A-36. STS-9 prelaunch/launch jimsphere profiles of wind speed, wind direction, in-plane and out-of-plane wind components, 1615 GMT November 29, 1983.

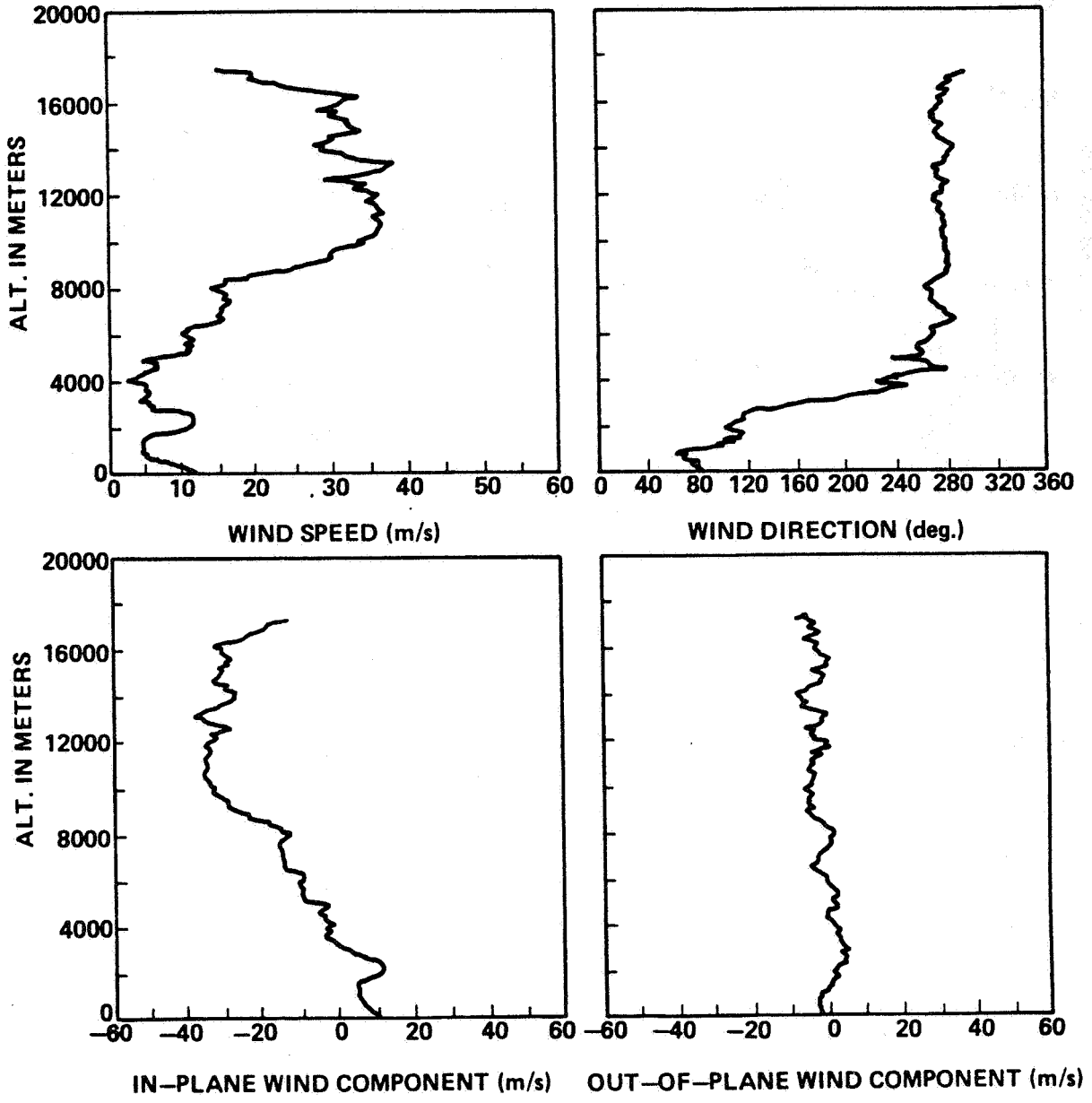

Figure A-37. STS-11 prelaunch/launch jimsphere profiles of wind speed, wind direction, in-plane and out-of-plane wind components, 0000 GMT February 3, 1984.

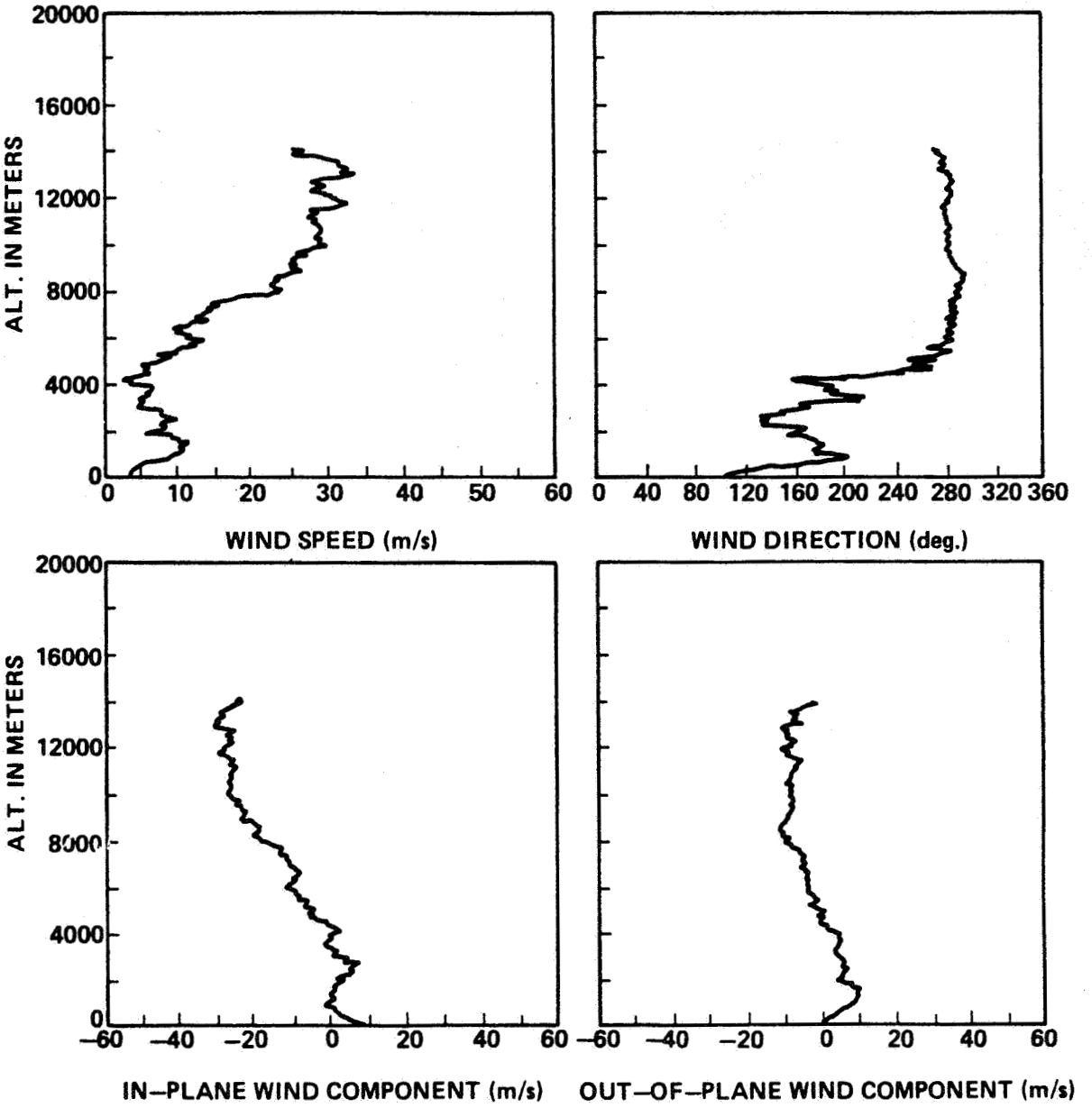

Figure A-38. STS-11 prelaunch/launch jimsphere profiles of wind speed, wind direction, in-plane and out-of-plane wind components, 0545 GMT February 3, 1984.

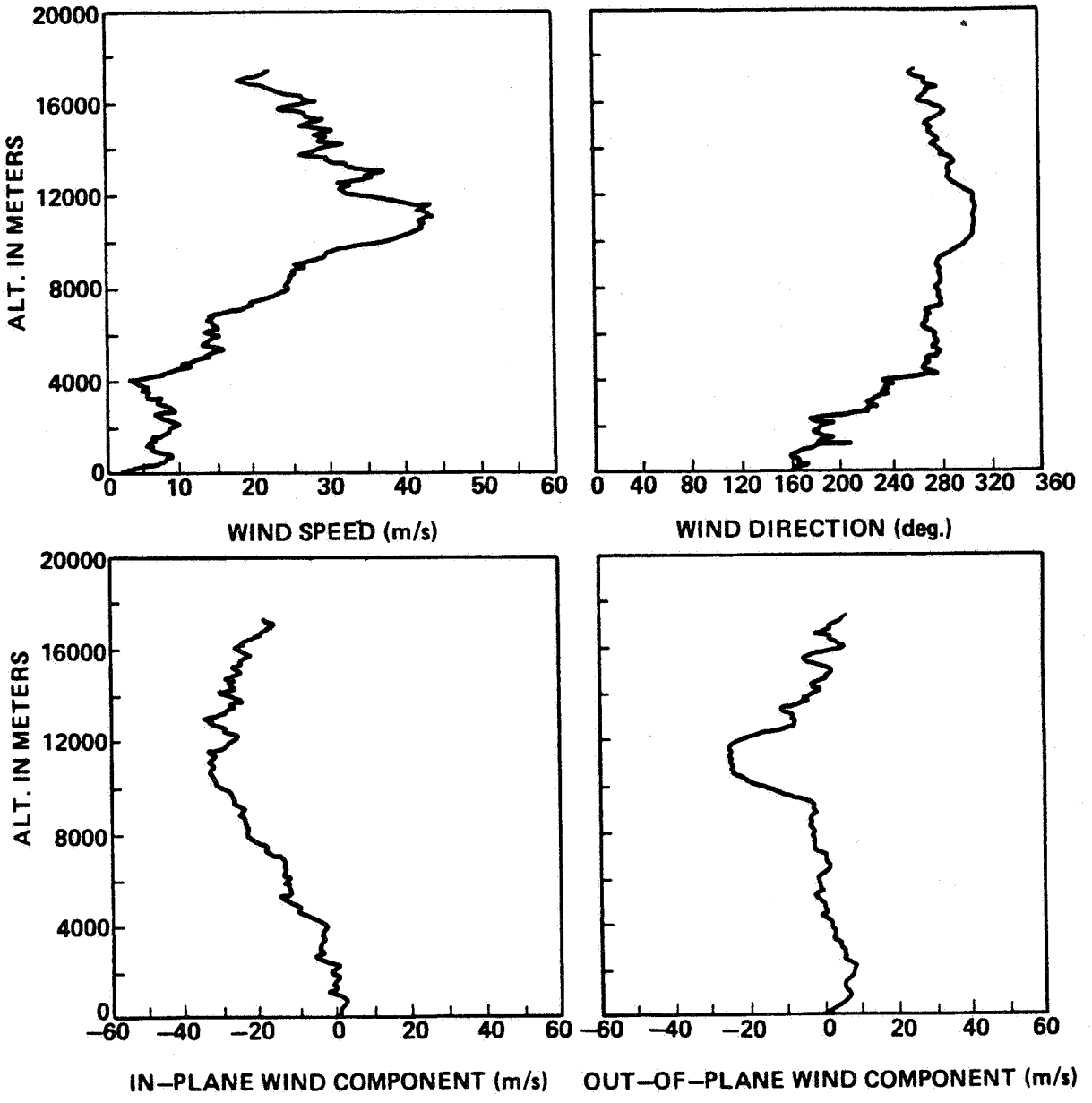

Figure A-39. STS-11 prelaunch/launch jimsphere profiles of wind speed, wind direction, in-plane and out-of-plane wind components, 0930 GMT February 3, 1984.

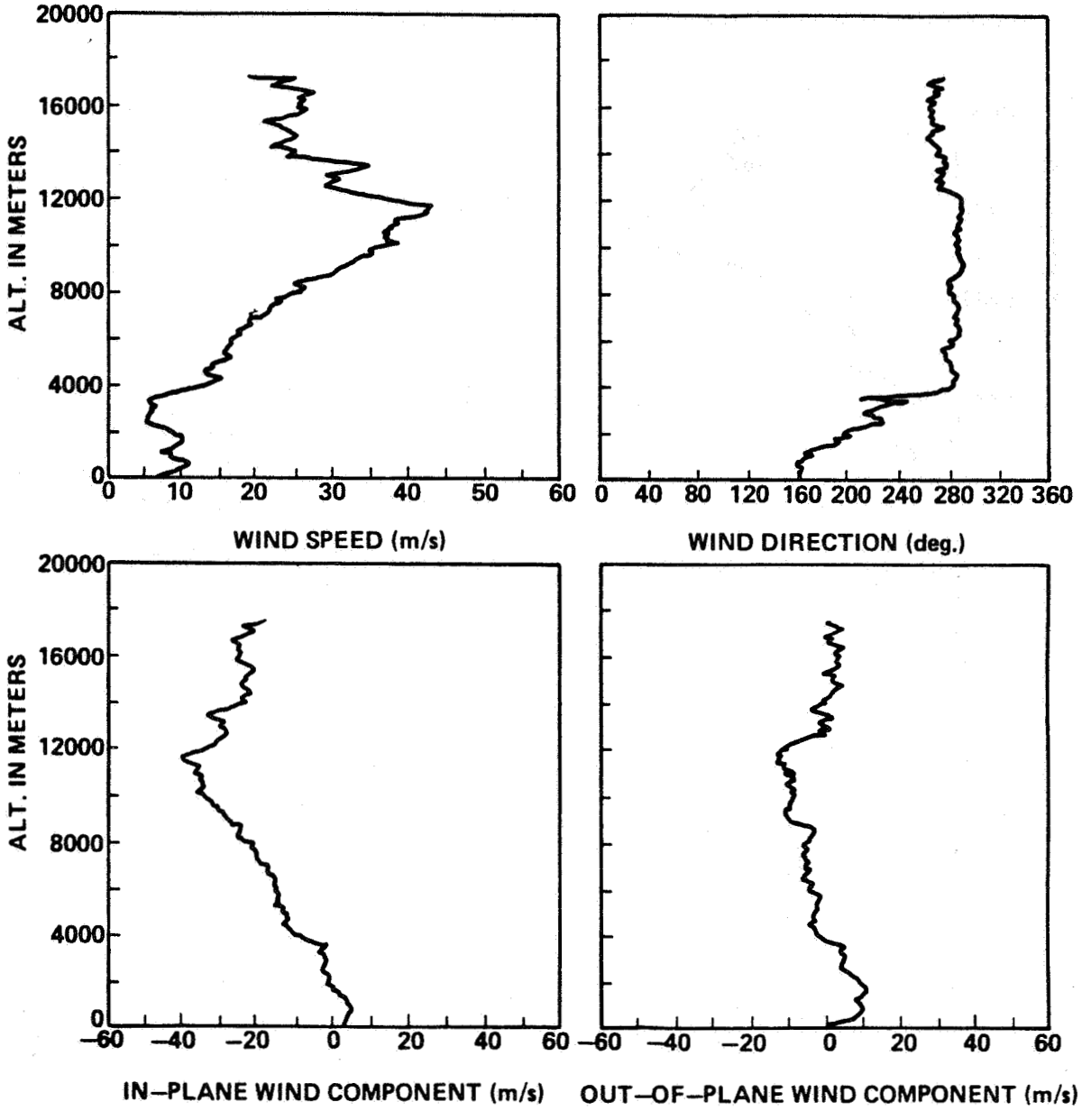

Figure A-40. STS-11 prelaunch/launch jimsphere profiles of wind speed, wind direction, in-plane and out-of-plane wind components, 1320 GMT February 3, 1984.

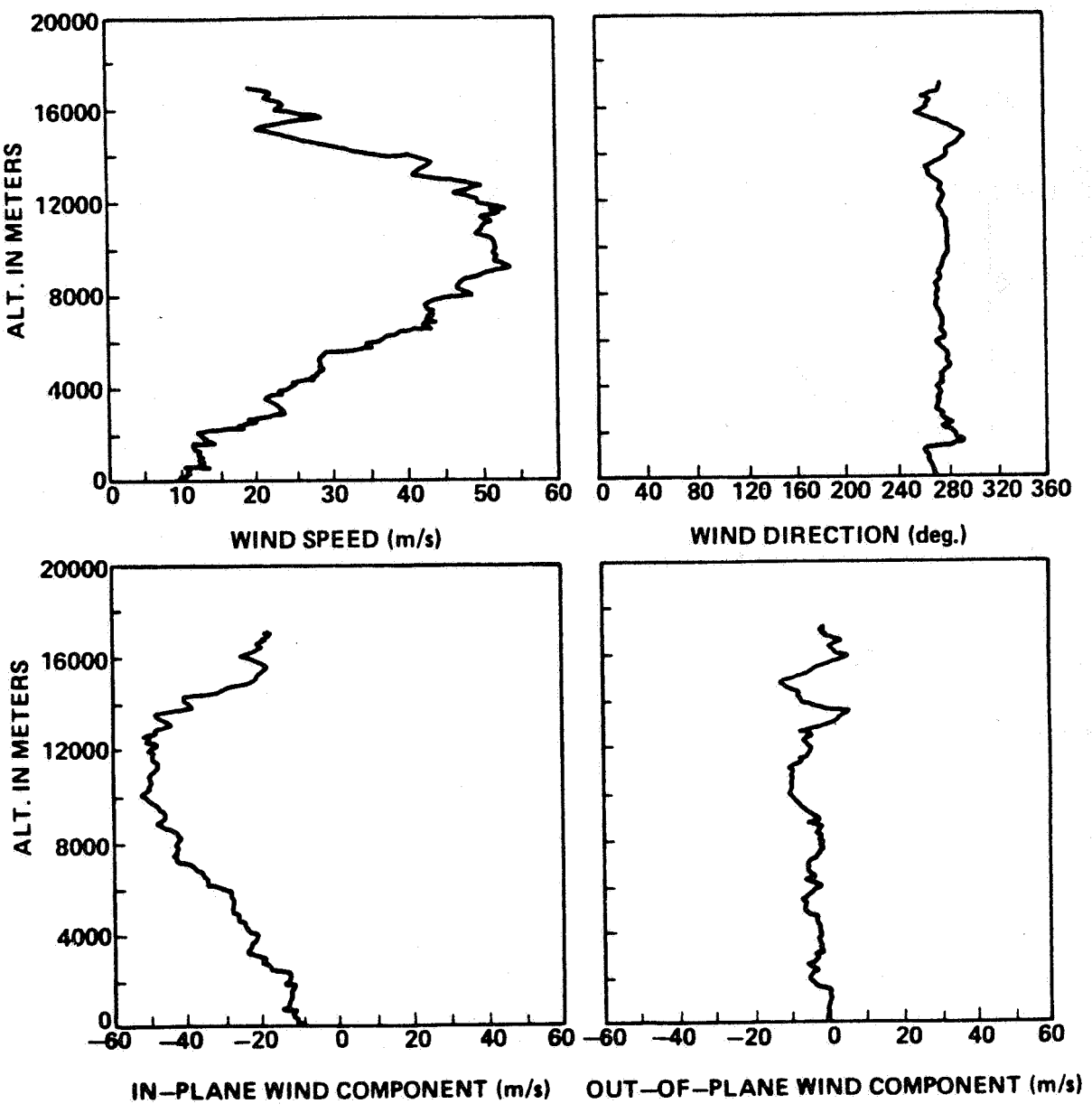

Figure A-41. STS-13 prelaunch/launch jimsphere profiles of wind speed, wind direction, in-plane and out-of-plane wind components, 0058 GMT April 6, 1984.

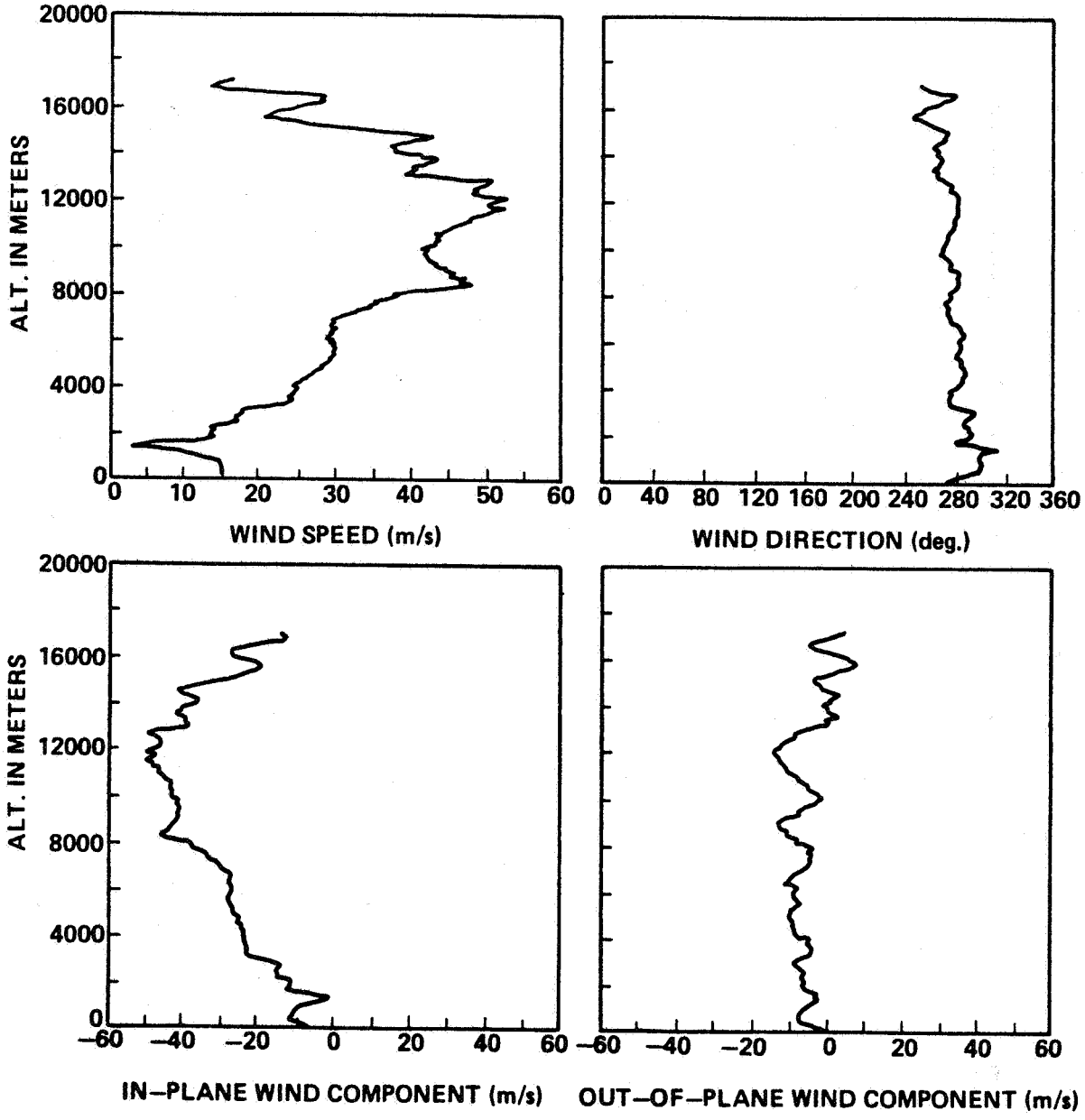

Figure A-42. STS-13 prelaunch/launch jimsphere profiles of wind speed, wind direction, in-plane and out-of-plane wind components, 0643 GMT April 6, 1984.

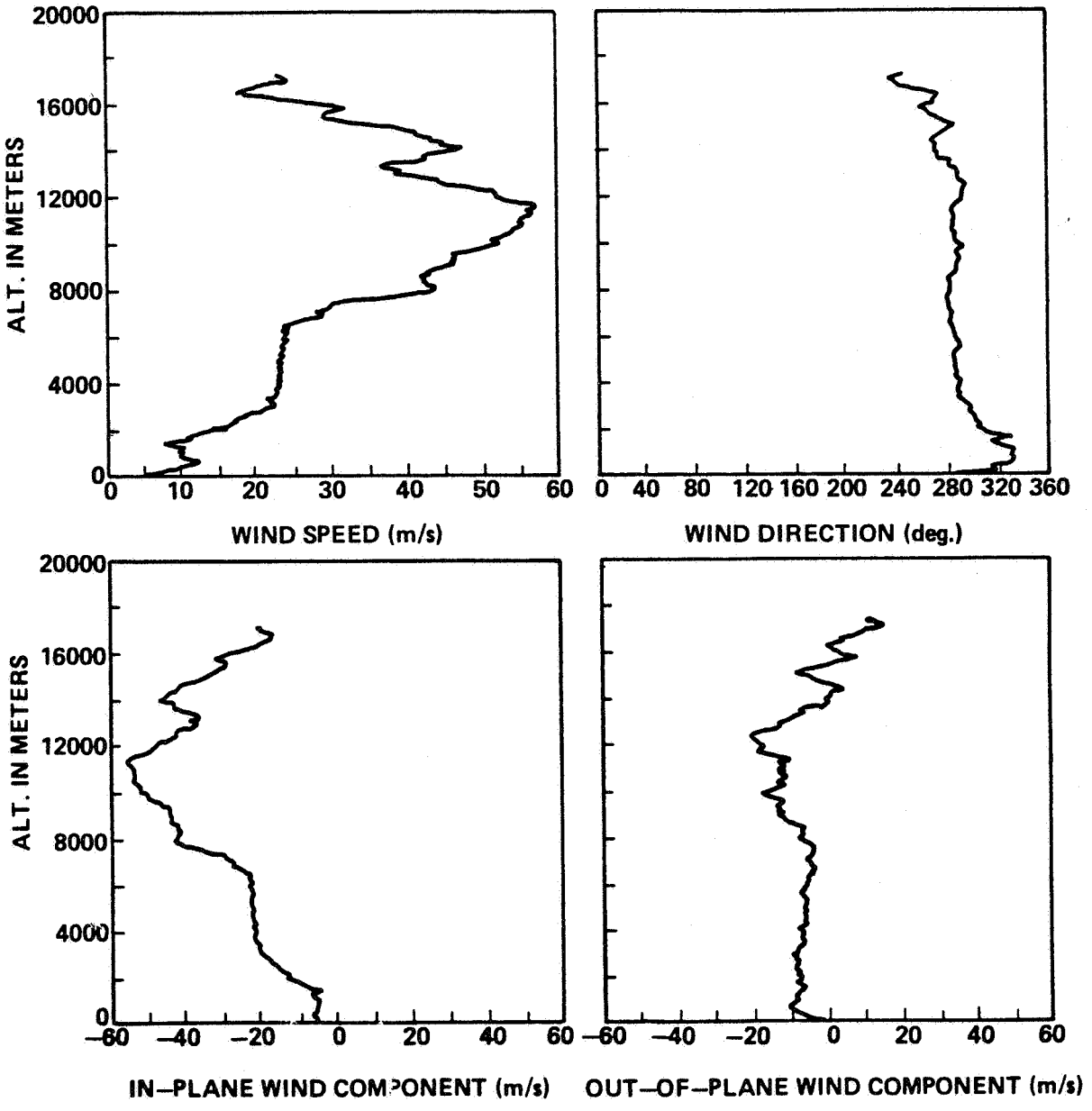

Figure A-43. STS-13 prelaunch/launch jimsphere profiles of wind speed, wind direction, in-plane and out-of-plane wind components, 1028 GMT April 6, 1984.

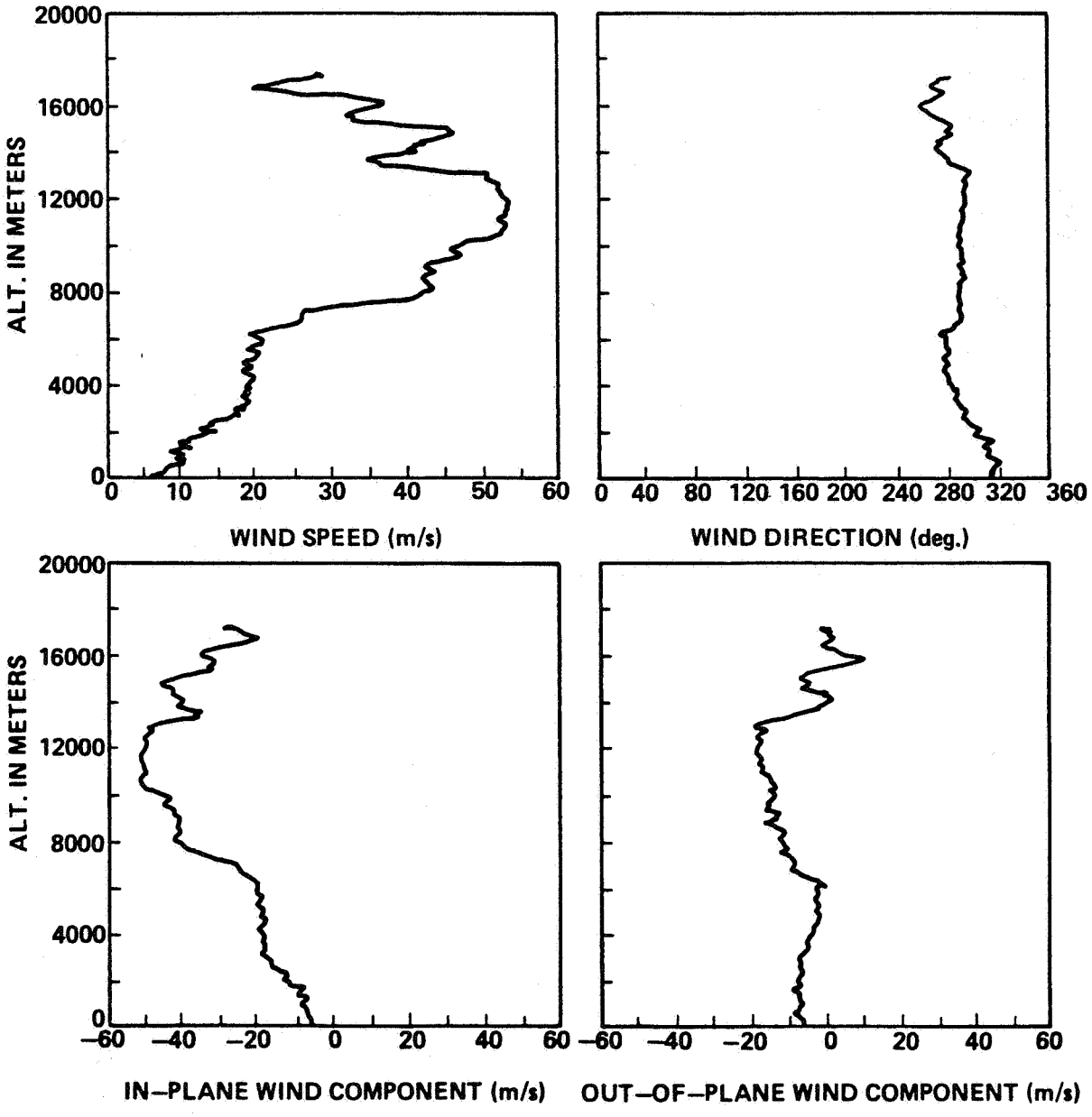

Figure A-44. STS-13 prelaunch/launch jimsphere profiles of wind speed, wind direction, in-plane and out-of-plane wind components, 1413 GMT April 6, 1984.

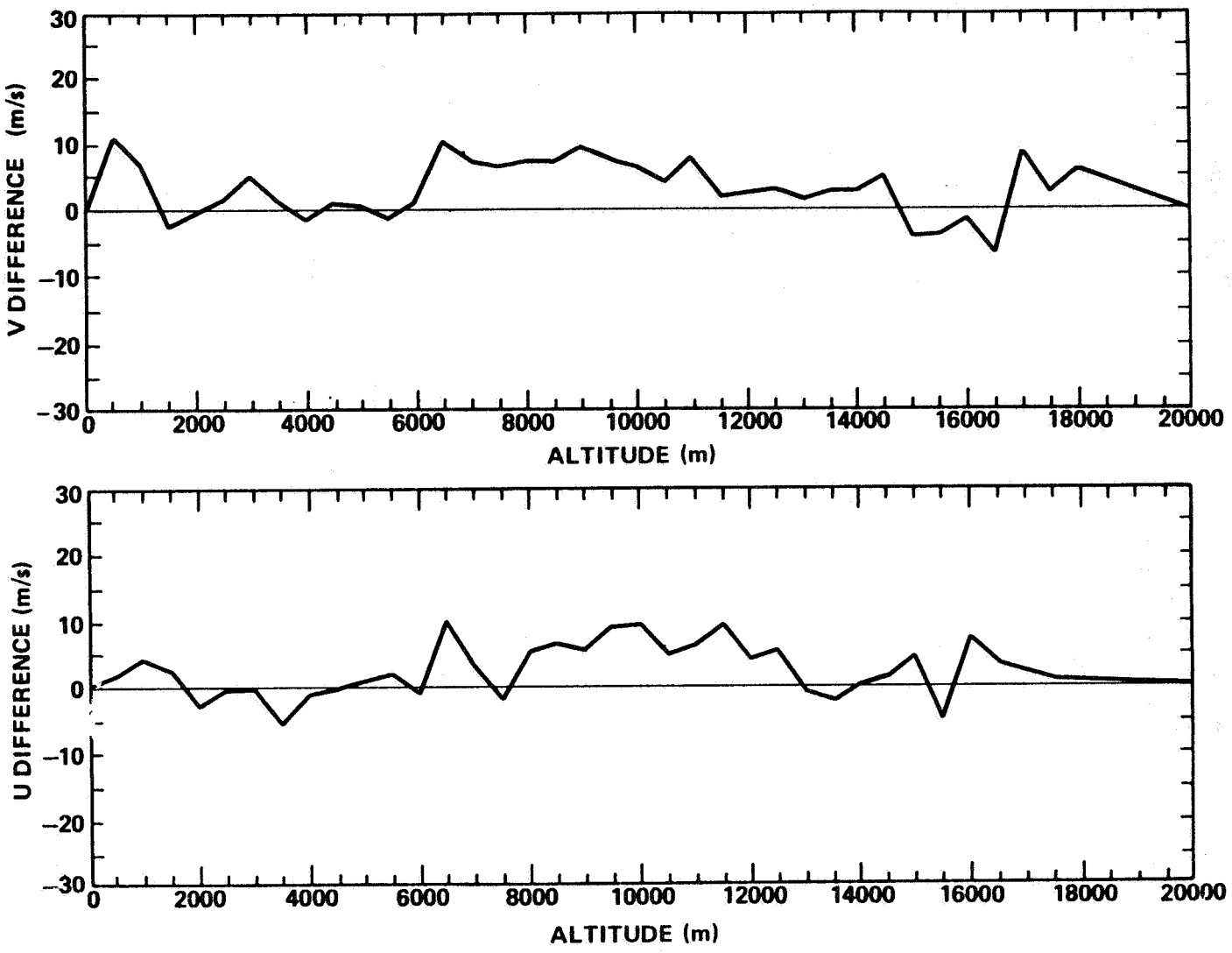

Figure A-45. Jimsphere-measured wind component changes (u,v) observed at Kennedy Space Center, Florida, between 0200 GMT and 0430 GMT November 12, 1981, during NASA's STS-2 countdown.

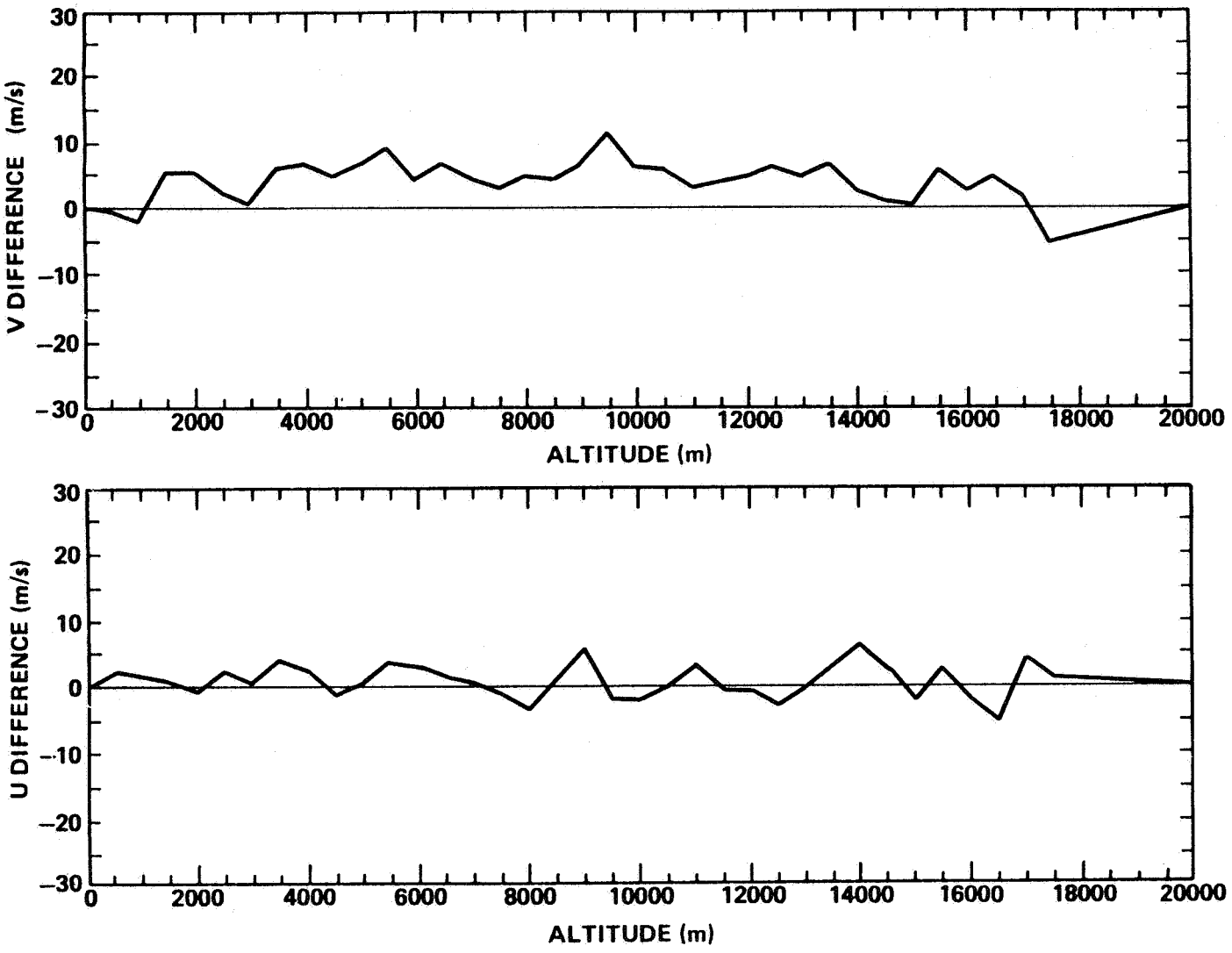

Figure A-46. Jimsphere-measured wind component changes (u,v) observed at Kennedy Space Center, Florida, between 0430 GMT and 0800 GMT November 12, 1981, during NASA's STS-2 countdown.

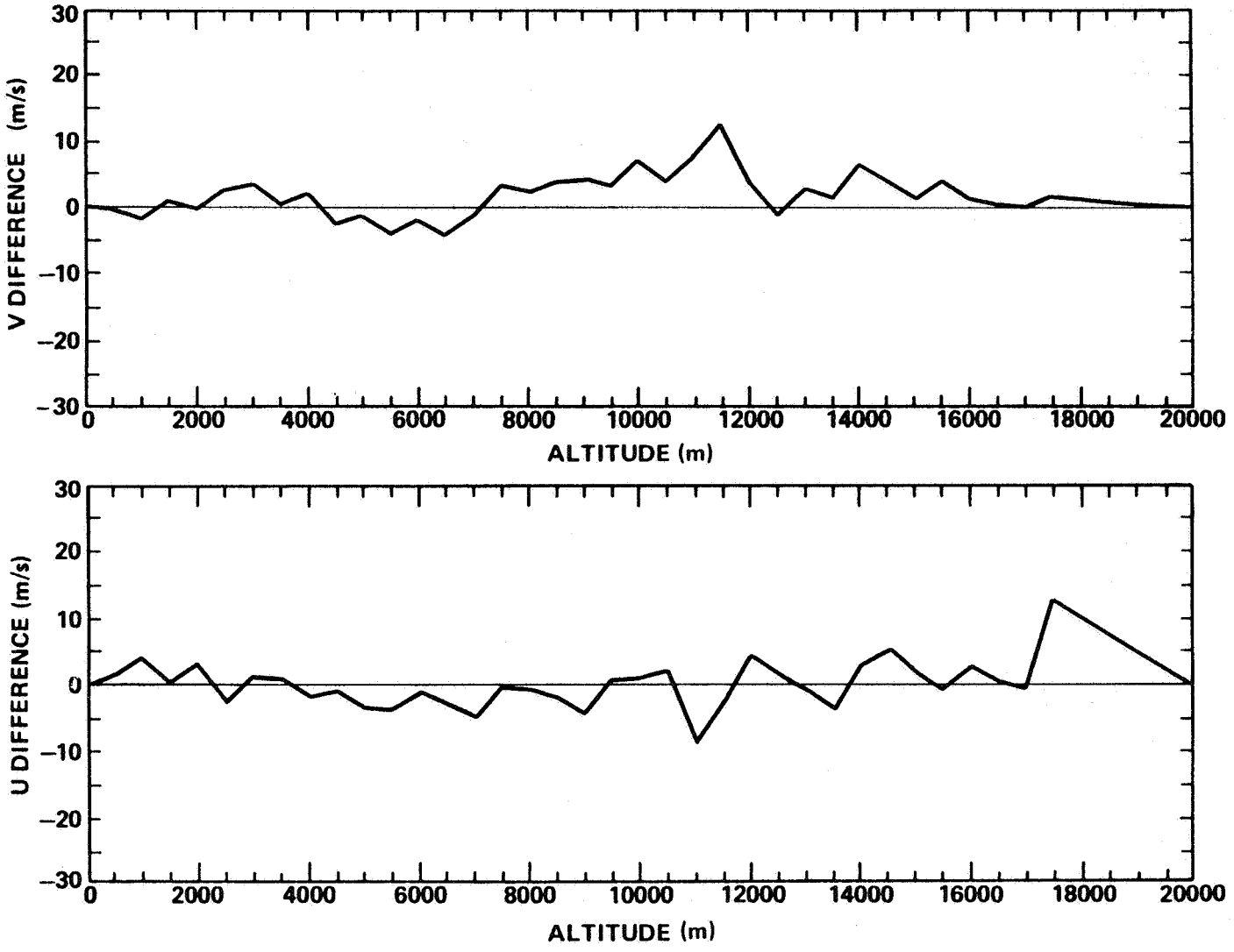

Figure A-47. Jimsphere-measured wind component changes (u,v) observed at Kennedy Space Center, Florida, between 0800 GMT and 1130 GMT November 12, 1981, during NASA's STS-2 countdown.

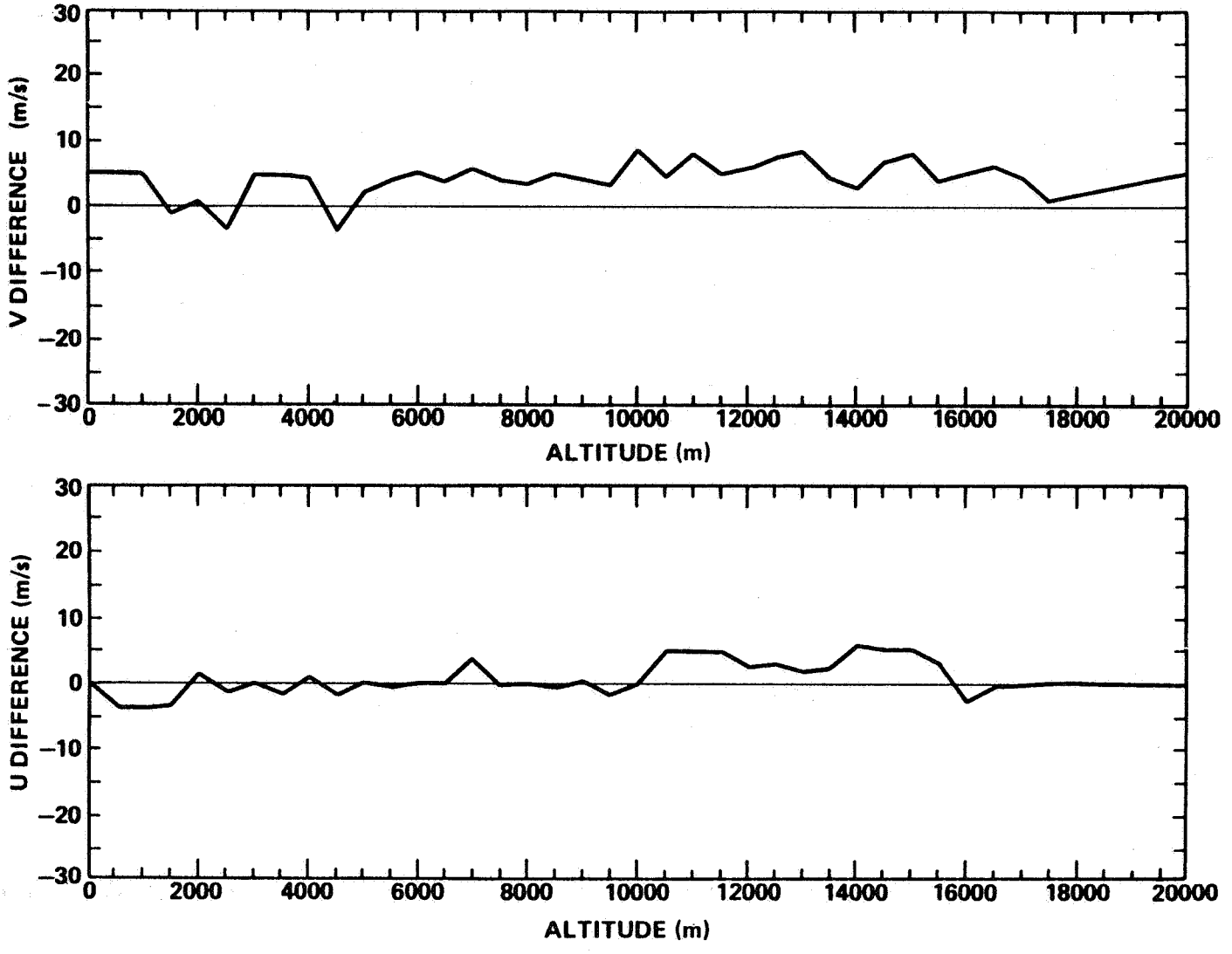

Figure A-48. Jimsphere-measured wind component changes (u,v) observed at Kennedy Space Center, Florida, between 1230 GMT and 1417 GMT March 22, 1982, during NASA's STS-3 countdown.

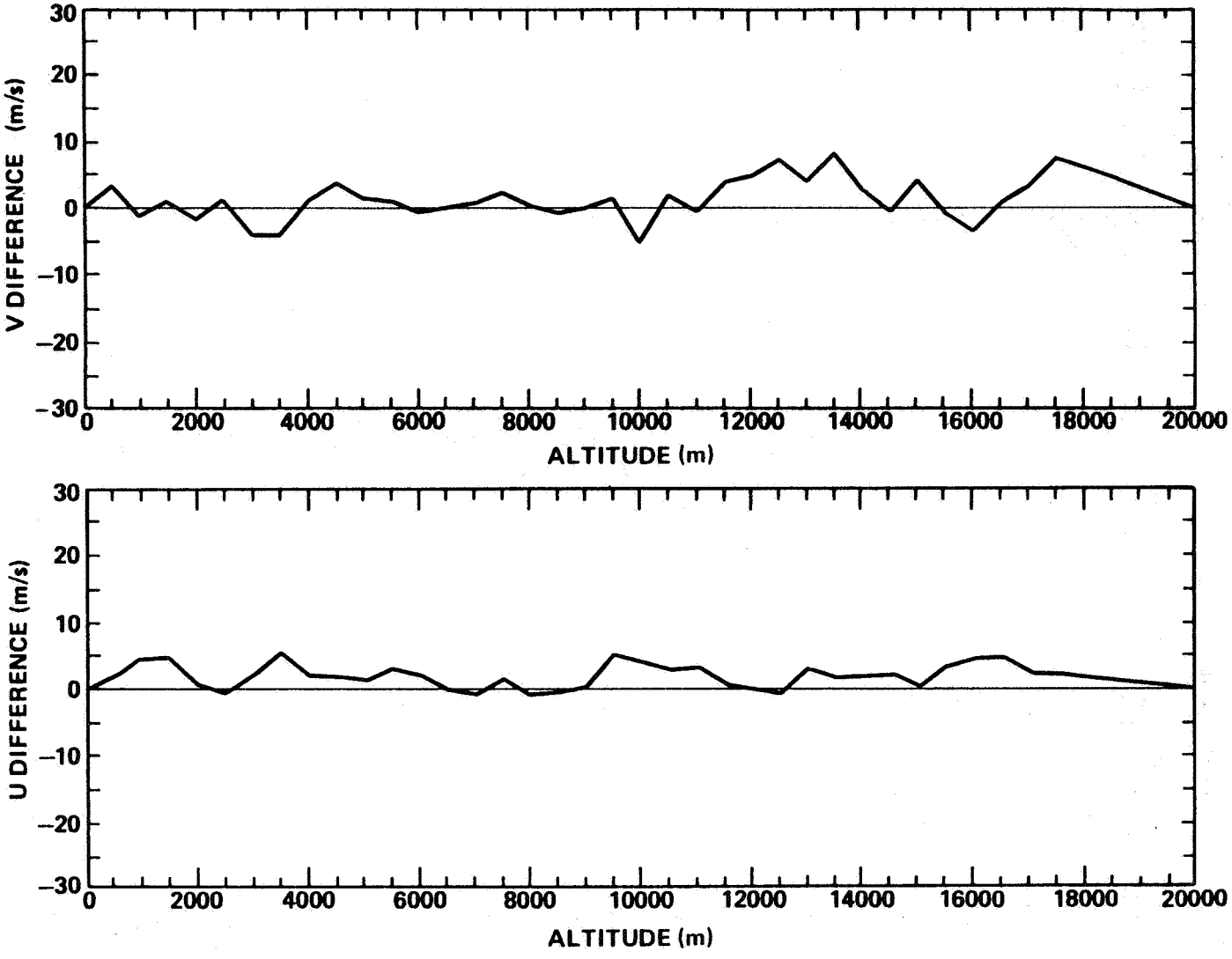

Figure A-49. Jimsphere-measured wind component changes (u,v) observed at Kennedy Space Center, Florida, between 0200 GMT and 1430 GMT March 22, 1982, during NASA's STS-3 countdown.

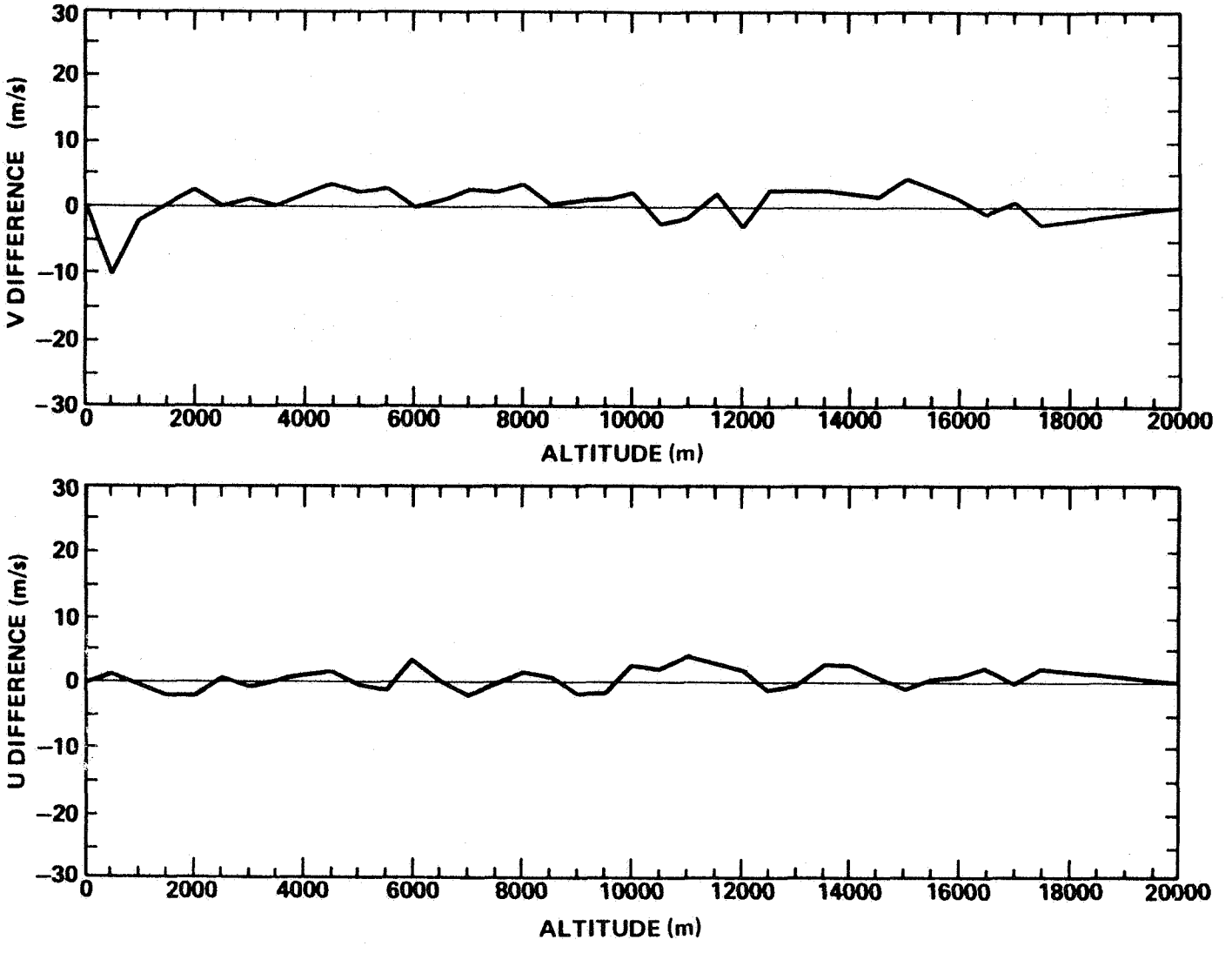

Figure A-50. Jimsphere-measured wind component changes (u,v) observed at Kennedy Space Center, Florida, between 0430 GMT and 0800 GMT March 22, 1982, during NASA's STS-3 countdown.

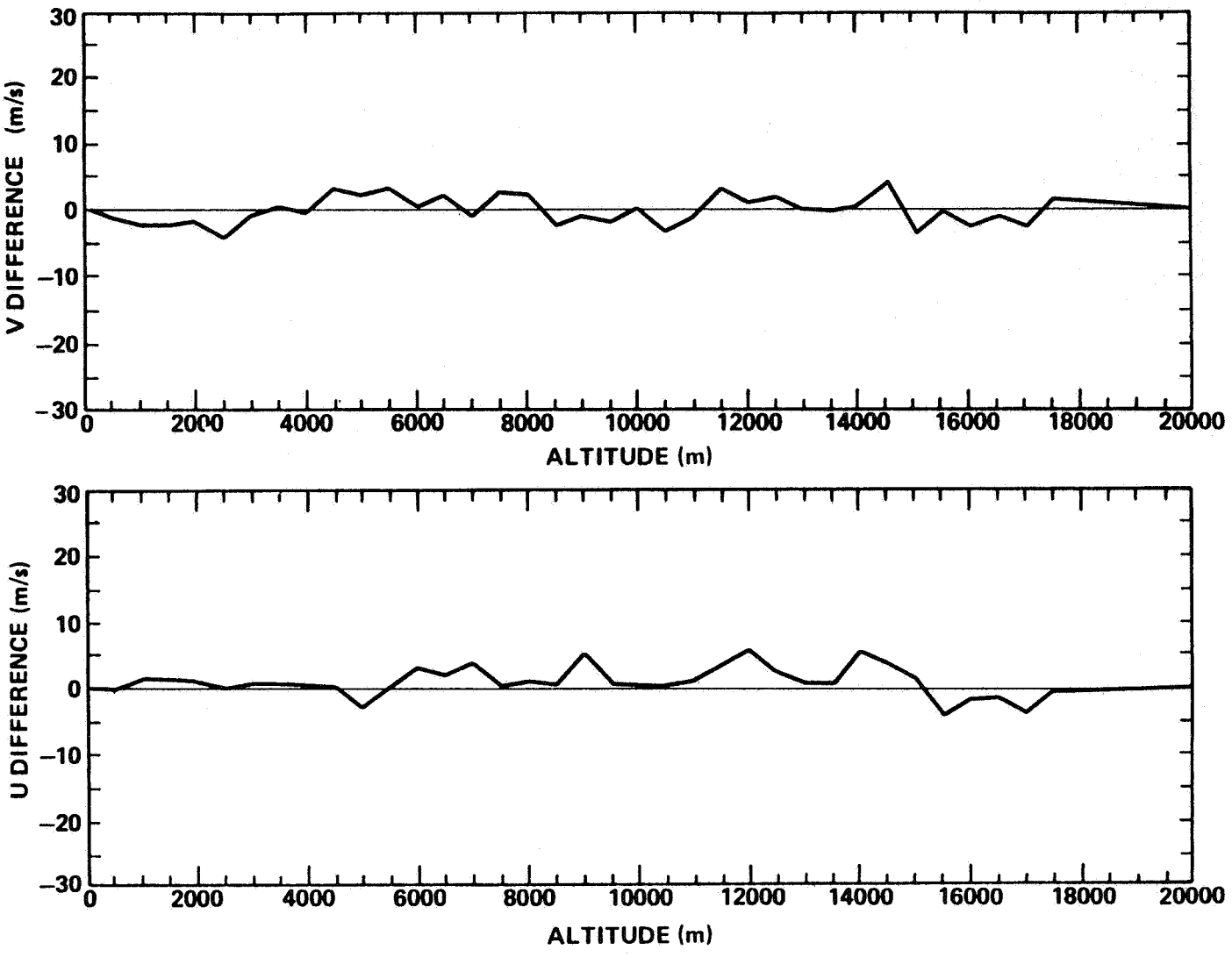

Figure A-51. Jimsphere-measured wind component changes (u,v) observed at Kennedy Space Center, Florida, between 0100 GMT and 0330 GMT June 27, 1982, during NASA's STS-4 countdown.

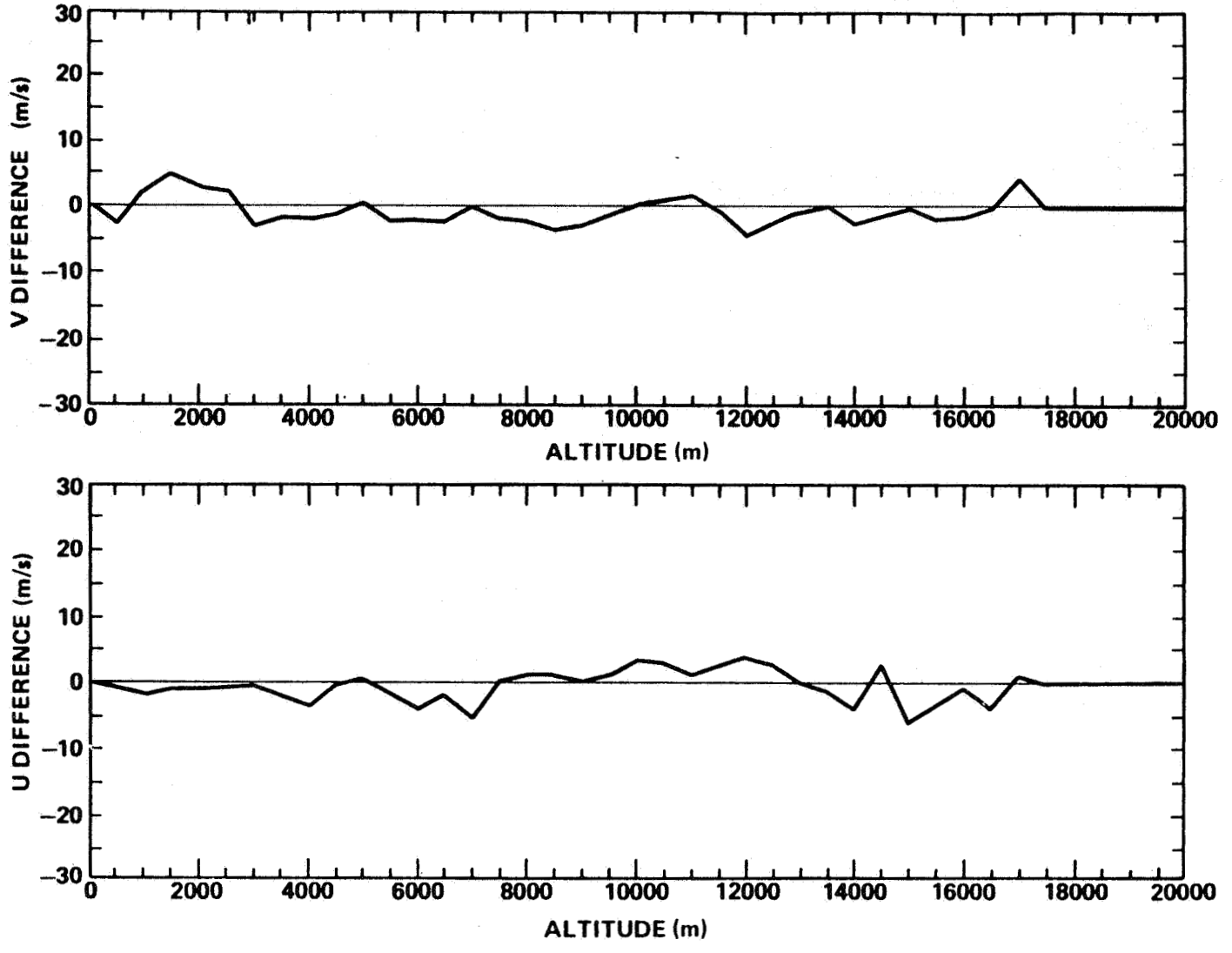

Figure A-52. Jimsphere-measured wind component changes (u,v) observed at Kennedy Space Center, Florida, between 0330 GMT and 0745 GMT June 27, 1982, during NASA's STS-4 countdown.

C-2

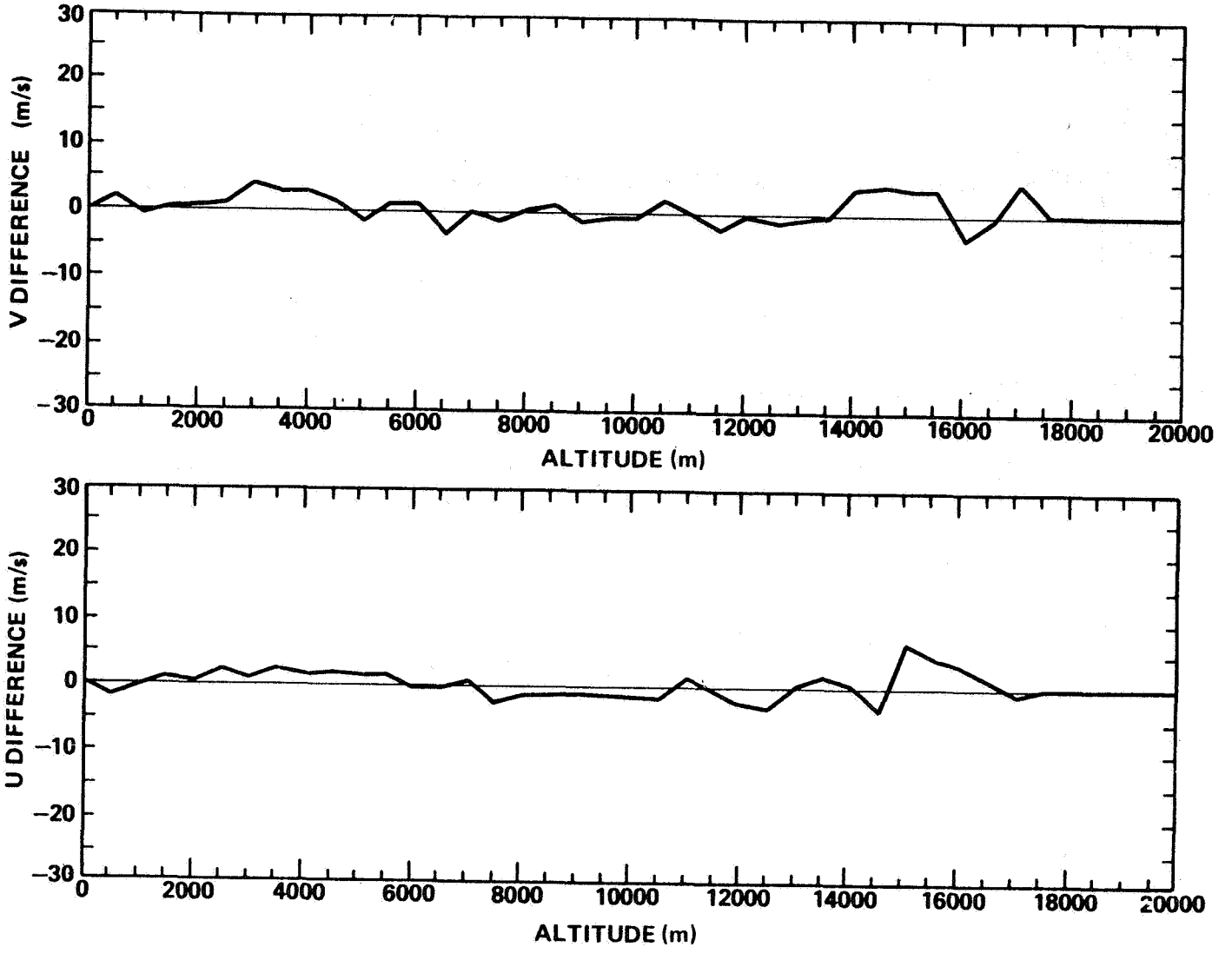

Figure A-53. Jimsphere-measured wind component changes (u,v) observed at Kennedy Space Center, Florida, between 0745 GMT and 1130 GMT June 27, 1982, during NASA's STS-4 countdown.

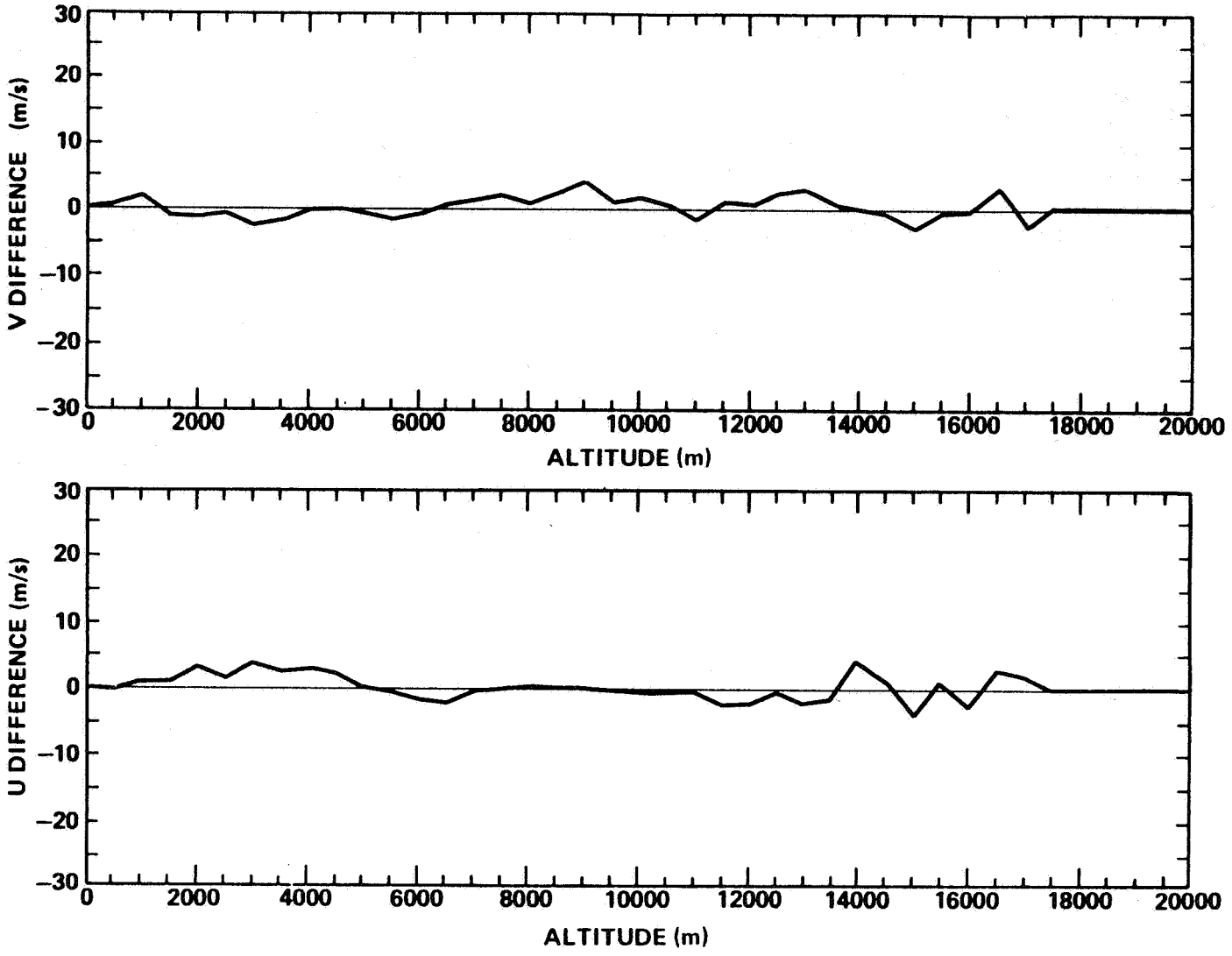

Figure A-54. Jimsphere-measured wind component changes (u,v) observed at Kennedy Space Center, Florida, between 1130 GMT and 1515 GMT June 27, 1982, during NASA's STS-4 countdown.

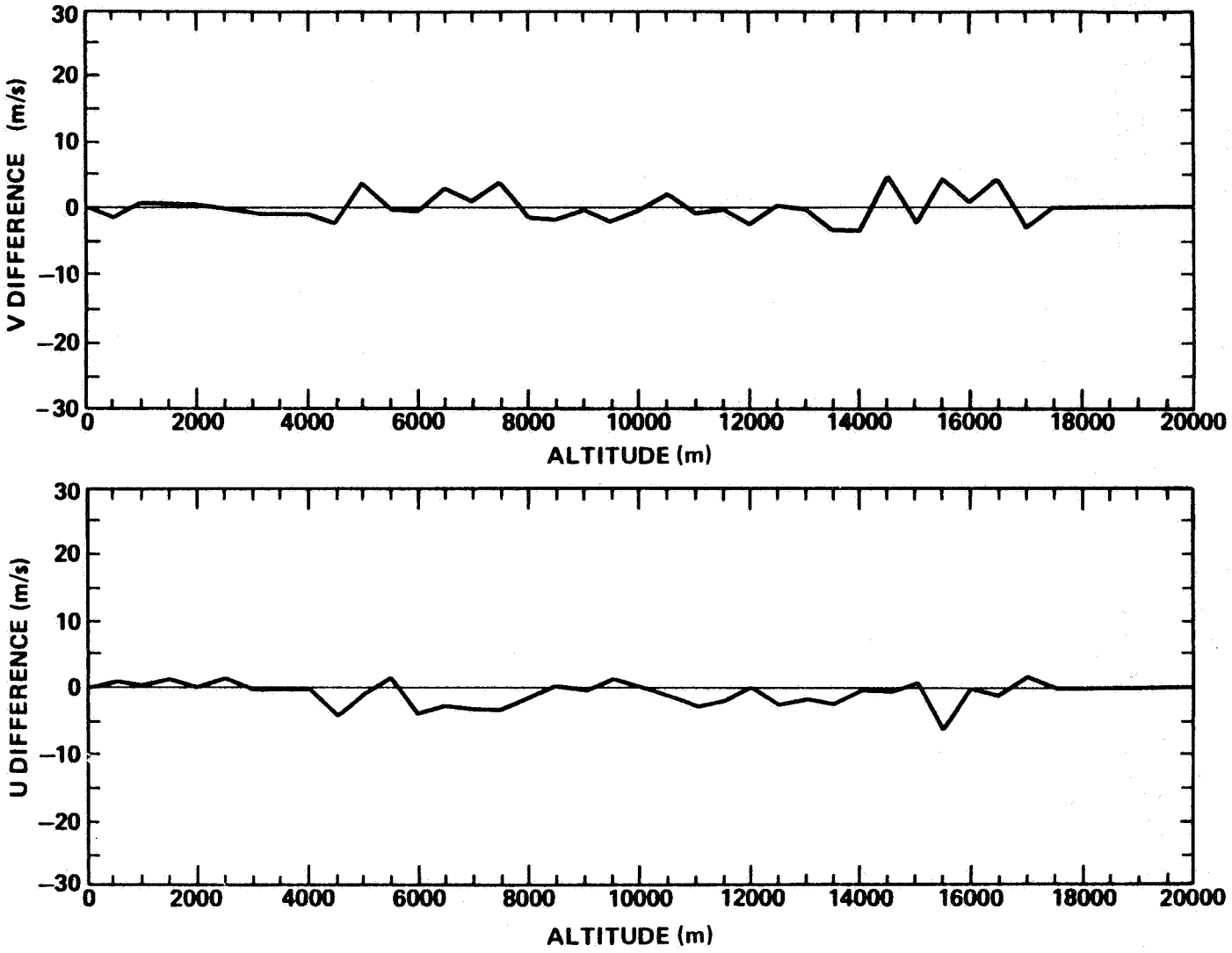

Figure A-55. Jimsphere-measured wind component changes (u,v) observed at Kennedy Space Center, Florida, between 2219 GMT and 0019 GMT November 10 and 11, 1982, during NASA's STS-5 countdown.

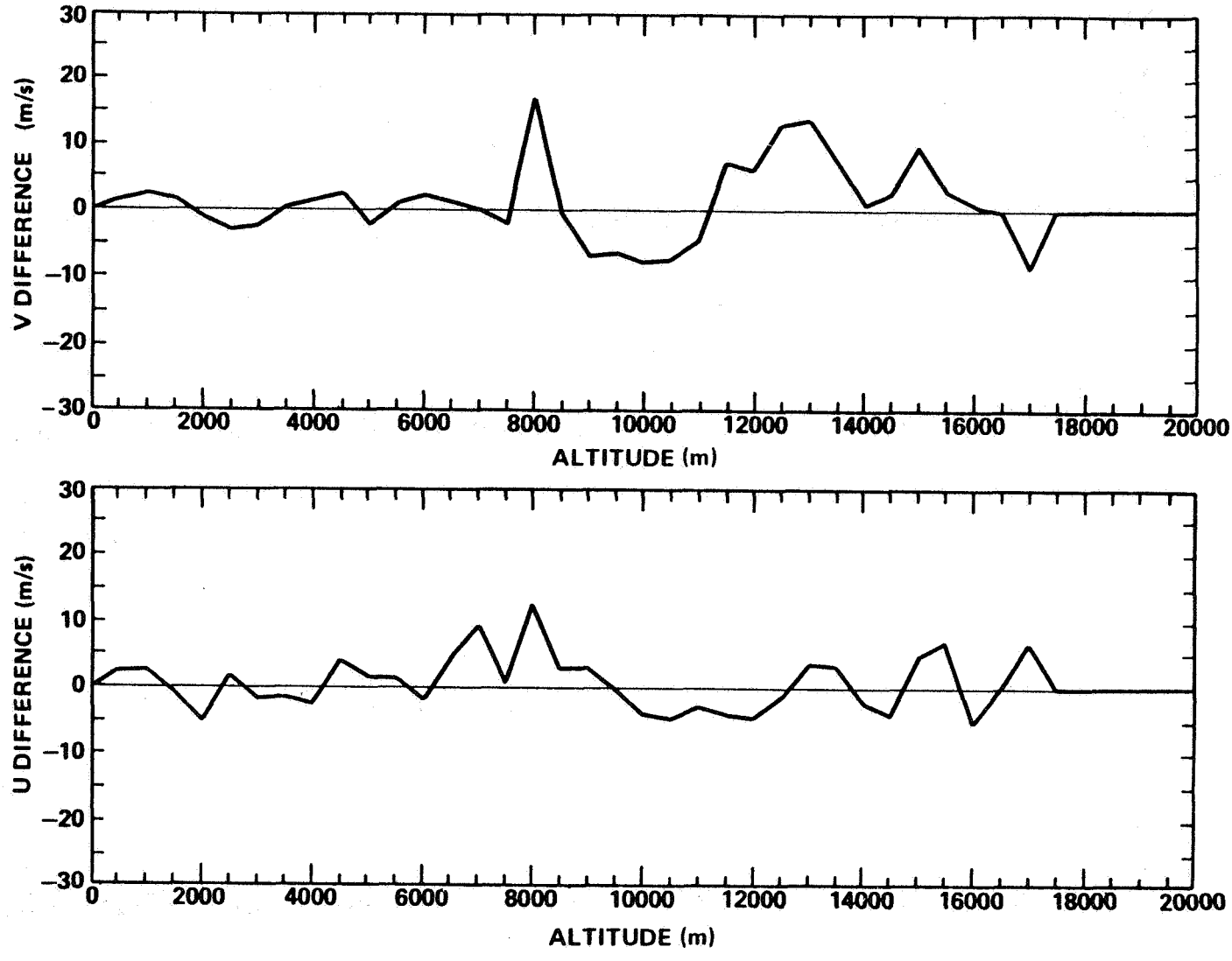

Figure A-56. Jimsphere-measured wind component changes (u,v) observed at Kennedy Space Center, Florida, between 0504 GMT and 0849 GMT November 11, 1982, during NASA's STS-5 countdown.

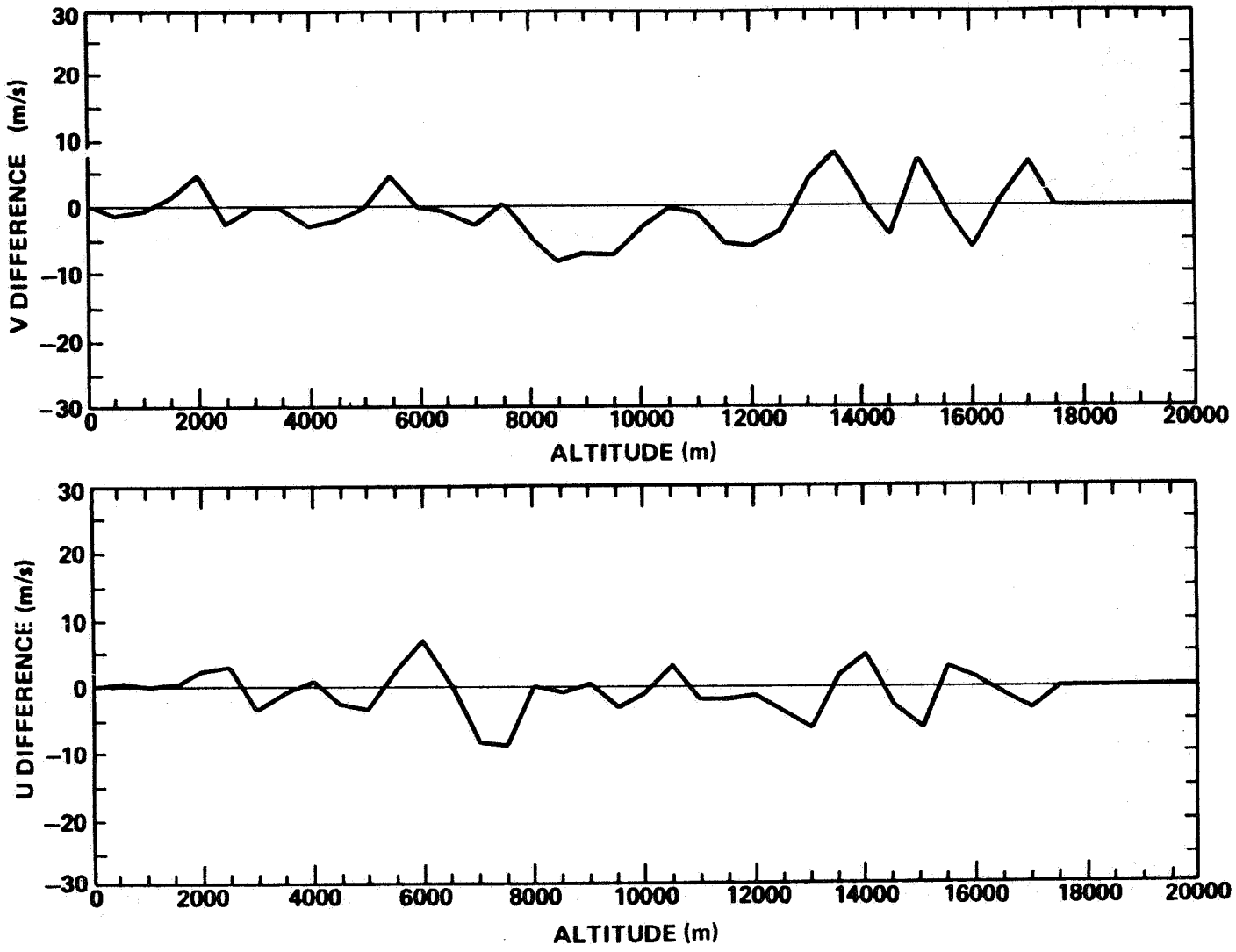

Figure A-57. Jimsphere-measured wind component changes (u,v) observed at Kennedy Space Center, Florida, between 0849 GMT and 1235 GMT November 11, 1982, during NASA's STS-5 countdown.

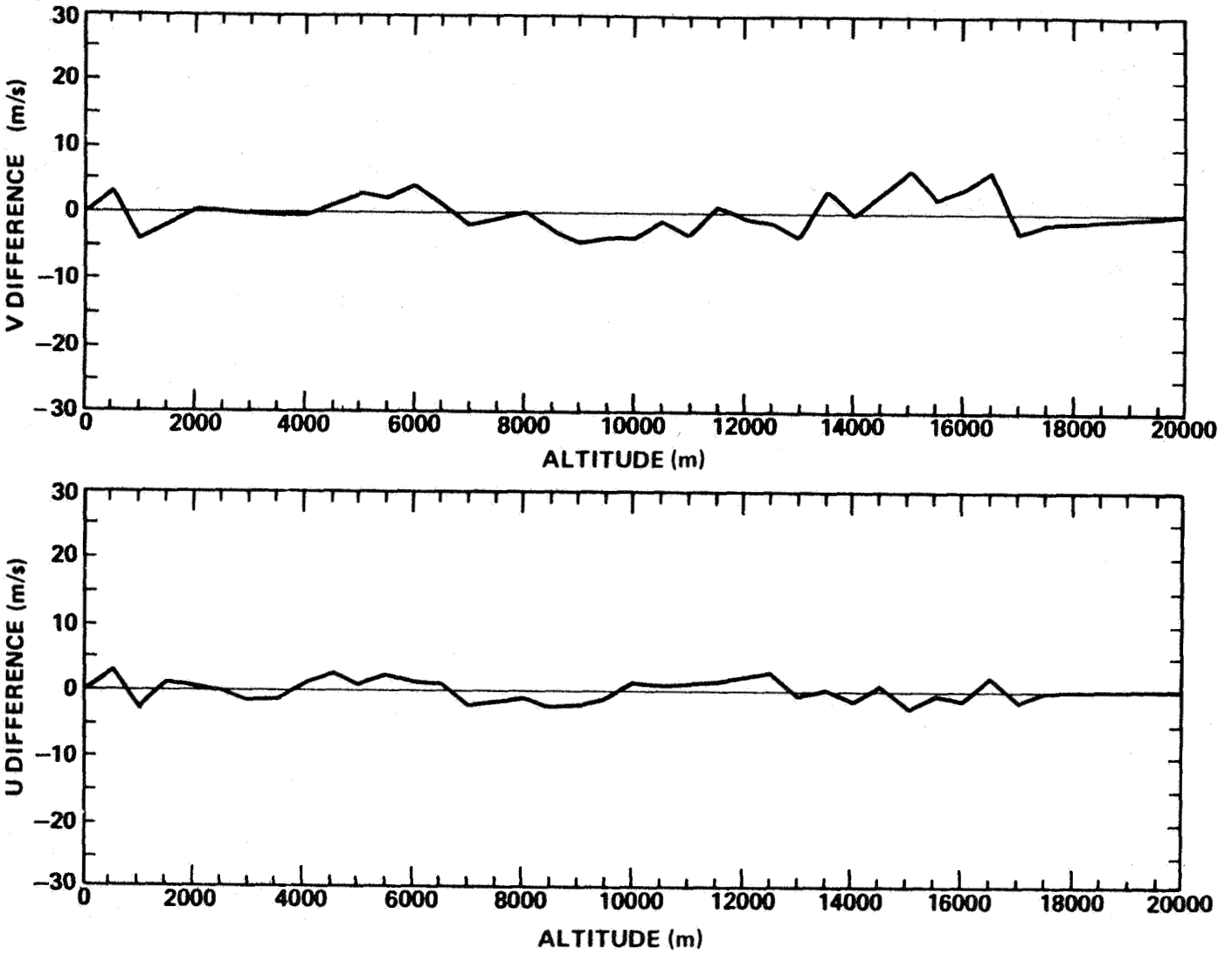

Figure A-58. Jimsphere-measured wind component changes (u,v) observed at Kennedy Space Center, Florida, between 0430 GMT and 0630 GMT April 4, 1983, during NASA's STS-6 countfown.

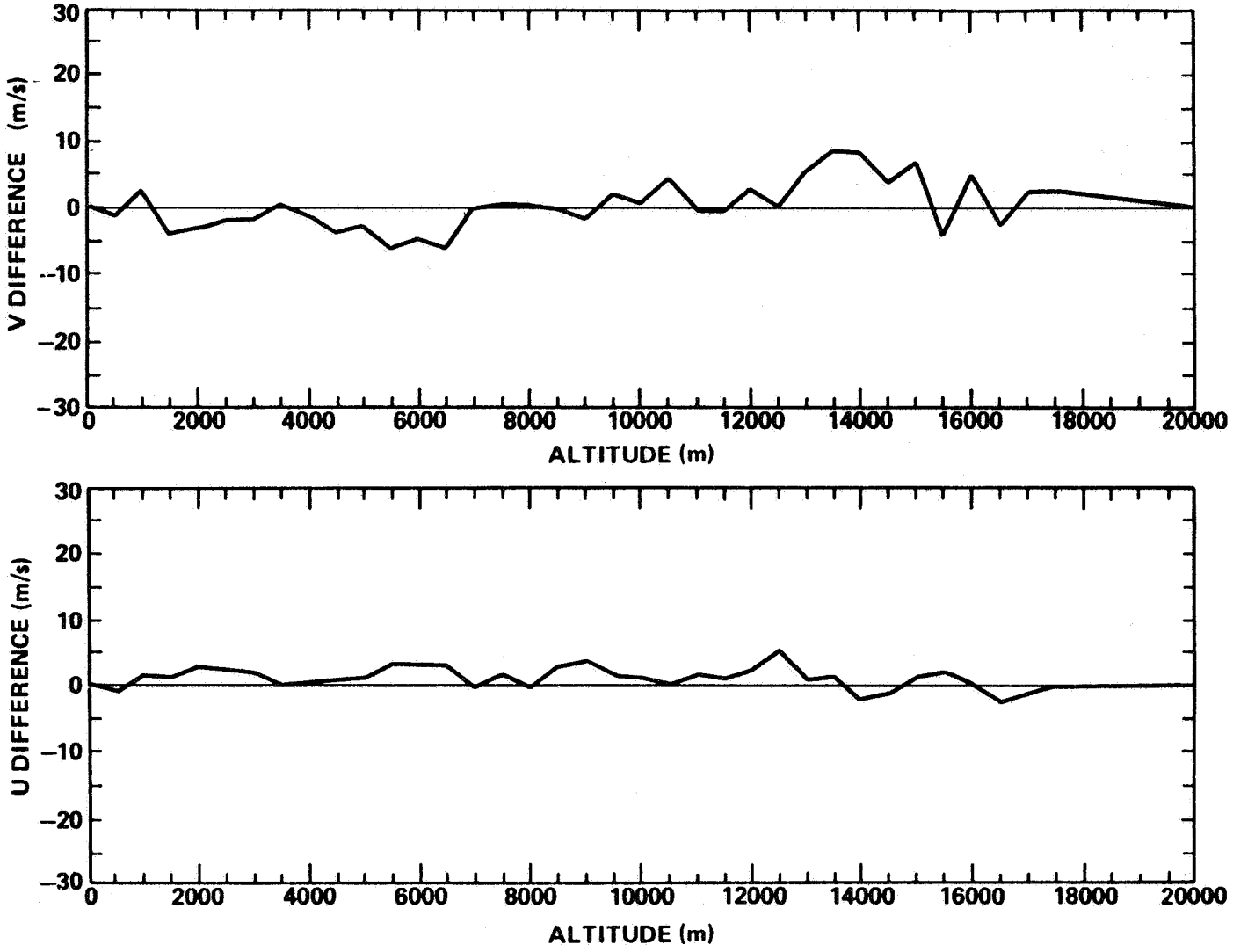

Figure A-59. Jimsphere-measured wind component changes (u,v) observed at Kennedy Space Center, Florida, between 1145 GMT and 1515 GMT April 4, 1983, during NASA's STS-6 countdown.

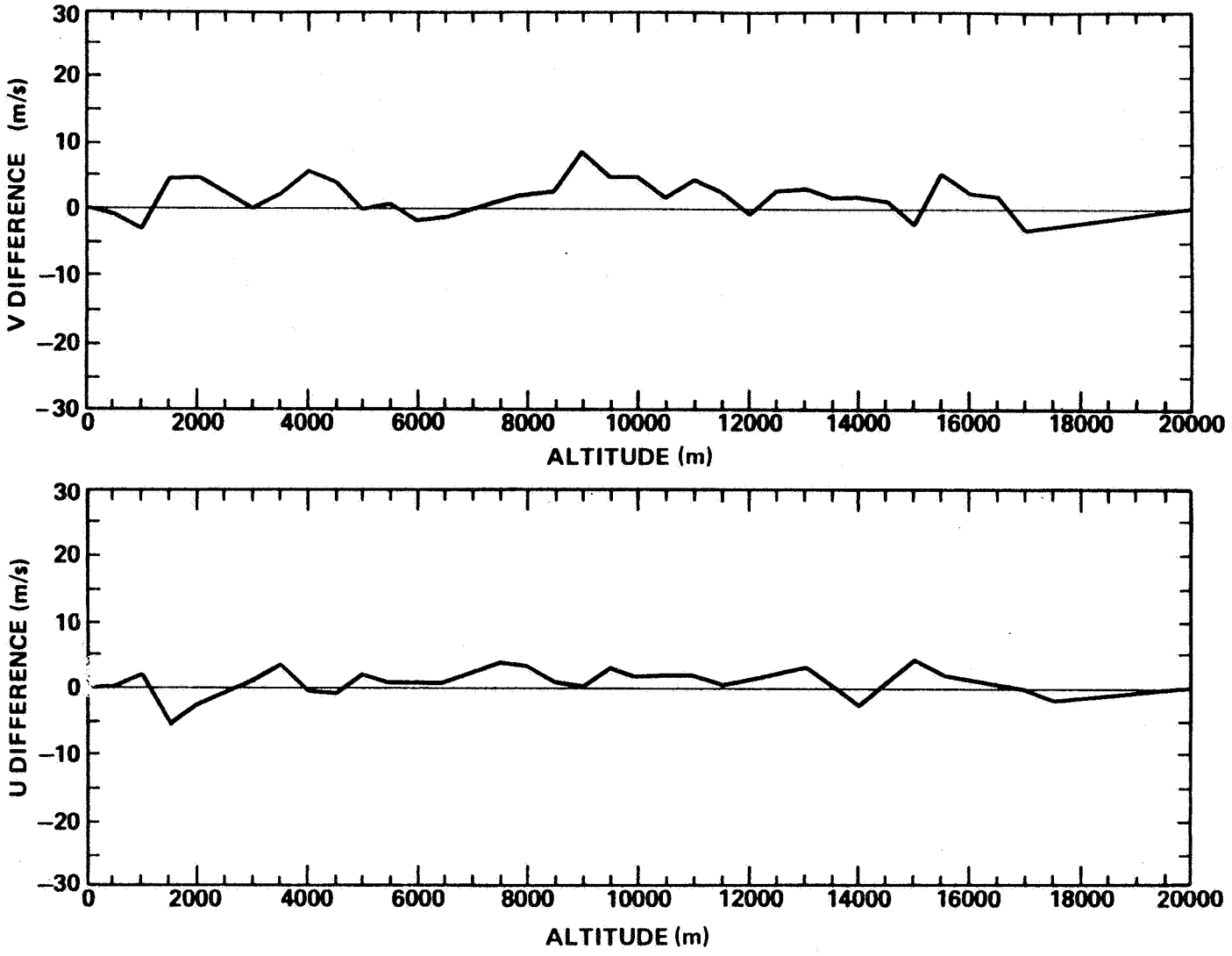

Figure A-60. Jimsphere-measured wind component changes (u,v) observed at Kennedy Space Center, Florida, between 1515 GMT and 1845 GMT April 4, 1983, during NASA's STS-6 countdown.

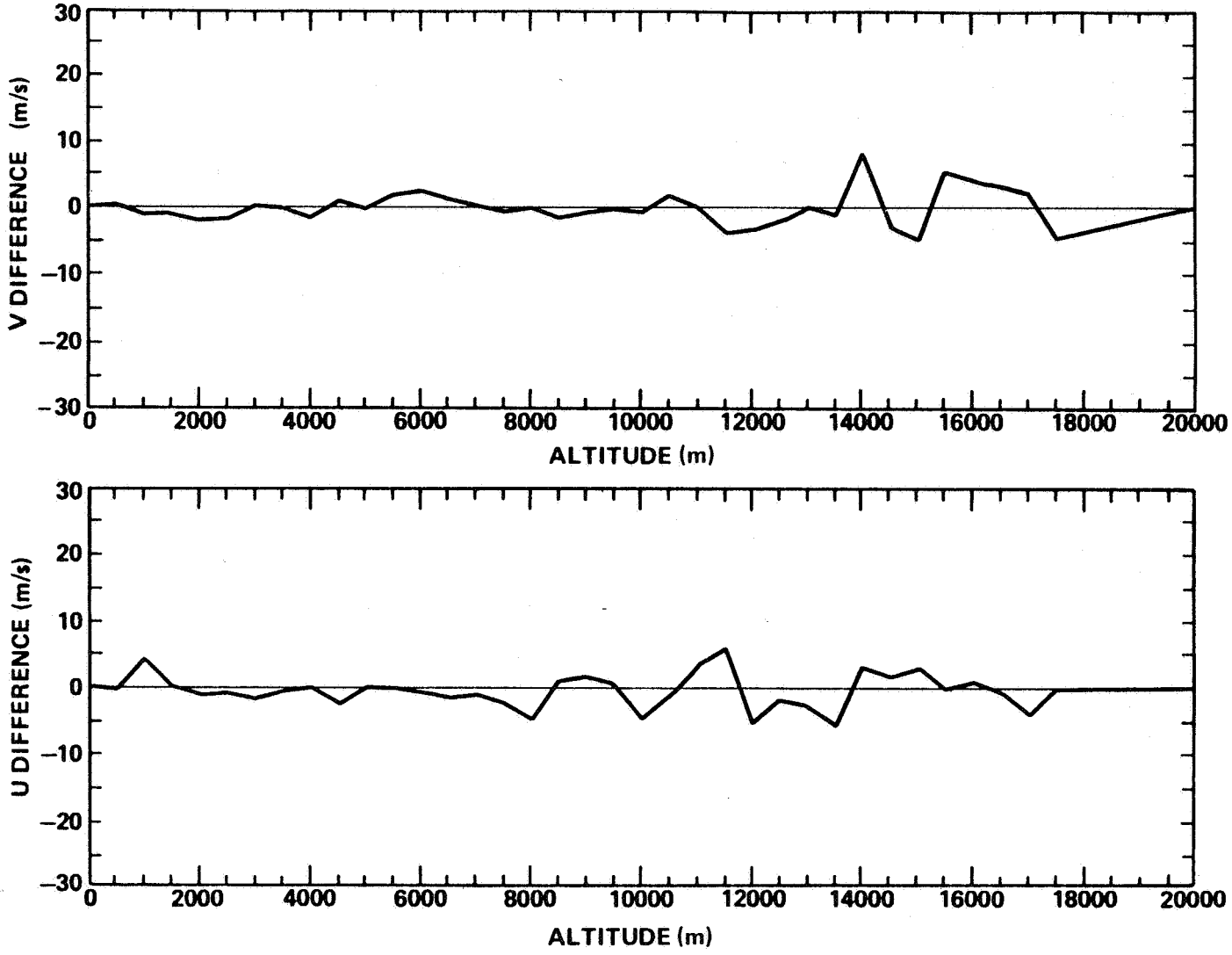

Figure A-61. Jimsphere-measured wind component changes (u,v) observed at Kennedy Space Center, Florida, between 0803 GMT and 1150 GMT June 18, 1983, during NASA's STS-7 countdown.

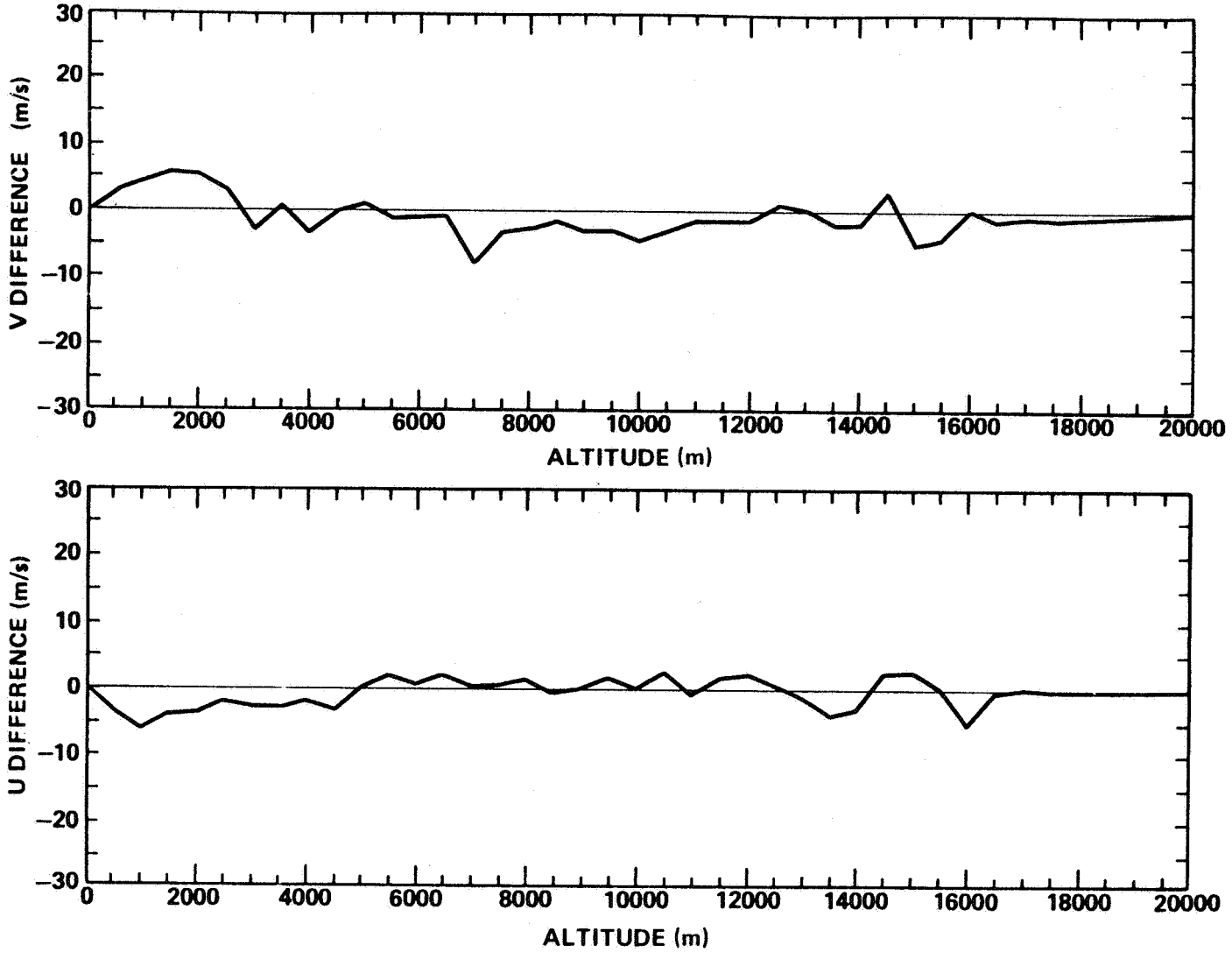

Figure A-62. Jimsphere-measured wind component changes (u,v) observed at Kennedy Space Center, Florida, between 0845 GMT and 1230 GMT November 28, 1983, during NASA's STS-9 countdown.

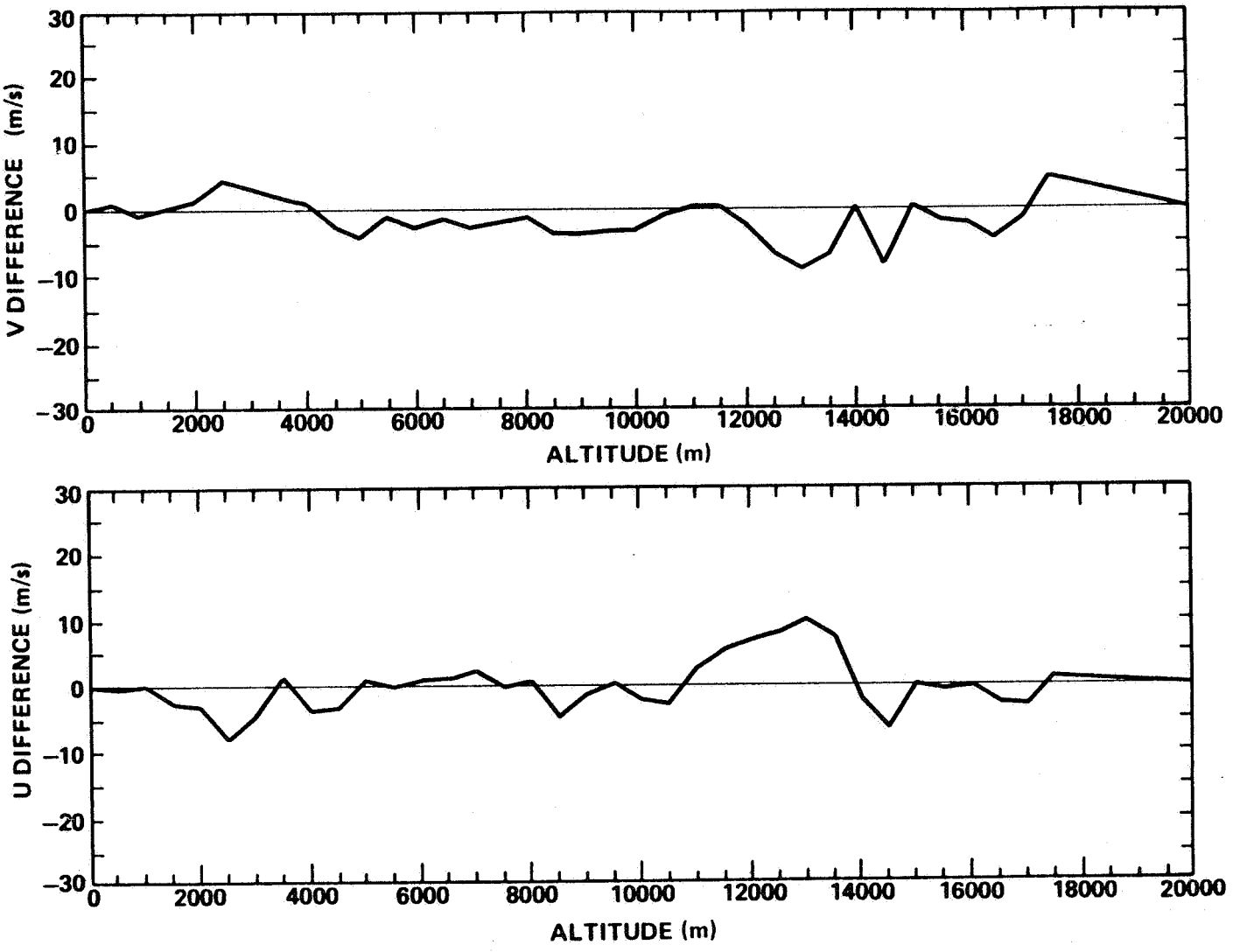

Figure A-63. Jimsphere-measured wind component changes (u,v) observed at Kennedy Space Center, Florida, between 1230 GMT and 1615 GMT November 29, 1983, during NASA's STS-9 countdown.

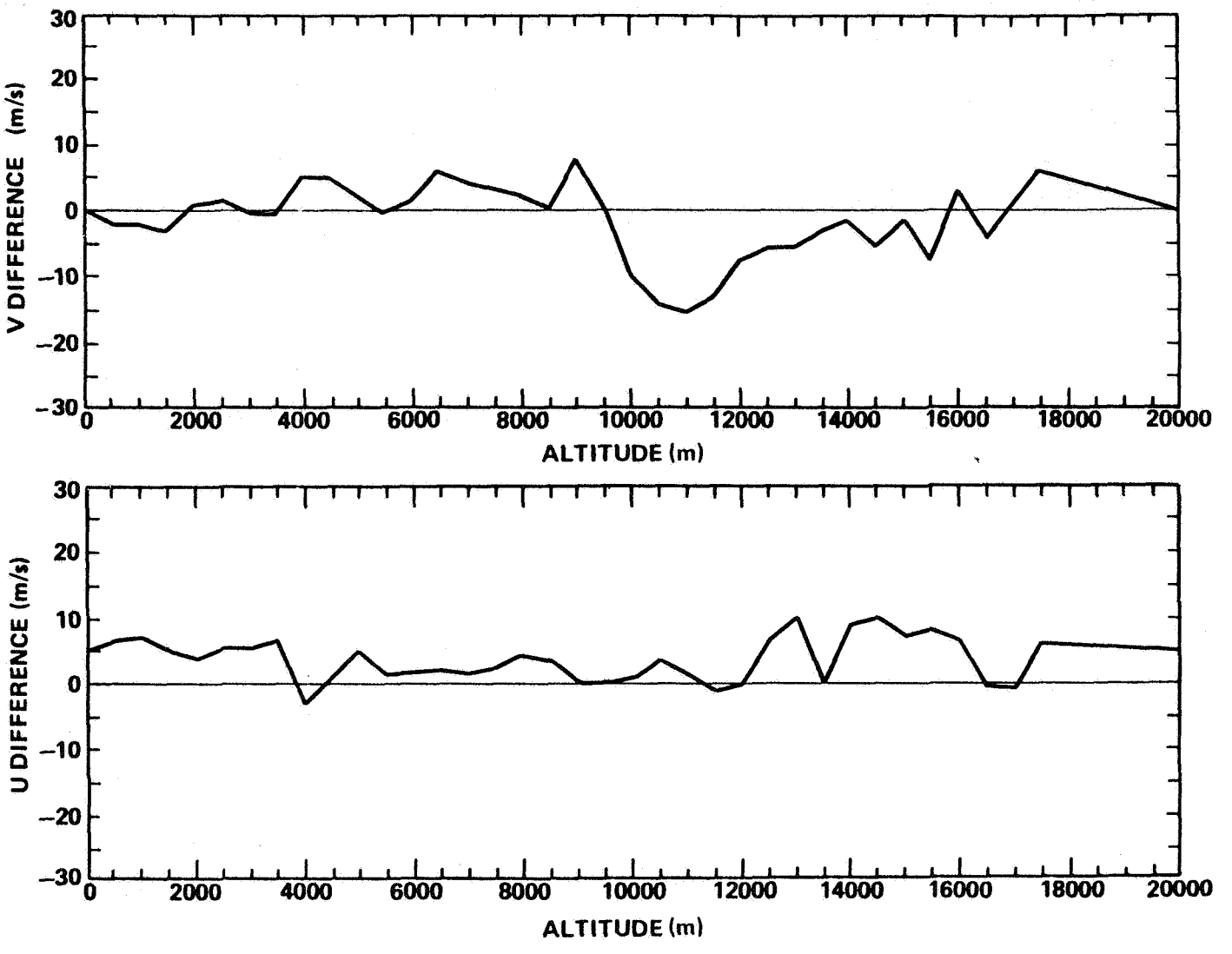

Figure A-64. Jimsphere-measured wind component changes (u,v) observed at Kennedy Space Center, Florida, between 0930 GMT and 1320 GMT February 3, 1984, during NASA's STS-11 countdown.

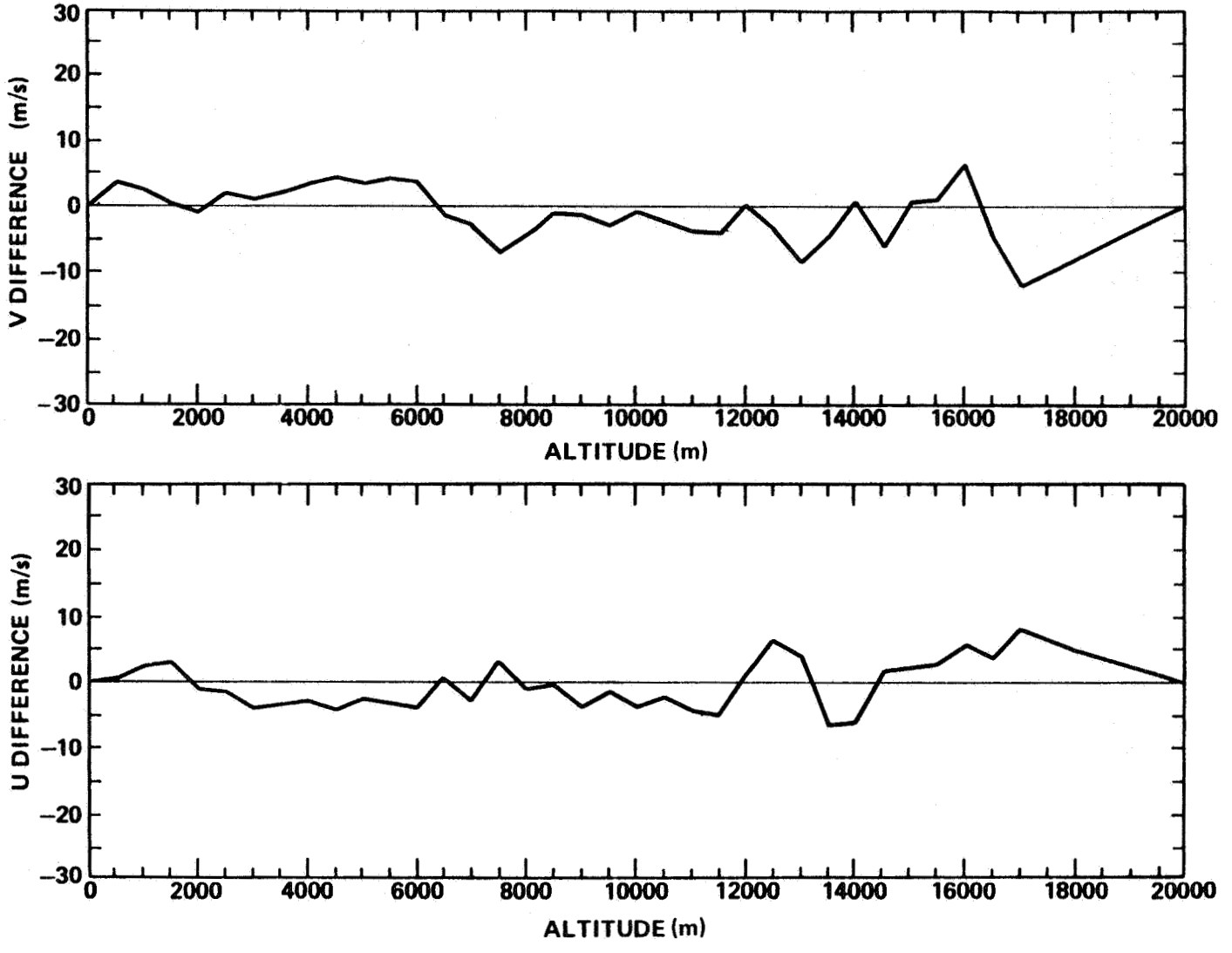

Figure A-65. Jimsphere-measured wind component changes (u,v) observed at Kennedy Space Center, Florida, between 1028 GMT and 1413 GMT April 6, 1984, during NASA's STS-13 countdown.

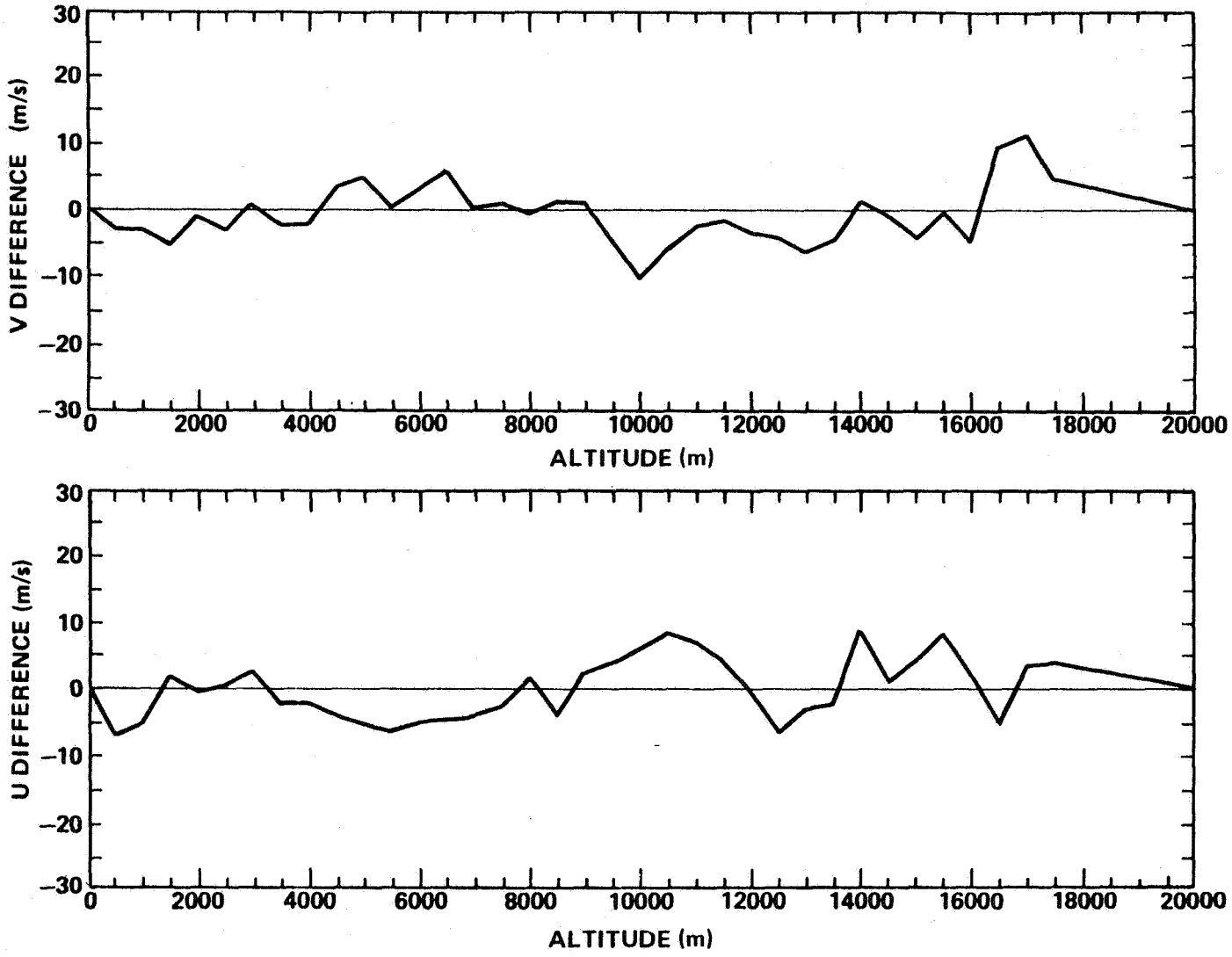

Figure A-66. Jimsphere-measured wind component changes (u,v) observed at Kennedy Space Center, Florida, between 0643 GMT and 1028 GMT April 6, 1984, during NASA's STS-13 countdown.

1. REPORT NO.	2. GOVERNMENT ACCESSION NO.	3. RECIPIENT'S CATALOG NO.
NASA TP -2573		

4. TITLE AND SUBTITLE	5. REPORT DATE
Analysis of Jimsphere Pairs for Use in Assessing Space Vehicle Ascent Capability	March 1986
	6. PERFORMING ORGANIZATION CODE
7. AUTHOR(S)	8. PERFORMING ORGANIZATION REPORT #
Charles K. Hill	
9. PERFORMING ORGANIZATION NAME AND ADDRESS	10. WORK UNIT NO.
George C. Marshall Space Flight Center Marshall Space Flight Center, Alabama 35812	M-516
	11. CONTRACT OR GRANT NO.
	13. TYPE OF REPORT & PERIOD COVERED
12. SPONSORING AGENCY NAME AND ADDRESS	Technical Paper
National Aeronautics and Space Administration Washington, D.C. 20546	14. SPONSORING AGENCY CODE

15. SUPPLEMENTARY NOTES

Prepared by Systems Dynamics Laboratory, Science and Engineering Directorate.

16. ABSTRACT

The purpose of this research was to develop a data base of paired detailed wind profiles for use in evaluating Shuttle Transportation System (STS) ascent capability. Since launch decision is based on a wind measured about 3.5 hr before launch, a data base of paired detailed profiles is needed. Method and technique on the reduction process and analysis is also presented. Guidelines used in selecting the pairs of profiles were established to insure a valid and representative data base. σu values for 3.5 hr at 12 km altitude show 8 percent increase from the transition case to the winter case and 18 percent decrease from the transition case to the summer case. σv values for 3.5 hr at 12 km altitude shows 12 percent increase from the transition case to the winter case and 17 percent decrease from the transition case to the summer case. A special feature of the 7- and 10.5-hr cases is that σv increases by as much as 30 percent from the transition to the winter profiles. This large increase does not appear in the σu data. Comparisons of the calculated values of 3.5-hr standard deviations of u and v with actual component deviations measured during Space Shuttle launch conditions confirm that the statistical values are representative.

17. KEY WORDS	18. DISTRIBUTION STATEMENT
Wind Shear Wind Variability Space Shuttle Performance Temporal Variability of Wind	Unclassified-Unlimited Subject Category: 02

19. SECURITY CLASSIF. (of this report)	20. SECURITY CLASSIF. (of this page)	21. NO. OF PAGES	22. PRICE
Unclassified	Unclassified	114	A06

For sale by National Technical Information Service, Springfield, Virginia 22161

NASA-Langley, 1986